

Dissertation
submitted to the
Combined Faculties for the Natural Sciences and for Mathematics
of the Ruperto-Carola University of Heidelberg, Germany
for the degree of
Doctor of Natural Sciences

presented by

Stefan Welti, Diplom-Biologe

born in: Heidelberg

Oral exam:

**Biochemical Characterization
of the Sec14-PH Module
from the Neurofibromatosis Type I Protein**

Referees: PD Dr. Klaus Scheffzek
Prof.Dr. Michael Brunner

Contents

1	Abstracts	8
1.1	Abstract	8
1.2	Zusammenfassung	9
2	Abbreviations	10
3	Introduction	13
3.1	Neurofibromatosis Type I	13
3.2	The <i>NF1</i> gene	14
3.3	Animal models of NFI	15
3.3.1	Mouse	15
3.3.2	<i>Drosophila melanogaster</i>	16
3.4	The <i>NF1</i> gene product Neurofibromin	17
3.4.1	The GAP related domain and Ras	20
3.4.2	The tubulin binding region	23
3.4.3	The syndecan binding region	25
3.4.4	The CSRD domain	26
3.4.5	The Sec14 homology - PH like module	27
3.5	Current situation and goals	29
4	Results and discussion	31
4.1	Improved overlay assays and PIP binding	31
4.1.1	New tools: the α NF1-SecPH antibody	31
4.1.2	Overlay assays and the PIP binding Site	32
4.2	Assessment of typical PH- and Sec14-domain activities	39
4.2.1	NF1-SecPH does not bind phosphotyrosine	39
4.2.2	Localization studies in life cells	41
4.3	Structural investigation of lipid bound NF1-SecPH	45
4.3.1	Improved purification procedure for NF1-SecPH	45
4.3.2	Crystallization of detergent free NF1-SecPH	47
4.3.3	Structure of glycerophospholipid bound NF1-SecPH	49
4.4	Properties of the lipid binding cage	52

4.4.1	Identification of the bound ligands as PtdEtn and PtdGro	52
4.4.2	NF1-SecPH has lipid exchange activity	56
4.5	Patient derived mutations of NF1-SecPH	58
4.5.1	Purification and characterization of NF1-SecPH mutants	58
4.5.2	Structure of the Δ K1750 mutant	62
4.5.3	Structure of the TD mutant	66
4.6	Access to the lipid binding cage can be inhibited with PIPs	69
4.7	Conclusions and outlook	71
5	Materials and methods	77
5.1	Common Methods	77
5.2	Expression and purification of NF1-SecPH	78
5.3	Protein - lipid overlay assays	79
5.3.1	Generation of α NF1-SecPH antibodies	79
5.3.2	Protein lipid overlay assays	80
5.3.3	Site directed mutagenesis	81
5.4	Crystallographic techniques	82
5.4.1	Crystallization	82
5.4.2	X-ray data collection	83
5.4.3	Structure determination by molecular replacement	85
5.5	Analysis of the NF1-SecPH - glycerophospholipid interaction	86
5.5.1	Lipid extraction	86
5.5.2	Preparation of liposomes	87
5.5.3	Lipid exchange reactions and inhibition	88
5.5.4	Mass spectrometry analysis	88
5.6	Protein characterization	90
5.6.1	Analytical size exclusion chromatography	90
5.6.2	Circular dichroism spectroscopy	90
5.6.3	Isothermal titration calorimetry	91
5.7	Mammalian cell culture and microscopy	92

6 Appendix	94
6.1 Publication list	94
6.2 Abbreviations used in Fig. 3-4 (p.24)	95
6.3 Key to the lipid arrays	97
6.4 Units, amino acids and prefixes	98
References	99

Acknowledgement

Foremost, I want to thank my supervisor Klaus Scheffzek for arousing my fascination for structural biology, introducing me to X-ray crystallography and for offering me the opportunity to elaborate this thesis. For further valuable input and discussions I would like to thank the members of my Thesis Advisory Committee Philippe Bastiaens, Michael Brunner, Luis Serrano and Jochen Wittbrodt. In addition, I would like to thank Thomas Rausch for participating in the disputation.

This thesis would not have been possible without the help of many people - I want to thank especially Igor D'Angelo for uncounted help and advice, Sven Fraterman and Matthias Wilm for a great and fruitful collaboration as well as Massimiliano Mazza, Ivan Yudushkin, Wolfram Antonin and Fabien Bonneau for patience and showing me new techniques. For years of friendship, help and a good working atmosphere I am further grateful to Annabel Parret, Esther Lenherr, Jeanette Seiler, Vladimir Pena, Vadim Sidorovitch, Kanchan Anand, Ulrike Laabs, Michael Hothorn, Stefan Reinelt, Hüsseyin Besir, Ann-Marie Lawrence, Ines Racke and Uli Steuerwald. A big thank also to Sonja Kühn who gave me the chance to guide her to her Diploma and who managed to advance two projects at once, as well as to Uli Karst, a summer student I had the privilege to work with. For additional valuable help I also want to thank Oriol Galego, Stefanie Kandels-Lewis, Simone Prinz, Stephanie Kronenberg, Christopher Roome and Frank Thommen.

Furhtermore, I am grateful to my parents, Friederike and my brother Wilfried for their support and I want to address a very special thank to my wife Henriette for her continuous help, encouragement and understanding; without you, this thesis would not have been possible.

*für Henriette und
meine Eltern*

1 Abstracts

1.1 Abstract

Neurofibromatosis type I (NF1) is an inherited neurocutaneous disorder with a high incidence of 1 in 3500 newborns. Clinical manifestations include pigment anomalies, Lisch nodules and the formation of different tumors like neurofibroma. NF1 is caused by alterations of the *NF1* gene, encoding the Ras specific GTPase activating protein Neurofibromin, which participates in several major signaling pathways. A structural proteomics approach recently led to the discovery of an unpredicted pleckstrin homology (PH)- and a Sec14-like domain.

In this thesis I have investigated the biochemical properties of the NF1-SecPH module. NF1-SecPH can bind glycerophospholipids with a preference for phosphatidylethanolamine and -glycerol (PtdEtn, -Gro), of which PtdEtn is abundant in Neurofibromin containing cells and thus a likely physiological ligand. It was furthermore possible to crystallize NF1-SecPH in complex with glycerophospholipids which is the first structure of a CRAL-Trio domain bound to such ligands and shows that PtdEtn binds to the interior of the Nf1-Sec portion. Lipid exchange experiments revealed that PtdEtn and PtdGro are readily exchanged, but phosphatidylcholine, -serine and -inositol (PtdCho, -Ser, -Ins) are only incorporated to a minor degree. The lipid exchange activity can be modulated by soluble headgroups of phosphorylated PtdIns derivatives (PIPs), which is consistent with a regulatory interaction between Nf1-Sec and NF1-PH. While some patient derived mutants show significant structural alterations compared to the cellular NF1-SecPH module, their properties with respect to lipid content and PIP binding are only affected slightly. Localization studies in the presence and absence of stimuli did not reveal a specific compartment association compared to other PH domain containing proteins.

Taken together, PtdEtn is probably a physiological ligand of NF1-SecPH, which seems able to incorporate membrane derived lipids in a regulated fashion.

1.2 Zusammenfassung

Neurofibromatose Typ I (NF1) ist eine neurokutane Erbkrankheit, die bei einem von 3500 Neugeborenen auftritt. Häufige Symptome sind Pigmentanomalien, Lisch-Knoten und verschiedene Tumore, wie Neurofibrome. Die Erkrankung wird durch Mutationen im *NF1* Gen verursacht, das mit dem Ras spezifischen GTPase aktivierenden Protein Neurofibromin einen Regulator zentraler Signalwege kodiert. Durch strukturbezogene Proteomik wurde kürzlich eine unerwartete Pleckstrin Homologie- (PH) und eine Sec14-ähnliche Domäne entdeckt.

In der vorliegenden Arbeit untersuchte ich die biochemischen Eigenschaften des NF1-SecPH Moduls. NF1-SecPH bindet Glycerophospholipide – im Besonderen Phosphatidylethanolamin und -glycerol (PtdEtn, -Gro) – was zusammen mit seiner Häufigkeit in Neurofibromin enthaltenden Zellen für PtdEtn als wahrscheinlichen physiologischen Liganden spricht. Zudem konnte NF1-SecPH im Komplex mit Glycerophospholipiden kristallisiert werden, was die erste Struktur einer CRAL-Trio Domäne mit solchen Liganden darstellt und zeigt, dass PtdEtn im Inneren von NF1-Sec bindet. Während PtdEtn und PtdGro leicht austauschbar sind, werden Phosphatidylcholin, -serin und -inositol (PtdCho, -Ser, -Ins) nur schlecht inkorporiert. Die Austauschreaktion kann zudem mit hohen Konzentrationen löslicher Kopfgruppen phosphorylierter PtdIns Derivate (PIPs) moduliert werden, was konsistent mit einer regulatorischen Interaktion zwischen NF1-Sec und NF1-PH ist. Obwohl die Strukturen einiger Mutanten von Patienten signifikante Änderungen zum zellulären NF1-SecPH aufweisen, sind hinsichtlich gebundener Lipide oder der Bindung von PIPs kaum Unterschiede feststellbar. Lokalisierungsstudien bei An- oder Abwesenheit von Stimuli zeigten keine Assoziierung mit bestimmten Zellbereichen, im Gegensatz zu anderen Proteine mit PH Domänen.

Zusammenfassend ist PtdEtn ein wahrscheinlicher physiologischer Ligand von NF1-SecPH, das anscheinend auf regulierte Art und Weise Membranlipide inkorporieren kann.

2 Abbreviations

AC	adenylyl cyclase
α -TTP	α -tocopherol transfer protein
AMP	adenosine monophosphate
ArA	arachidonic acid
Arp2/3	actin related proteins 2/3
BEACH	Beige and Chédiak-Higashi domain
Bp	base pair
BSA	bovine serum albumin
cAMP	cyclic adenosine monophosphate
CASK	calcium/calmodulin-dependent serine protein kinase
CBD	caveolin binding domain
CD	circular dichroism
CNS	central nervous system
CRAL_Trio	domain type named after CRALBP and Trio
CRALBP	cellular retinaldehyde binding protein
CREB	cAMP response element binding
CSRD	cysteine and serine rich domain
CRMP-2	collapsin response mediator protein 2
Dab	disabled
DNA	deoxyribonucleic acid
D-GD3	disialoganglioside-GD3
ECL	enhanced chemiluminescence
ECM	extracellular matrix
EDTA	ethylenediaminetetraacetic acid
EGF	epidermal growth factor
EM	electron microscopy
Ena	enabled
ER	endoplasmatic reticulum
ESI	electrospray ionisation
EVH1	enabled / VASP homology 1
EVI2A	ecotropic viral integration site 2A
EVI2B	ecotropic viral integration site 2B
<i>E.coli</i>	<i>Escherichia coli</i>
FFDM	fat free dry milk powder
GAP	GTPase activating protein
GDP	guanosine diphosphate
GEF	guanosine nucleotide exchange factor
GFP	green fluorescent protein
GPCR	G-protein coupled receptor
GRD	GAP related domain
GRP1	general receptor for phosphoinositides isoform 1
GST	glutathion-S-transferase
GTP	guanosine triphosphate

HeLa	Henrietta Lacks
HEPES	N-1-Hydroxyethylpiperazine N'-2-ethanesulfonic acid
HRP	horseradish peroxidase
Ins-3-P	1D- <i>myo</i> -Inositol-3-phosphate
InsP ₆	<i>myo</i> -Inositol-1,2,3,4,5,6-hexakisphosphate
IRA1	inhibitory regulator of the RAS-cAMP pathway 1
IRA2	inhibitory regulator of the RAS-cAMP pathway 2
IRS	insulin receptor substrate
ITC	isothermal titration calorimetry
LOH	loss of heterozygosity
LPA	lysophosphatidic acid
LPtdCho	lyso-PtdCho
MAPK	mitogen-activated protein kinase
MAP1	microtubule-associated protein 1
MES	2-(N-Morpholino)-ethanesulfonic acid
MPNST	malignant peripheral nerve sheet tumor
MR	molecular replacement
mRNA	messenger RNA
MS	mass spectrometry
mTOR	mammalian target of rapamycin
MWCO	molecular weight close out
M-GM1	monosialoganglioside-GM1
NF1	Neurofibromatosis type I
NF1-CSRD	cysteine and serine rich domain of Neurofibromin
NF1-GRD	gap related domain of Neurofibromin
NF1-PH	PH-like domain of human Neurofibromin
NF1-SecPH	SecPH domains of human Neurofibromin
NF1-Sec	Sec14-like domain of human Neurofibromin
NF1-Syn	syndecan binding domain of Neurofibromin
NF1-Tub	tubulin binding domain of Neurofibromin
NLS	nuclear localization signal
OD	optical density
OMPG	oligodendrocyte myelin glycoprotein
PA	phosphatidic acid
PBS	phosphate buffered saline
PDB	protein data bank
PDGF	platelet derived growth factor
PEG	polyethylene glycol
<i>pfu</i>	<i>Pyrococcus furiosus</i>
PH	pleckstrin homology
PI	phosphatidylinositol = PtdIns
PIPs	phosphorylated PtdIns derivatives
PITP	phosphatidylinositol transfer protein
PI3K	phosphatidylinositol 3-kinase
PKA	protein kinase a
PKC α	protein kinase C α

PLC- β 2	phospholipase C- β 2
PMFS	phenylmethanesulfonyl fluoride
Pob3	polymerase 1 binding protein 3
PSn1P	phosphatidylserine-1-phosphate
PTB	phosphotyrosine binding
PtdCho	phosphatidylcholine, (3- <i>sn</i> -phosphatidyl)choline
PtdEtn	phosphatidylethanolamine
PtdGro	phosphatidylglycerol
PtdIns	phosphatidylinositol, 1-(3- <i>sn</i> -phosphatidyl)-D- <i>myo</i> -inositol
PtdIns-3-P ₁	PtdIns-3-phosphate
PtdSer	phosphatidylserine
pTyr	phosphotyrosine
Q-ToF	quadrupole-time of flight
Rac	ras related C3 botulinum toxin substrate 1
Ral	ras-like protein
Ran	ras-related nuclear protein
RanBD	ran binding domain
Ras	rat sarcoma viral oncogene homolog
RdgB	retinal degeneration B (α I / α II)
RMSD	root mean square deviation
RNA	ribonucleic acid
RTK	receptor tyrosine kinase
rutAC	rutabaga adenylyl cyclase
SCF	stem cell factors
SDS-PAGE	sodium dodecyl sulfate polyacrylamide gel electrophoresis
Shc	src homology 2 domain containing
Sn1P	sphinganine-1-phosphate
SPCho	sphingosylphosphorylcholine
src	v-Src avian sarcoma (Schmidt-Ruppin A-2) viral oncogene
S1P	sphingosine-1-phosphate
TAP-TAG	tandem affinity purification - tag
TD	tandem duplication mutation
TEV	tobacco etch virus
TFIIH	transcription factor IIH
ToF	time of flight
TRIO	triple functional domain protein
Tris	tris-(hydroxymethyl)-aminoethane hydrochloride
TGF- β	transforming growth factor β
UV	ultra violet
VASP	vasodilator-stimulated phosphoprotein
WASP	Wiscott-Aldrich syndrome proteins
YFP	yellow fluorescent protein
4x	mutant of NF1-SecPH: K1670A-R1674A-R1748A-K1750A

3 Introduction

3.1 Neurofibromatosis Type I

Neurofibromatosis type I (NF1), also referred to as von Recklinghausen disease, is a common inherited neurocutaneous disorder classified as a Phakomatosis.¹⁻⁴ The disease was first described by the German professor Friedrich Daniel von Recklinghausen in 1882⁵ and since then, no cure or efficient treatment could be found. Causative for the autosomal dominant disorder are alterations of the *NF1* gene, which has one of the highest mutation rates in the human genome of about $0.3 - 1.0 \times 10^{-4}$. Correspondingly, 50% of new cases arise from spontaneous mutations.^{6,7} NF1 has a relative high incidence of 1 in 3500 and a minimum prevalence of 1 in 5000. Although the disorder is completely penetrant, both severity and the individual phenotype are unpredictable and differ even between family members carrying the same mutation.⁷⁻⁹

The most frequent clinical manifestations of NF1 include several benign pigmented lesions called café-au-lait spots, Neurofibroma, axillary or inguinal freckling and hamartomas of the iris termed lisch nodules.^{2,9,10} Neurofibroma are benign peripheral nerve sheath tumors which mainly consists of fibroblasts, Schwann-, mast- and perineurial cells, large amounts of collagenous extracellular matrix and a traversing neuron.¹ While cutaneous neurofibroma are nearly symptomless except itching, subcutaneous ones can cause pain and neurological deficits by compression of nearby peripheral nerves. Similar symptoms emerge from plexiform neurofibroma which in addition diffusely infiltrate the surrounding tissue and grow along nerves to large size. In some cases cutaneous and plexiform neurofibroma can progress to highly aggressive malignant peripheral nerve sheath tumors (MPNSTs) which widely metastasize and usually portend a poor outcome.^{1,9} Tumor formation is induced by *NF1*^(-/-) Schwann cells, but depends on a *NF1*^(-/+) microenvironment and recruitment of inflammatory cells.^{1,11-13} Other features affect bone homeostasis (scoliosis,

pseudoarthrosis¹⁴), brain function (attention deficit,¹⁵ learning problems,¹⁶ epilepsy¹⁷) and include further types of tumors (phaeochromocytoma,¹⁸ optic pathway glioma,¹⁹ rhabdomyosarcoma,^{20,21} juvenile myelomonocytic leukemia²²) to exemplify some of the many possible complications.^{9,10,23,24}

3.2 The *NF1* gene

The *NF1* gene is located on the long arm of chromosome 17 near the centromere,²⁵⁻²⁸ consists of about 280 Kbp of genomic DNA²⁹⁻³² and is divided into 60 alternatively spliced exons.³³ Although, a large number of different *NF1* splicing products are known,^{33,34} only five of them have also been detected on the protein level so far (fig. 3-1).^{33,35-37}

The expression of the different *NF1* splicing products is regulated in a complex way, including tissue specific expression, mRNA editing³⁸⁻⁴⁰ and developmental changes as shown with cultured human cells and murine *NF1* homologues.⁴¹⁻⁴⁵ Expression of *NF1* during development is ubiquitous between the onset of organogenesis and midstage embryonic development, but decreases then in many tissues until expression in adults is mainly observed in neurons, Schwann cells and oligodendrocytes.⁴⁶⁻⁴⁸ While the splice products type I and II are widely expressed with a focus on the nervous system,⁴⁹⁻⁵¹ the *NF1* isoforms 3 and 4 are exclusively expressed in muscle tissue^{35,36} and isoform 9br in CNS neurons.^{37,45,52}

It is noteworthy, that the three pseudogenes OMGP (oligodendrocyte myelin glycoprotein), EVI2A and EVI2B (ecotropic viral integration site) are located on the antisense strand of the *NF1* gene. OMGP is a cell adhesion molecule and ligand of the NgR receptor, while EVI2A/B are transmembrane glycoproteins whose murine homologues are linked to leukemia formation. However, no mutations associated with *NF1* could be found in this genes so far.⁵³⁻⁵⁶

3.3 Animal models of NFI

In different animal systems defects of NFI could be modeled, revealing a number of mechanisms involved in the pathogenesis of the disease, especially regarding tumor formation. In many aspects, the acquired information is valid for the human organism and might help to further the development of therapies. The best characterized model systems of NF1 are mouse (*Mus musculus*) and the fruit fly (*Drosophila melanogaster*).

3.3.1 Mouse

The mouse *Nf1* gene has a sequence homology of 98% to human *NF1*, including both, the coding sequence and promoter region.⁵⁷ Therefore it can be expected that gene regulation, gene expression as well as the biochemical functions of the encoded proteins are very similar.

While mice with complete loss of Neurofibromin *Nf1*^{-/-} are embryonic lethal due to defects in heart development, *Nf1*^{+/-} mice recapitulate several symptoms of the human disease including abnormal brain function, learning disabilities, increased risk of myeloid leukemia and pheochromocytoma.⁵⁷⁻⁶¹ Although, the development of neurofibroma is not among the observed symptoms, they do occur in chimeric *Nf1*^{+/-} / *Nf1*^{-/-} mice, indicating that the required loss of heterozygosity (LOH) in Schwann cells is simply less frequent in mice.^{13,59,62}

To further characterize the prerequisites for tumor formation, mice were generated with the *Nf1* gene specifically disrupted in Schwann cells. Interestingly, these mice did not develop any tumors in contrast to *Nf1*^{+/-} mice with *Nf1*^{-/-} Schwann cells. While this result shows that neurofibroma have indeed a Schwann cell origin, it also demonstrates that tumor formation depends on a *Nf1*^{+/-} environment and interaction with other cell types. Similar observations could be made for the invasion of mast cells into nerve sheets, a process which seems to be a further prerequisite for tumor formation. Once attracted to nerve sheets by stem cell factors (SCF) secreting *Nf1*^{-/-} Schwann

cells, the mast cells start to produce mitogens, TGF- β (transforming growth factor β) and angiogenic factors which generates a permissive environment for the advancement of tumor formation.^{61,63-65}

In another mouse model the occurrence of MPNSTs could be observed. This required a so called second-hit mutation in *Nf1*^{+/-} mice, namely the disruption of the *p53* allele located at the same chromosome like *Nf1*. Investigations of MPNSTs showed, that during malignant transformation these tumors had lost the remaining alleles of *Nf1* and *p53*, displaying the full range of features observed in the human malignancy.^{59,61} Also NF1 related learning disabilities could be investigated in mice, revealing that missing of exon 23a is responsible for these symptoms. On a molecular level, the removal of exon 23a results in the reduction of Neurofibromins GAP activity (p. 20) and leads to an excess of active K-Ras. Downregulation of K-Ras activity is in turn sufficient to rescue the phenotype, as shown with *Nf1*^{+/-} / *K-Ras*^{+/-} mice and indirect K-Ras inhibitors.^{57,66}

3.3.2 *Drosophila melanogaster*

The *Drosophila melanogaster Nf1* gene has a size of about 13 Kbp and a sequence identity of 60% with human *NF1*.⁶⁷ Deletion of one *Nf1* allele seems to have no severe effects, but *Nf1*^{-/-} flies have a decreased body size, learning disabilities and abnormalities in the regulation of circadian rhythm effectors.⁶⁷⁻⁶⁹ Similar to mice, the described learning defects are reversible, which was shown by inducible expression of transgenic *Nf1*.⁷⁰

Interestingly, dependence on Ras signaling and the MAPK pathway could only be shown for some of the effects observed in *Nf1*^{-/-} flies, including impairment of long term memory formation as well as altered regulation of circadian controlled proteins like cAMP response element binding protein (CREB).^{69,71} In turn, the decreased body size and impairment of immediate memory seems to be associated with reduced PKA activity and cAMP signaling. Biochemical investigations point towards a potential direct interaction of Neurofibromin with the

rutabaga adenylyl cyclase (rutAC), leading to cAMP production and PKA activation.⁷⁰⁻⁷² However, the Ras signaling independence of at least the body size defects are discussed controversially in the literature.⁷³ In recent studies of *Nf1*^{-/-} flies, a number of additional effects have been reported, affecting the life span, stress response and mitochondrial activity. These effects could be reversed by overexpression of Neurofibromin and seem to be connected to AC activity and cAMP levels but not Ras signaling.⁷⁴

In summary, the *Drosophila* Neurofibromin proteins seems to act on a branching point of Ras and AC / PKA mediated signaling in the fruit fly, affecting diverse processes like learning, development and longevity.^{60,70}

3.4 The *NF1* gene product Neurofibromin

The 2818 aa large Neurofibromin protein is the best characterized gene product of the *NF1* gene, corresponding to the splice variant type I. Neurofibromin has a central Ras specific GAP (GTPase activating protein) activity located in the GRD (GAP related domain)^{80,111,115} and is classified as a tumor suppressor protein,¹¹⁶⁻¹¹⁹ deficiency of which leads to an increased Ras activity as shown in at least some tumor cells^{116,120-123}(Fig.3-1). Sequence comparisons show similarities of GRD to the GAP domains of human p120GAP and the *Saccharomyces cerevisiae* proteins IRA1 and IRA2.^{80,115,116} As negative regulator of Ras, Neurofibromin effects a core element of several signal transduction pathways involved in processes like cell survival, -proliferation, -differentiation and -migration as well as learning and memory.^{10,12,53,58,124}

Since membrane attachment of Ras via lipid anchors is regulated in a complicated manner,¹²⁵⁻¹²⁷ it is tempting to speculate that Neurofibromin harbours membrane targeting activities as well to communicate with its target protein. Several studies addressing this topic could show Neurofibromin localization to the plasmamembrane (ker-

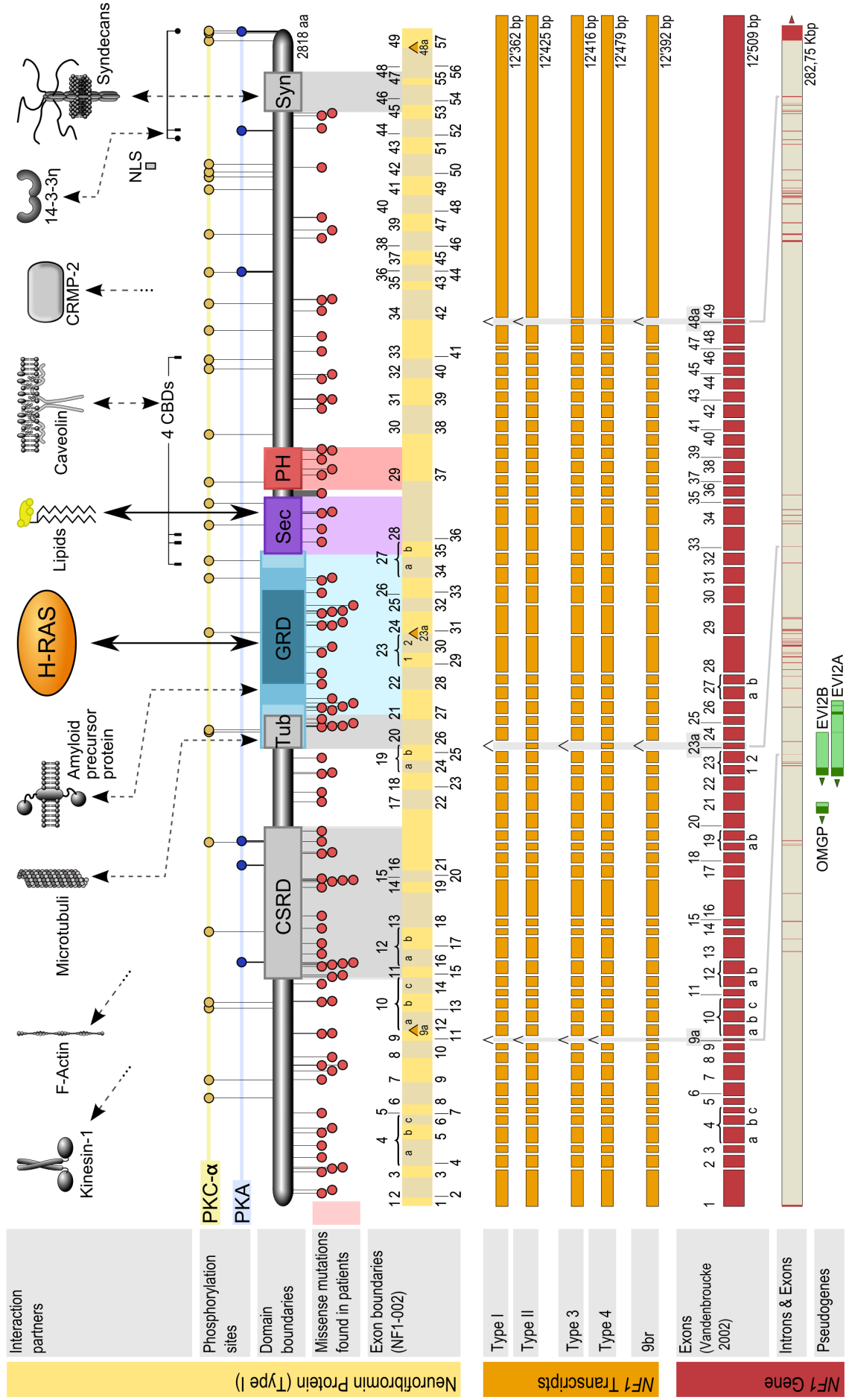


Fig. 3-1: *NF1*, Neurofibromin and interaction partners (legend see p.19).

◀ **Fig. 3-1 (p.18): *NF1*, Neurofibromin and interaction partners.**

***NF1* Gene:**²⁹ ‘Introns & Exons’ displays the 282.75 Kbps of genomic *NF1* DNA, with introns (gray) and exons (red) drawn to scale. ‘Pseudogenes’: Located on the antisense strand of the *NF1* gene are the pseudogenes OMGP,⁷⁵ EVI2A⁷⁶ and EVI2B,⁷⁷ drawn in dark (exons) and light green (introns). ‘Exons’ displays the common numbering (Vandenbrouck et.al.³³) and relative size of the *NF1* exons only, summing up to a total of 12509bps. ***NF1* Transcripts:** Exon schemes of the five alternatively spliced transcripts of *NF1*, translation of which could be confirmed on the protein level.^{33,35-37} Alternatively spliced exons are indicated with a circumflex and a gray underlay. **Neurofibromin Protein (Type I):** ‘Domain boundaries’ shows a scheme of the 2818 aa Neurofibromin protein, with the six known protein regions CSRD,⁷⁸ Tub,⁷⁹ GRD,⁸⁰⁻⁸² Sec,^{83,84} PH⁸⁴ and Syn⁸⁵ displayed in scale as boxes. The light blue box of the GRD region corresponds to the p120GAP/IRA1/IRA2 homology region,⁸⁰ the blue box to the crystallized fragment⁸¹ and the dark blue one to the minimal GAP domain.⁸² Potential PKA^{28,78} and PKC α ⁸⁶ phosphorylation sites (‘Phosphorylation sites’) are indicated with blue and yellow circles. Red circles (‘Missense mutation found in patients’) indicate currently know missense mutations, single aa deletions and one tandem duplication located between the Sec and the PH domain.⁸⁷⁻¹⁰⁵ Corresponding to the protein scheme ‘exon boundaries’ shows the 57 exons of isoform I, with the common numbering on top and continuous numbering below. Orange triangles indicate the exons 9a, 23a and 48a, which are removed by alternate splicing in Neurofibromin Type I. ‘Interaction Partners’ shows the reported nuclear localization signal (NLS),¹⁰⁶ the four caveolin binding domains (CBDs) where caveolin is predicted to bind Neurofibromin¹⁰⁷ and the remaining interaction partners Kinesin-1,¹⁰⁸ F-Actin,¹⁰⁹ Microtubule,⁷⁹ amyloid precursor protein,¹¹⁰ H-Ras,¹¹¹ Lipids,^{84,112} CRMP-2,¹¹³ 14-3-3 η ¹¹⁴ and Syndecans.⁸⁵ Arrows indicate the interacting Neurofibromin domain if known.

atinocytes),¹²⁸ the endoplasmatic reticulum (ER; in CNS neurons),¹²⁹ mitochondria and microtubules (fibroblasts, leptomenigeal cells, astrocytoma cells).^{130,131} There is also the presence of a nuclear localization signal (NLS) in Neurofibromin reported,¹⁰⁶ however the biological meaning of this finding is rather unclear. In the described experiments only the C-terminal half of the protein was used and despite several studies of other research groups, a similar observation has not been reported until now (see above).

To identify further domains of Neurofibromin, patient derived mutations of the *NF1* gene have been analyzed revealing a huge number of different alterations, 90% of which result in truncated protein products due to premature stop codons or splicing defects. Patient derived missense mutations and single amino acid deletions are found distributed over the whole *NF1* gene and cluster in regions corresponding to the GRD and CSRD (cysteine and serine rich domain) of the protein⁹⁰(fig.

3-1). This underlines the importance of the GRD domain, but indicates likewise that the CSRD and other regions of Neurofibromin are likely to be of functional relevance as well.⁸⁷⁻¹⁰⁵ Biochemical analysis revealed phosphorylation of Neurofibromin by protein kinase A (PKA)⁷⁸ and C (PKC)⁸⁶ as well as several interaction partners including Syndecan,⁸⁵ amyloid precursor protein,¹¹⁰ Caveolin,¹⁰⁷ tubulin,⁷⁹ kinesin-1,¹⁰⁸ collapsin response mediator protein-2 (CRMP-2)¹¹³ and 14-3-3 η .¹¹⁴ For most of these interactions, the physiological significance and the precise mode of interaction with Neurofibromin is not clarified yet.

3.4.1 The GAP related domain and Ras

The best understood part of Neurofibromin is the GAP related region (GRD) which spans aa 1095 to 1569 and functions as negative regulator of the proto-oncogene Ras.^{79,82,111,132}

Ras acts as a molecular switch in the cell and can either be in an GTP bound 'on' state allowing target proteins to bind and trigger further signaling, or a GDP bound 'off' state (Fig.3-2). Structurally, in the 'on' state the else flexible Switch I and II regions of Ras become stabilized by the γ -phosphate of GTP and adopt thereby a more defined conformation capable of target protein binding, which leads to further stabilization of the switch regions. The continuous cycling of Ras between 'on' and 'off' states establishes a sensitive equilibrium and maintains a certain amount of 'on' state Ras which is tightly regulated by two protein classes. The first one are Guanine nucleotide exchange factors (GEFs), which can switch Ras to the 'on' state by facilitating the release of GDP, followed by a quick noncatalyzed re-binding to abundant intracellular GTP. The second one are GTPase activating proteins (GAPs) like Neurofibromin, which can stop the 'on' state of Ras by accelerating its slow intrinsic GTP hydrolysis activity resulting in GDP bound 'off' state Ras.^{80,111,115,116,127,132}

The activation of Ras catalyzed GTP hydrolysis by Neurofibromin is well investigated in biochemical and structural detail, suggesting

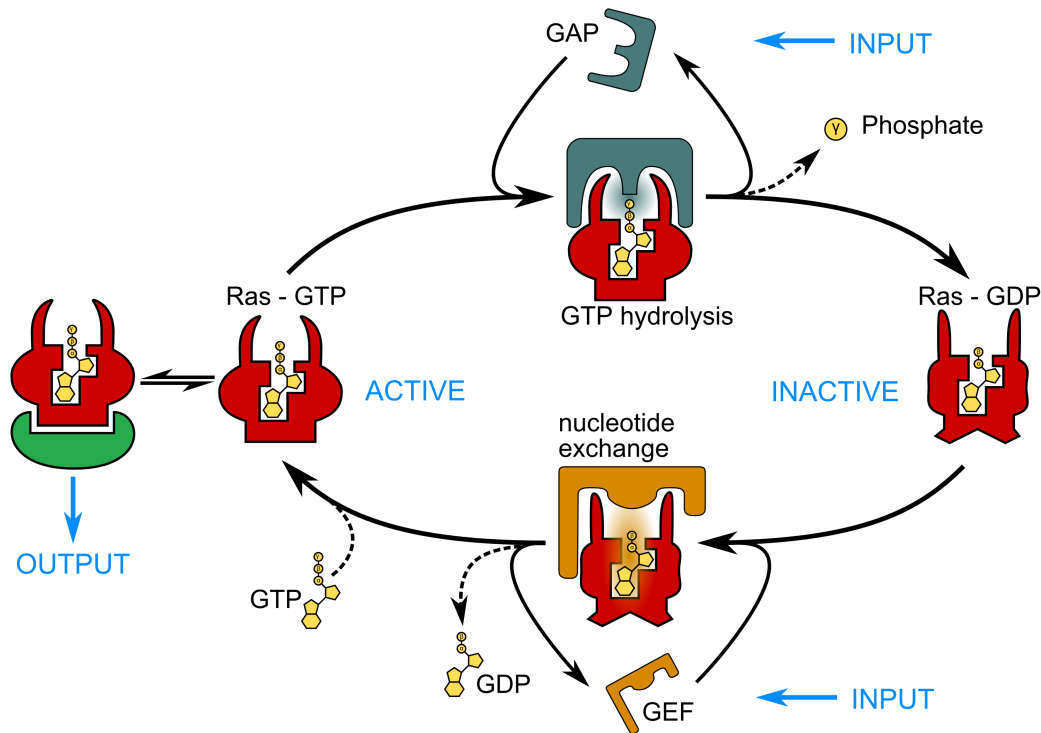


Fig. 3-2: The Ras cycle Inactive Ras-GDP binds to a GEF protein, which removes the GDP from the Ras active site. Due to the high GTP concentration in the cell, Ras immediately picks up a GTP molecule and becomes active. Ras effectors can now bind and trigger downstream signaling events. Inactivation of Ras can either occur by its very slow intrinsic GTPase activity or by interaction with GAP proteins like Neurofibromin, which complement the Ras active site and accelerate the GTP hydrolysis extremely. Both GEFs and GAPs are regulated themselves, providing the means of signal input into the Ras cycle.

complementation of the Ras active site by the Arg1276 containing finger loop of GRD as main catalytic mechanism (fig. 3-3). Arg1276 stabilizes the transition state of the hydrolysis reaction by neutralization of negative charges emerging from the nascent inorganic phosphate.^{81,132-134} The importance of Arg1276 for the physiological functionality of Neurofibromin was underlined by the observation of a missense mutation changing Arg1276 to proline in a patient with malignant tumors, which results *in vitro* in a 8000-fold reduction of Neurofibromin's GAP activity, without changing the binding affinity towards Ras.¹³⁵ Other features important for catalysis are the Switch II region, which needs to be stabilized by GRD interactions to maintain the geometry of the active site, as well as Ras-Gln61 and a Mg^{2+} ion for further stabilization of the transition state. On the GRD side, the FLR motif is stabilizing the conformation of the finger-loop as well

as the Switch I and II regions, while the variable loop ensures the specificity of the GRD - Ras interaction.^{81, 132, 133, 136, 137}

Experiments with a GRD containing fragment of Neurofibromin showed that the GAP activity can be inhibited by phosphatidic and (PA) arachidonic acid (ArA),¹³⁸ while the same observation was also made with the full length protein using different stearic or oleic acid derivatives.^{139, 140} Although, Neurofibromin has with NF1-Sec (see below) a lipid binding module, this inhibitory effect seem to be feature of GRD alone, at last for PA and ArA.

As outlined in fig. 3-4 (p.24), Neurofibromin influences a number of signal transduction pathways, especially by GRD mediated negative regulation of Ras. Ras is an important target of RTK signaling and influences in turn a number of other signaling pathways and cellular

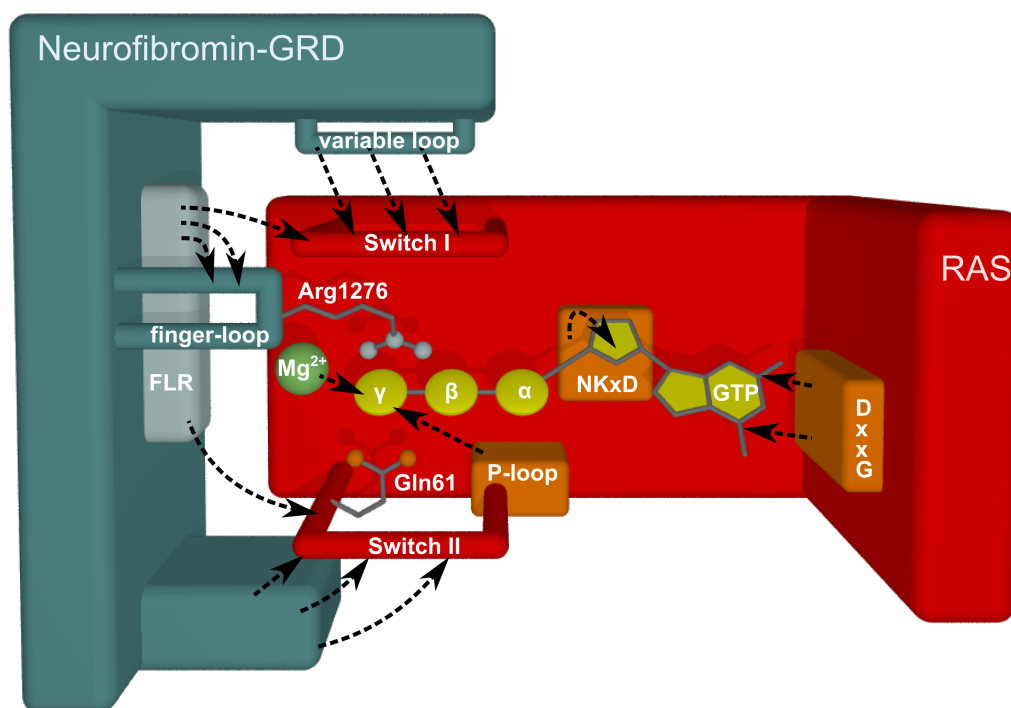


Fig. 3-3: The Ras - RasGAP complex. Scheme of Neurofibromin interactions with the Ras active site during catalysis: Neurofibromin complements the Ras active site by insertion of the Arg1276 containing finger loop. Furthermore, several parts of Neurofibromin including the FLR motive and the variable loop, stabilize the Ras switch I and II regions in a reaction competent conformation as indicated by arrows. Hydrolysis of the GTP- γ phosphate is performed by Neurofibromin-Arg1276, Ras-Gln61, the P-loop and a Mg^{2+} ion. The binding affinity and ligand specificity of Ras for GTP is mediated by the Mg^{2+} ion, P-loop, NKxD- and DxxG motive.

processes. This includes proliferation by MAPK signaling, membrane trafficking through Ral, actin cytoskeleton dynamics and cell cycle progression via Rac and PI3K as well as enhanced cell growth and protein translation by mTOR signaling. Furthermore, Neurofibromin affects signaling pathways independent of Ras, for example via AC / PKA and is in turn influenced by GPCR signaling, PKA and PKC α . A number of further connections to signaling pathways can be expected, taken into account the number of Neurofibromin interaction partners, especially receptors like syndecans.

3.4.2 The tubulin binding region

Stretching from residue 1095 to 1176, the tubulin binding domain (NF1-Tub) is located inside the p120GAP homology region of Neurofibromin which harbours the GRD domain. The NF1-Tub region was shown to bind to α/β -tubulin heterodimers as well as whole microtubules. Furthermore, the GAP activity of Neurofibromin and the affinity towards Ras is reduced upon tubulin binding *in vitro*,^{79,131} an effect which is probably even stronger in the cell since binding to microtubules removes Neurofibromin from the plasma membrane and Ras. The finding of a patient derived mutation in GRD, which disrupts tubulin binding but does not influence GAP activity, underlines the relevance of this observations.¹⁹⁶ This interaction potentially connects Ras signaling with important microtubule dependent processes like chromosome segregation, axonal transport and organelle movement.¹⁹⁵

It is noteworthy, that just recently an interaction between Neurofibromin and collapsin response mediator protein-2 (CRMP-2) was reported, which seems to be involved in the regulation of neurite outgrowth.¹¹³ CRMP-2 was furthermore reported to be able to form a heterotrimeric complex with α/β -tubulin and kinesin-1,¹⁹⁴ which are both interaction partners of Neurofibromin as well.^{79,108,131} In addition, Ras was reported to regulate neuronal polarity via a pathway finally affecting CRMP-2,¹⁶⁴ suggesting a feedback loop to Neurofi-

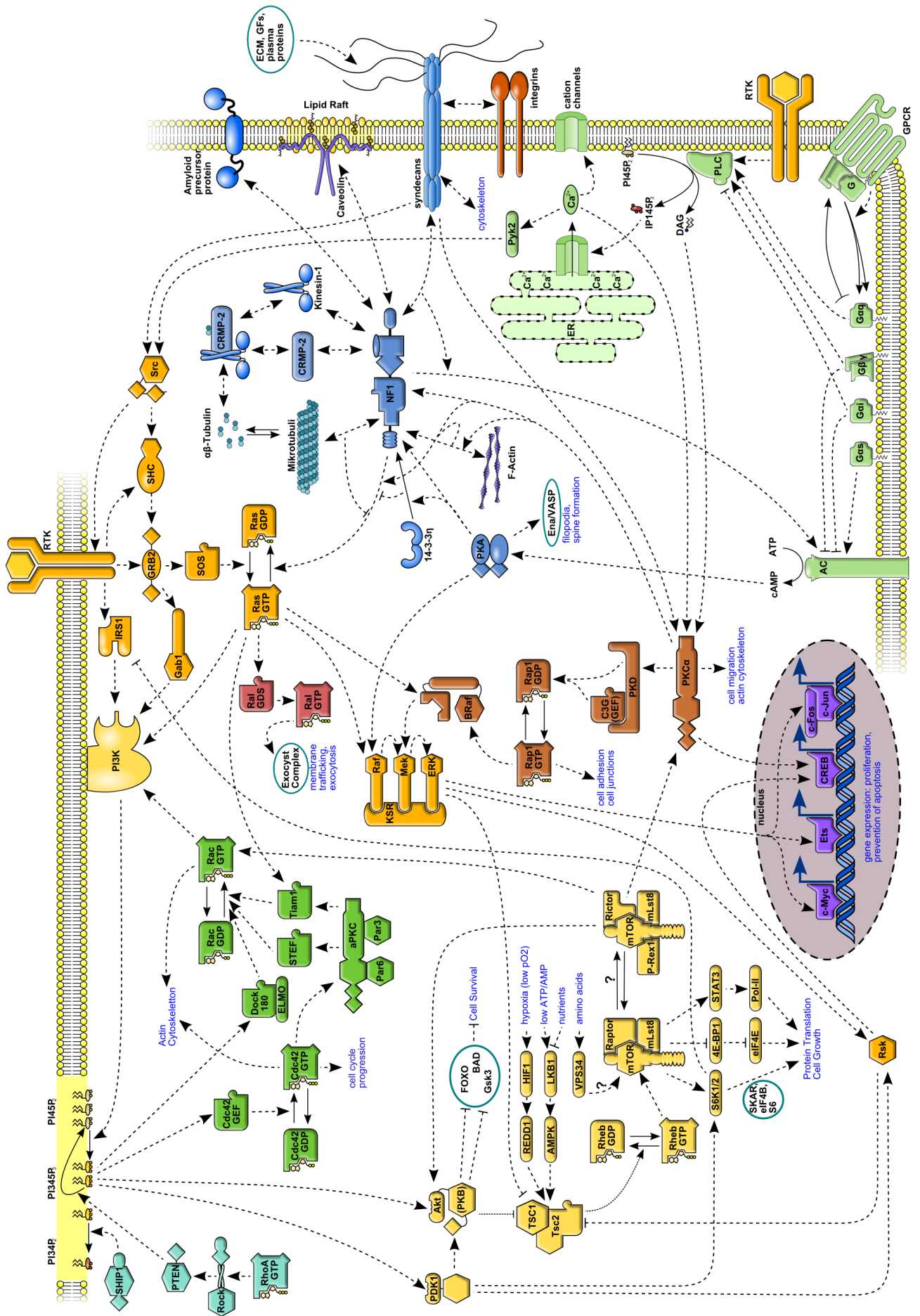


Fig. 3-4: Simplified scheme of Neurofibromin and chosen signaling pathways (legend see p.25)

◀ **Fig. 3-4 (p.24): Simplified scheme of Neurofibromin and related signaling pathways in consideration of the most recent findings.**

The best characterized function of Neurofibromin is the negative regulation of Ras, which connects the protein to various signaling pathways. Ras is a main effector of RTK signaling and transduces the incoming signals towards different targets including the MAP kinase pathway, PI3K / mTOR signaling, Rac / cytoskeleton as well as membrane trafficking and exocytosis via Ral. Furthermore, Neurofibromin influences these signaling events via AC / PKA and is in turn influenced by GPCR, syndecan and integrin signaling. Taking into account the number of Neurofibromin interaction partners reported, it can be expected that future research will reveal a number of additional connections to cellular signaling.^{16, 78, 79, 81, 85, 86, 107–110, 113, 114, 132, 133, 141–195} The abbreviations of protein names are itemized in the appendix p.95. Please note that the interaction scheme does not include all reported interactions, not even if both components are displayed. Only chosen proteins are shown, not accounting for all existing isoforms. Colors are used for the purpose of clarity only. Arrowheads indicate functional activation of the target molecule or reaction by catalysis, recruitment, phosphorylation ect., while flat bars indicate functional inhibition or inactivation. Arrows with two heads symbolize interaction.

bromin.

3.4.3 The syndecan binding region

The syndecan binding region (NF1-Syn) is located at the C-terminus of Neurofibromin (aa 2619 to 2719) and was shown to bind syndecans in yeast two hybrid screens, which is supported by the finding that syndecan-2 induced filopodia and dendritic spine formation is Neurofibromin dependent.^{85, 159}

Syndecans are transmembrane receptors carrying 3 to 5 heparan- or chondroitin-sulfate sugar chains on their extracellular part. With their intracellular domains, syndecans can bind cytoskeletal and signaling molecules like CASK, synthenin, PKA and Src, while their extracellular part interacts with plasma proteins, growth factors and extracellular matrix (ECM) proteins. Thereby syndecans couple ECM and cytoskeleton, affecting processes like organ morphogenesis, cell motility and -adhesion, often by synergistic signaling in cooperation with integrins. Syndecans were also shown to act as co-receptors of RTKs, modulating their signaling output dependent on the current extracellular environment.

The signaling events affecting the regulation of filopodia and spinogenesis are apparently mediated by the subsequent actions of Neurofi-

bromin, AC, cAMP, PKA and finally Ena/VASP (enabled / vasodilator-stimulated phosphoprotein) proteins which are key regulators of the actin cytoskeleton. However, these findings seem to reflect only parts of the full regulatory mechanism, since PKA activation alone is not sufficient to trigger spinogenesis and the extracellular part of syndecan-2 is needed as well for productive signaling. Whether additional pathways are triggered by syndecan-2 via ECM / integrin contacts or by other mechanisms is unclear, but it should be noted that PKA and actin are both direct interactors of Neurofibromin and enhance Ras signaling by GRD inhibition. Taken together, syndecans seem to recruit Neurofibromin to adhesion sensitive signaling complexes involved in the coupling of extracellular signaling and actin dynamics.^{85, 158–160, 197}

3.4.4 The CSRD domain

Analysis of patient derived missense mutations revealed a clustering of mutations in the Neurofibromin region spanning from residues 593 to 909, suggesting the presence of a further functional unit which was termed cysteine and serine rich domain (CSRD). Features of the CSRD are three cysteine pairs suggestive of ATP binding as well as potential phosphorylation sites for PKC α and PKA.⁹⁰

It was demonstrated, that PKA can phosphorylate CSRD *in vitro* and speculated that this could have an effect on microtubule binding. This idea is based on the finding that one of the amino acid stretches (815-834) carrying a PKA site has sequence homology to the microtubule associated proteins MAP-2 and tau.^{90, 131}

Phosphorylation of CSRD by PKC α was observed *in vivo* as consequence of EGF stimulation and enhances both, GRD activity and the association of Neurofibromin with the actin cytoskeleton. EGF stimulation can simultaneously activate Ras and PLC γ signaling, leading to cell migration and/or cell proliferation. This PLC γ - PKC α mediated negative feedback on Ras signaling is in this context hypothesized to represent a mechanism shifting the cellular EGF response towards cell migration.⁸⁶

3.4.5 The Sec14 homology - PH like module

The Sec14 homologous region (NF1-Sec) resides C-terminally of GRD ranging from residues 1560 to 1698 and is directly followed by the pleckstrin homology like domain (NF1-PH) extending from residue 1715 to 1816. Bioinformatic studies predicted NF1-Sec⁸³ due to weak homology to the CRAL_TRIO motive (Prosite¹⁹⁸ PS50191), which could be confirmed after we solve the structure of the NF1-SecPH module.^{84,199} In contrast, NF1-PH is a crystallographic discovery and was only recognized as PH domain after structural comparison with databases, supporting our project approach.

The CRAL_TRIO motif was first observed in the *Saccharomyces cerevisiae* phosphatidylinositol (PI) transfer protein (PITP) Sec14p and consists of a large hydrophobic cage which is closed by a special amphipatic helix. With this cage, PITPs are able to transfer hydrophobic lipids between membranes through the aqueous medium. The amphipatic helix seems to be the key element in this process and is believed to be able to enter a membrane, extract a single lipid and seal the lipid-binding cage during the transport (“bulldozer mechanism”).^{200–205} PITPs are found in most organisms excluding bacteria and can be divided into two different domain types which are unrelated to each other in structure and sequence. In mammals, the first domain type includes the protein classes containing PITP α , PITP β , RdgBaI and RdgBaII which mainly have a transfer activity for 1-(3-*sn*-phosphatidyl)-D-*myo*-inositol (PtdIns, PI) and (3-*sn*-phosphatidyl)choline (PtdCho). The lipid PtdIns and especially its phosphorylated derivatives (PIPs) are essential components of many signaling pathways effecting cytoskeleton dynamics, membrane transport and traffic.²⁰⁶ The second domain type consists of the Sec14p-like proteins, which have strongly diversified in terms of physiological functions and ligand specificity, transporting for example pigments and vitamins.^{207–213}

PH domains consists structurally of two stacked β -sheets which

are interconnected by three variable loops and flanked by an α -helix (β -sandwich). This structural scaffold is able to carry several different binding sites for various ligands, which are usually located in the variable loops region.^{214,215} A short overview of the different groups of PH domains is given here, since the associated functions might also be relevant for NF1-PH: Classic PH domains are mainly PIP binders of varying specificity and affinity for single PIPs. While some of them bind strong enough to localize the host protein to a membrane upon the availability of one specific target PIP, others are only capable of doing so in cooperation with additional domains and lack the stringent PIP specificity (dual-key strategy²¹⁶). It is noteworthy, that such a cooperative mode of action has the features of a logical AND switch, allowing localization only if all required ligands are present simultaneously. In return, this means that each combination of domains is specific for a certain membrane microenvironment and/or the occurrence of defined signaling events.^{206,217–223} Phosphotyrosine binding domains (PTB) can bind simultaneously to PIPs and proteins with an Asn-Pro-X-Tyr (NPXY) motive, often requiring phosphorylation of Tyr. Subgroups of PTB domains include Shc-, IRS- and Dab-like protein modules, mostly found in proteins functioning as adaptors or scaffolds in signal transduction pathways.^{214,224–227} Also polyproline helices can be bound by PH domains, which is typical for enabled / VASP homology 1 (EVH1)-, Wiscott-Aldrich syndrome proteins (WASP) and homer-vessel scaffold proteins. EVH1 proteins are multidomain modulators of actin cytoskeleton dynamics,^{197,228} while WASP proteins are scaffolds coupling several signaling pathways with the Arp2/3 actin filament nucleation complex.²²⁹ Homer-Vessel proteins are found in excitatory synapses and are involved in memory formation and long term potentiation.^{228,230} The last group of protein modules with a PH fold are Ran binding domains (RanBD), which are components of the nucleocytoplasmatic transport system and help to dissociate and recycle Ran-GTP importin / exportin complexes.^{214,231,232} It should be noted that some PH domains do not count to the above mentioned

groups and were only identified after structure determination like in Neurofibromin. An example is the PH domain of TFIIH, which is important for nucleotide excision repair.²³³

The crystal structure of the NF1-Sec domain of Neurofibromin shows a similar fold like other CRAL-TRIO containing protein modules,^{84,200,212,213,234} with the amphipatic helix (lid helix) blocking the entry to the lipid binding cage.²³⁴ Inside, a Triton X-100 molecule is located which is a detergent from the purification process. The NF1-PH domain is closely interacting with the NF1-Sec domain and has besides its normal PH fold an additional β -protrusion (lock) inserted between the strands $\beta 3$ and $\beta 4$. This β -protrusion folds in the crystal structure on top of the lid-helix and would prevent an opening movement if inflexible. Such a close interaction between a Sec14- and PH-domain is uncommon and was not reported previously, suggesting that the combination of these two domains generates a novel functionality. Mutational analysis in combination with PIP binding assays showed furthermore a second binding site for PIPs at the lid - lock interface, composed of residues provided by both Neurofibromin domains.⁸⁴

3.5 Current situation and goals

Recently, we could crystallize and determine the structure of a Neurofibromin fragment next to GRD, containing a Sec14-like and an unpredicted PH domain. Inside the NF1-Sec lipid binding cage, a triton-X100 detergent molecule from the purification process was bound, replacing any previously contained cellular ligand. Furthermore, binding of the module to phosphorylated PtdIns (PIPs) was shown with a fusion-tag based assay and the binding site mapped by mutational analysis. Also first localization experiments were done in several cell lines, but without a clear result.

The main aim of this thesis is to address the question which role

the Nf1-SecPH module plays in context of the Neurofibromin protein. Suggestive possibilities include that NF1-SecPH provides membrane association or works as a lipid sensor affecting the GAP activity, it however might also serve another purpose. To address this questions, a number of points require clarification:

- What is the function of the NF1-Sec lipid binding cage ?
- Is there a regulatory interaction between the NF1-Sec and NF1-PH domain ?
- What alterations are caused by patient derived missense mutants ?

Therefore, the thesis work will focus on the further characterization of the NF1-SecPH module utilizing biochemical and structural methods with a special emphasis on the various missense mutations observed in patients.

4 Results and discussion

4.1 Improved overlay assays and PIP binding

4.1.1 New tools: the α NF1-SecPH antibody

Although a number of assays could be performed so far with tagged NF1-SecPH protein, several problems were associated with this setup. The combination of His-Tag, GST (glutathion-S-transferase)-Tag and TEV (tobacco etch virus) cleavage site adds about 250 aa to the protein in question, which can lead to the obstruction of binding sites or the impairment of biological activities, thereby generating false negative results. Furthermore, we observed the appearance of false positive signals while detecting the fused protein with α GST antibodies, which was caused by the combination of His- and GST-Tag. While this problem could be partly addressed by switching to a GST-tag, still the question remained if the additional domain does not falsify or impair the binding properties of NF1-SecPH (Igor D'Angelo, PhD thesis).

To establish a detection system for NF1-SecPH that circumvents the problems associated with fusion tags, α NF1-SecPH antibodies were raised in rabbits (animal handling by EMBL laboratory animal resources, (LAR)) and purified by means of a custom made NF1-SecPH affinity column. Typically 0.7 mg of antibody could be obtained from 5 ml of serum. The functionality of the antibody was

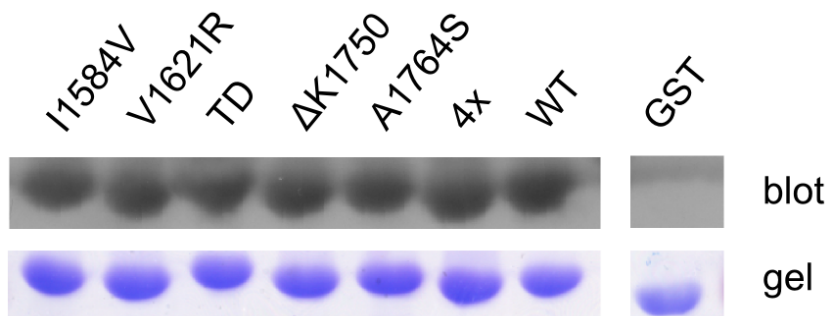


Fig. 4-1: Gel with several variants of NF1-SecPH and westernblot of the gel detected with Rabbit α NF1-SecPH / Goat α Rabbit-HRP (Sigma-Aldrich), ECL kit and autoradiography film (GE Healthcare). See 4.5 (p. 58) for mutants.

verified by westernblot experiments (fig. 4-1), and shown to recognize also a number of mutant versions of the module as well as the full length Neurofibromin protein (not shown, personal communication with Jeanette Seiler, EMBL).

4.1.2 Overlay assays and the PIP binding Site

Given the complicated regulatory mechanisms controlling the localization of Ras in the cell,¹²⁵ it is suggestive that Neurofibromin might have membrane targeting activities as well. Since a number of classical PH domains are known to support membrane association of their host protein,²¹⁷ NF1-SecPH was tested for such an activity by assessing its PIP binding abilities. Due to the availability of the new α NF1-SecPH antibody, it was possible to perform lipid-protein overlay assays with tag-free protein, excluding the previous problems with false positive (fig. 4-3 e)) and -negative signals.

For the assays, PIP-StripsTM, Spingo-Strips and PIP-ArraysTM from Echelon biosciences as well as custom made lipid arrays from Oriol Galego (EMBL Heidelberg) were used. In short, a lipid binding protein becomes attached to the immobilized lipids on the membrane and is still present after several wash steps. Detection is done with Rabbit α -NF1-SecPH and Goat α Rabbit-HRP (horseradish peroxidase) antibodies, followed by visualization with a chemiluminescence reaction and autoradiography film (fig. 4-2).

Before satisfactory results with the protein-lipid overlay assays could be obtained, a number of optimization steps had to be established.

- The replacement of fat free dry milk powder (FFDM) against fatty acid free BSA (Bovine serum albumin) was necessary, since FFDM completely blocks both, membrane and lipids (fig. 4-3 f)).
- Reduction of the high initial background to noise ration could be achieved by using the more sensitive ECL PlusTM- instead of

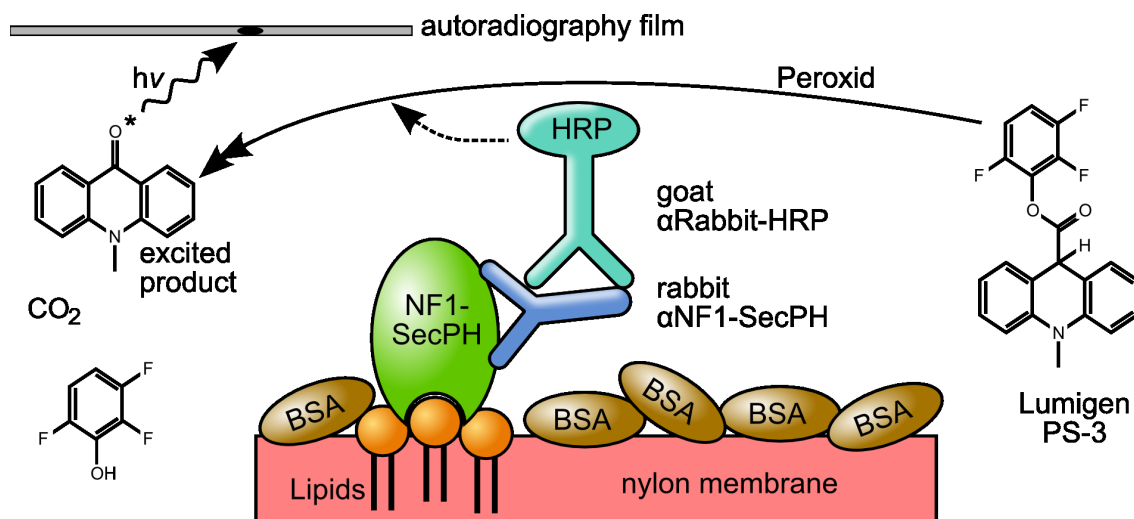


Fig. 4-2: PIP-StripTM assays. Lipids are spotted onto a nylon membrane, which is blocked with BSA before the experiment. While lipid binders become immobilized on the membrane, non-binders are removed in subsequent washing steps. Detection is done via rabbit α -NF1-SecPH and goat α -Rabbit-HRP antibodies followed by ECL visualization. In several reaction steps, Lumigen PS-3 is broken down to CO₂, a fluorinated phenol derivative and excited 9-hydro-10-methyl-9-oxoacridine, which is catalyzed by HRP in the presence of hydrogen peroxide and solvent. Upon decay of the excited state, 9-hydro-10-methyl-9-oxoacridine emits a photon which blackens the autoradiography film.²³⁵

the ECL kit (fig. 4-3, a) vs. f)).

- For some protein variants it was also necessary to perform the experiments at low temperature for a good signal to noise ratio (fig. 4-3, g)).
- Further parameters to be considered were to avoid multiple freeze-thaw cycles, the pH value and a very quick buffer exchange to prevent exposure of the membrane to air.

As displayed in fig. 4-3 a),b),d), NF1-SecPH binds only to phosphorylated PtdIns derivatives and sulfatide, with a preference for monophosphorylated PIP species. Although only PIPs are bound, the precise position of the charged group seems to have a rather weak effect on ligand binding. Similar to PIPs, also the galactolipid sulfatide contains a ring-structure with an attached charged group, here sulfate instead of phosphate, suggesting some adaptability of the binding region.

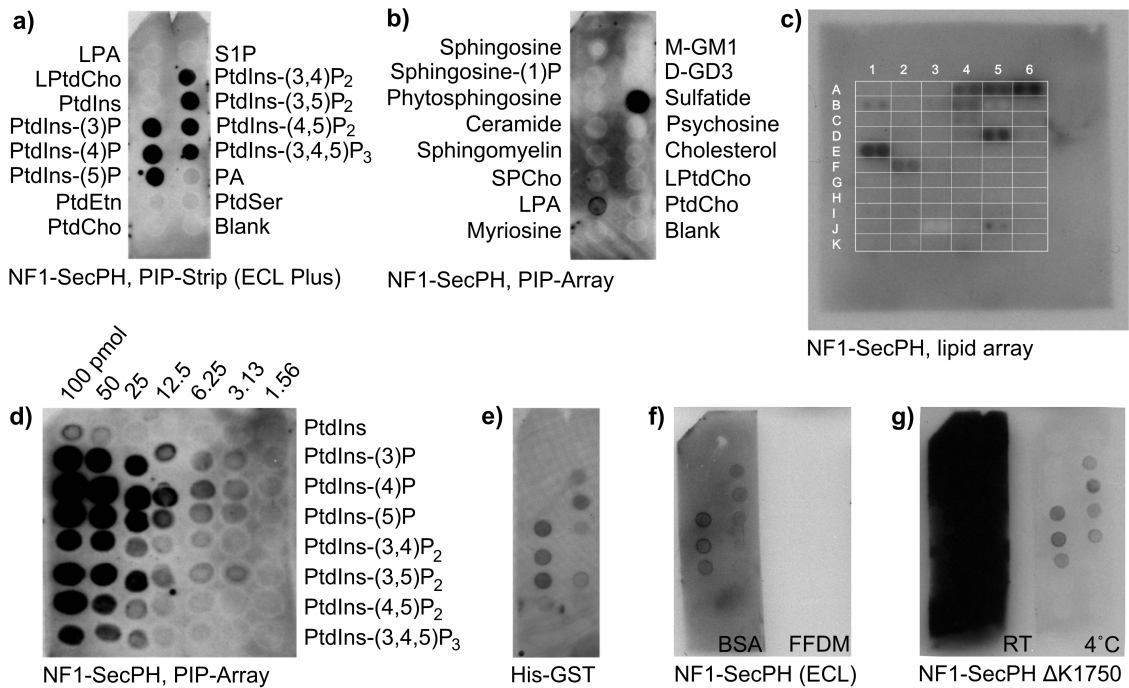


Fig. 4-3: Lipid protein overlay assays, see text for discussion of the results. **a)** PIP-StripTM with NF1-SecPH, membrane blocked with BSA, incubation at 4°C, detection with ECL PlusTM kit. **b)** Sphingo strip with NF1-SecPH, conditions like a). **c)** Lipid array with NF1-SecPH, produced by Oriol Galego (EMBL Heidelberg, annotation see appendix p. 97, treated like a). **d)** PIP-ArrayTM, conditions like a). **e)** PIP-StripTM with His-GST only, showing a false positive result. (BSA blocking, αGST, ECL detection). **f)** PIP-StripsTM with NF1-SecPH. Comparison of blocking reagents. On the left side BSA was used and on the right one fat free dry milk powder (FFDM). Detection with ECL kit. **g)** PIP-StripsTM, the temperature at which the assay is performed can change the signal to noise ratio for some proteins dramatically. Here, NF1-SecPH ΔK1750 was used for the assay at room temperature (RT, left side) and at 4°C (right side). For detection, the ECL PlusTM kit was used. **Abbreviations:** phosphatidic acid (PA), lyso-PA (LPA), Lyso-PtdCho (LPtdCho), sphingosin-1-phosphate (S1P), sphingosylphosphorylcholine (SPCho), monosialoganglioside-GM1 (M-GM1), disialoganglioside-GD3 (D-GD3)

Comparison of the GST-based detection with the tag-free system shows an overall similarity but also some visible differences: In contrast to the older system, a PtdIns-(3,4,5)P₃ signal is clearly visible while the previously observed PtdEtn and PtdSer signals (Igor D'Angelo, PhD thesis) are completely absent in the tag-free system. Although the GST-based detection system brought already a large increase of signal quality, the presence of the fusion tag still seems to somehow distort the outcome of the experiment. Since GST alone shows no lipid binding (Igor D'Angelo, PhD thesis), the interplay between NF1-SecPH and GST seems to permit an interaction with Ptd-

Etn and PtdSer. This could either mean that a further mutually provided binding region is present or that GST alters the NF1-SecPH lipid binding activity, which is in light of the diminished PtdIns-(3,4,5)P₃ binding signal more probable.

Lipid arrays revealed in addition to the previous results binding to Sphinganine-1-phosphate (Sn1P) and Phyto-Sn1P (PSn1P) (fig. 4-3 c)), but show also some discrepancies to the commercial strips regarding PtdIns-3-P₁ and Sphingosin-1-phosphate (S1P; fig. 4-3 compare c) with a),b)). Further experiments are necessary to verify this observations, especially since S1P shows clearly no interaction in commercial strips and differs by only one double bond from Sn1P.

The mutational analysis of the NF1-SecPH lid-lock interface is in good accordance with the GST-based detection system. As shown in fig. 4-4, PIP binding is completely abolished if the four residues K1670 - R1674 - R1748 - K1750 (fig. 4-5) are changed to alanine and strongly impaired for the double mutants K1670A - R1674A, R1748A - K1750A and R1666A - K1670A (not shown). Since the binding patterns of the double mutants indicate weaker interactions but do not change compared to wildtype NF1-SecPH, it seems that the absence of one residue can be partly compensated by others. These results clearly demonstrate that the PIP binding patch of NF1-SecPH is located in the interface region, containing residues from both the NF1-PH and NF1-Sec domain (fig. 4-5).

Besides the wildtype protein, a number of NF1-SecPH constructs containing patient derived mutations (see below) were analyzed for lipid binding properties, which would suggest a connection to the pathogenesis of NFI. The results of the overlay assays are depicted in fig. 4-6 and 4-7, showing mainly the same pattern as the wildtype protein except for Δ K1750 which has an overall weaker signal in PIPStripsTM and lipid array experiments. The deletion corresponds to the results of the mutational analysis and is comparable to the effect of the double mutants (K1670A - R1674A, R1748A - K1750A, R1666A - K1670A).

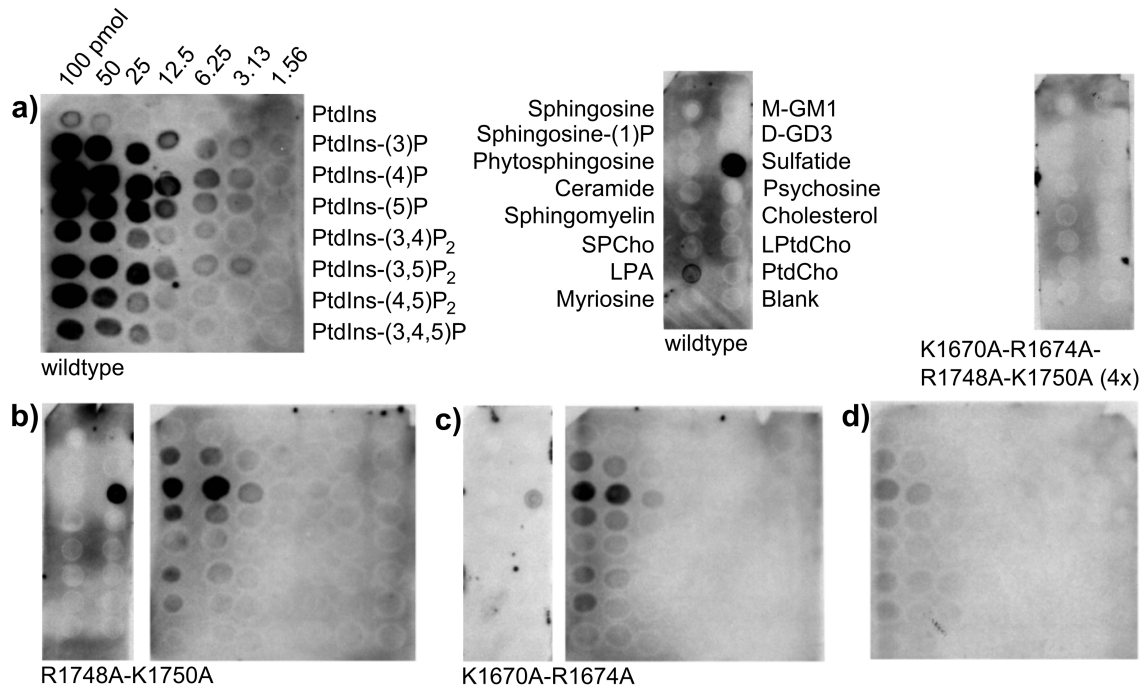


Fig. 4-4: Identification of the PIP binding site by mutational analysis. **a)** NF1-SecPH **b)** R1748A-K1750A **c)** K1670A-R1674A **d)** R1748A-K1750A-K1670A-R1674A (4x). For abbreviations see fig. 4-3

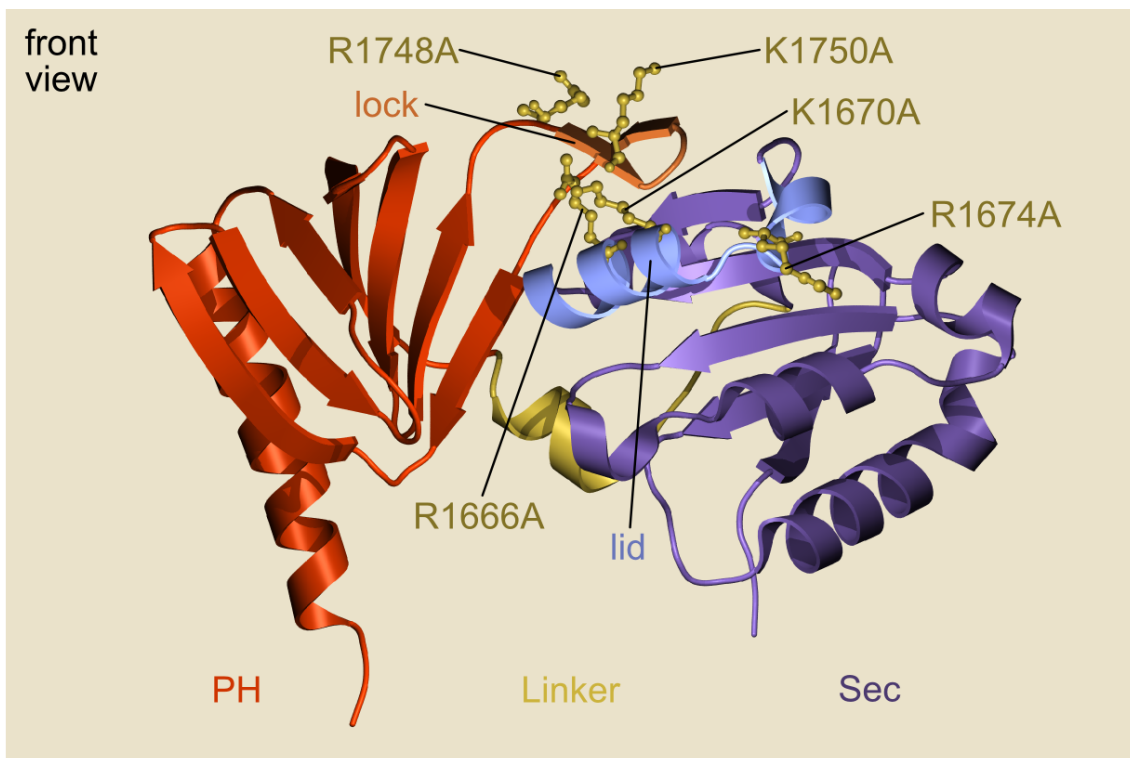


Fig. 4-5: Residues in the lid - lock interface region which are necessary for PIP binding (compare with fig. 4-4).

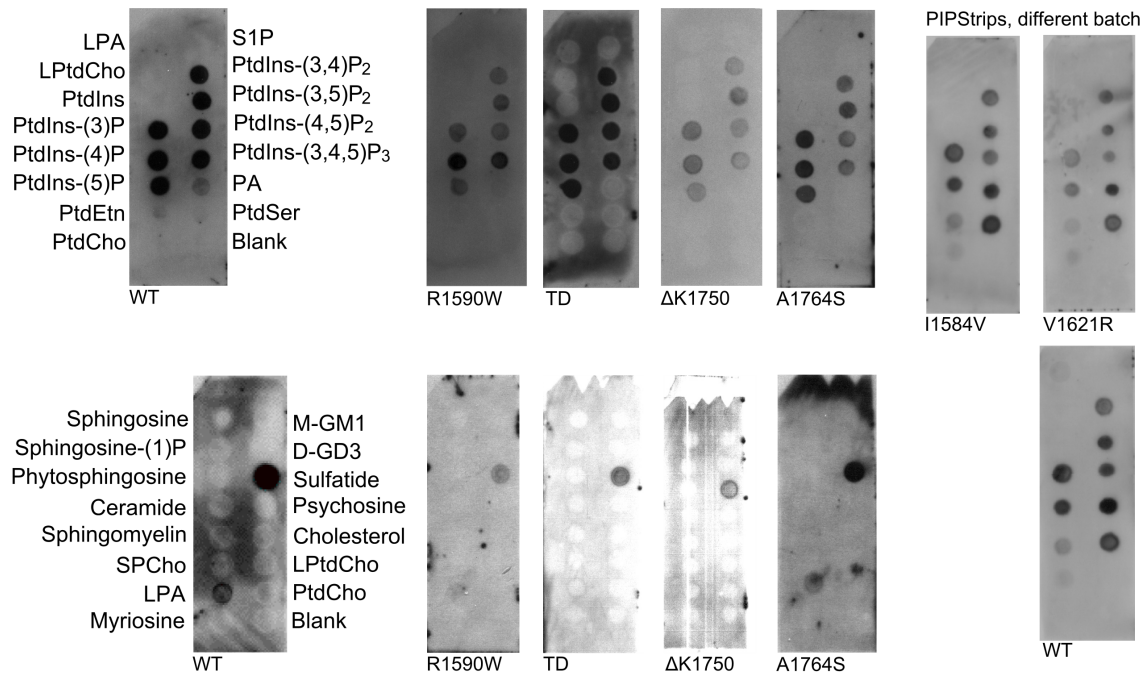


Fig. 4-6: PIPStrip™ experiments with different patient derived mutants of NF1-SecPH. The patterns of the mutants do not vary from the wildtype, except Δ K1750 which shows a weaker binding like the twofold mutations also located in the lid - lock interface region (fig. 4-3). On the right side, the mutations I1584V and V1621R show switched signals for PA and PtdIns-(5)P which is probably a manufacturing problem (see text).

Although NF1-SecPH seems not to have a high specificity for defined phospholipids, it can still contribute to a multivalent membrane association activity of the full length protein and the specificity of such an interaction towards a special membrane environment.^{206, 216, 217} Notably a number of small GTPases act as co-receptors together with PIPs to recruit GAP and GEF proteins to specific membrane subcompartments, which could also be imagined for Neurofibromin. However, since the remaining patient derived mutants do not show significant effects on PIP binding, it is likely that either an additional activity is present in NF1-SecPH or PIP binding is only part of a more complicated feature of the module. In this context, the special position of the PIP binding region could play a role, since it bridges the NF1-Sec α -helix which blocks access to the lipid binding cage and the closely interacting NF1-PH protrusion. A movement of both elements seems to be necessary for NF1-Sec to adopt an open conformation like the one in Sec14p²⁰⁰ or α -TTP,²³⁴ which the PIP ligand could prevent

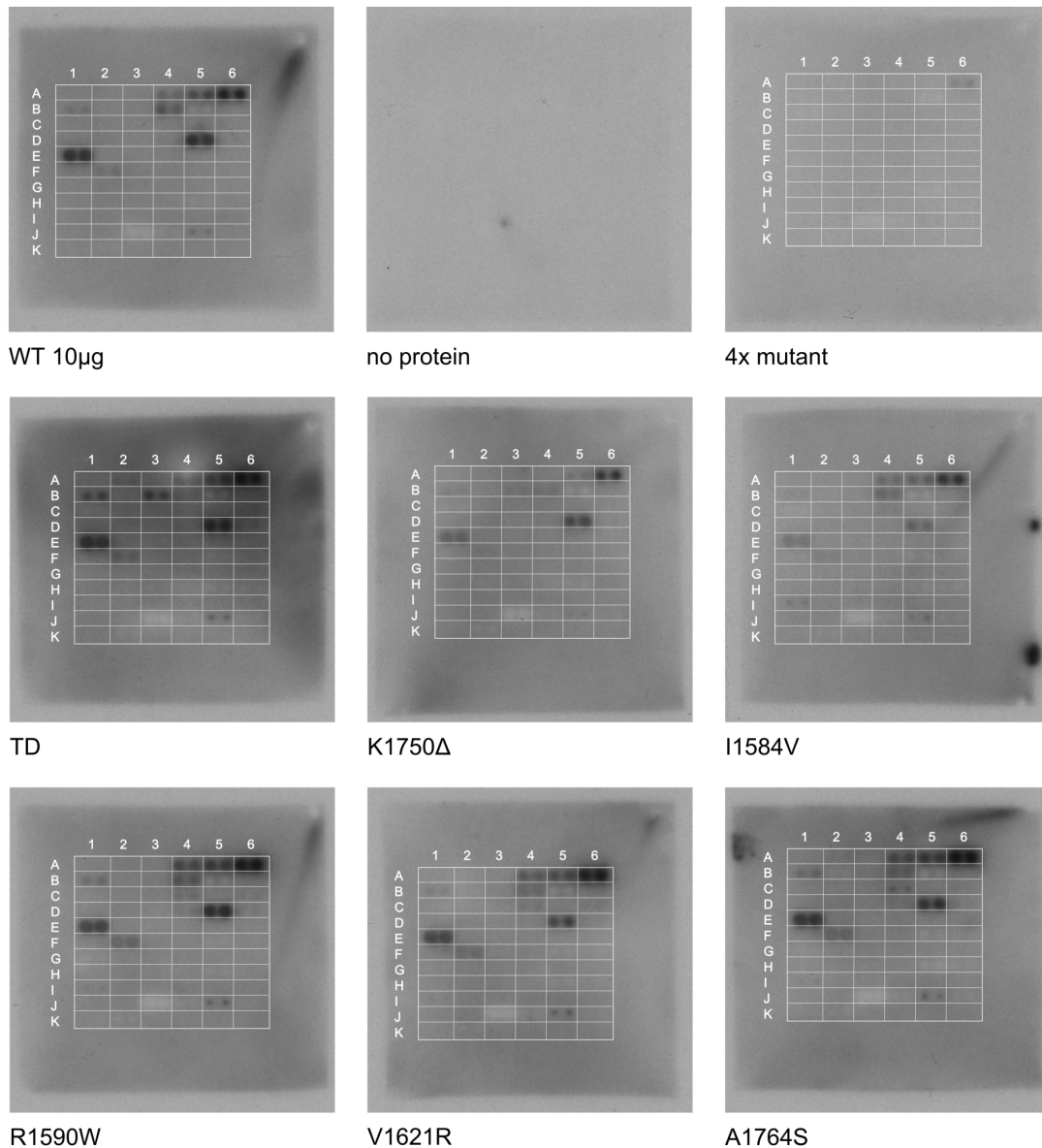


Fig. 4-7: Lipid Arrays with different patient derived mutants of Nf1-SecPH, showing similar results for wildtype and mutant proteins. The fourfold mutation K1670A - R1674A, R1748A - K1750A (4x) shows in consistence with previous results no binding to PIPs at all. Δ K1750 displays diminished binding signal like in PIPStripTM experiments fig. 4-6

by sticking helix and protrusion together. In this context, questions remaining open include whether the lipid binding cage is accessible at all, what kind of ligands could be accommodated in the cage and the effect of PIPs on such an activity.

Strangely, the PIPStripsTM of I1584V and V1621R (fig. 4-6) show switched signals for PA and PtdIns-(5)P. Since these mutants were investigated with a separate batch of PIPStripsTM and the wildtype control shows the same discrepancy to older results, there might have

been a problem in the manufacturing of this batch like a wrong spotting order. Previous PIPTripTM results were repeated many times (for WT $n > 20$) with different batches, never showing any variations. An appearance of a new dot, like here for PA, could eventually be explained with improved manufacturing procedures leading to increased stability of the immobilized lipid, but the disappearing of the PtdIns-(5)P signal while all other phosphorylated PIPs still bind lacks an explanation. Although these experiments should be repeated, the results from this batch are at least comparable with each other and do not show differences between the wildtype and the mutant binding patterns, indicating similar lipid binding properties. Also in the lipid array experiments, no differences in the ligand binding behavior between the wildtype, I1584V and V1621R is visible. The manufacturing of self spotted lipid strips was tried once in our group, but for small charges the storage of lipids and strips is problematic as well as the reproducible handling of the volatile organic lipid solutions. In case of the custom made lipid arrays, this problems could be circumvented since a special robot was used to fabricate large amounts of arrays for immediate use.

4.2 Assessment of typical PH- and Sec14-domain activities

4.2.1 NF1-SecPH does not bind phosphotyrosine

Although, protein-lipid overlay experiments showed clear binding signals for PIPs, the identity of a physiological ligand of NF1-SecPH is still not clear. Another group of protein modules containing a PH-like fold are the phosphotyrosine (pTyr) binding (PTB) domains, classical representatives of which usually have two separate binding sites, one for pTyr containing NPXY motifs and a second one for PIPs. Many proteins containing PTB domains are scaffolds or adapters which contribute to the organization of signaling complexes, affecting for example neuronal development.^{214, 224–227} Since pTyr has in addition some

similarity to PIPs and sulfatide in terms of a ring-structure which is decorated with a charged group, NF1-SecPH was assessed for pTyr binding capabilities.

To address this activity, the most meaningful experiment would be a large scale interaction screen with a combinatorial set of different phosphotyrosine NPXY motives, to elucidate not only the binding capability but as well the sequence specificity. Since the implementation of this experiment requires a considerable effort, a pilot experiment investigating the ability of NF1-SecPH to bind to phosphotyrosine alone was done first. Measurements with isothermal titration calorimetry (ITC) showed clearly no interaction between the two molecules, as displayed in fig. 4-8. Therefore, it seems to be unlikely that NF1-SecPH binds to phosphotyrosine NPXY motives and no further experiments were performed in this direction. Apparently the aromatic character

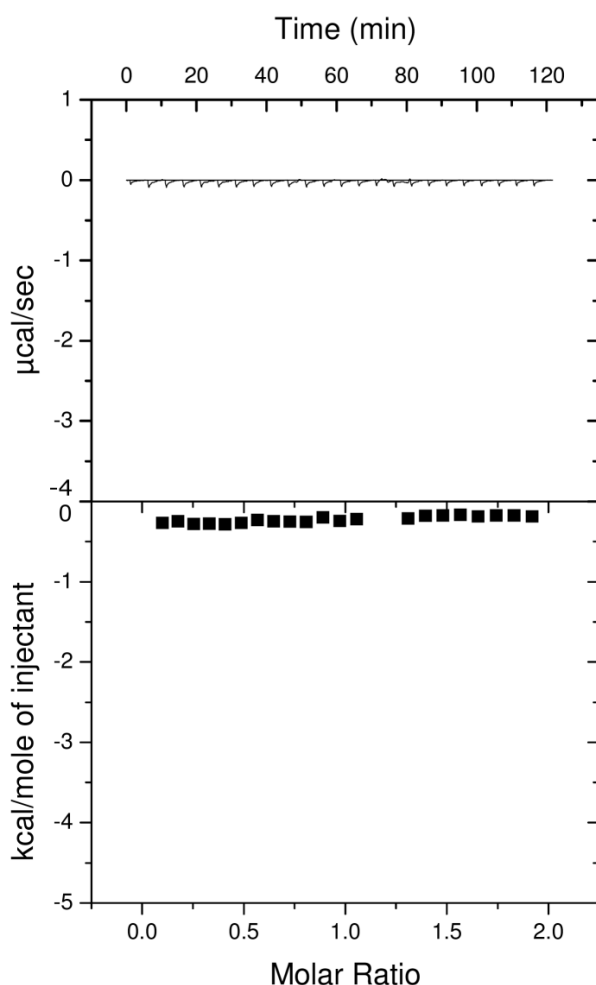


Fig. 4-8: Isothermal titration calorimetry (ITC) measurement with NF1-SecPH and phosphotyrosine. In the upper window, the heat generated upon injection of phosphotyrosine is plotted as $\mu\text{cal} / \text{sec}$ against time. The lower window displays the observed values as binding curve, with $\text{Kcal} / \text{mole}$ of injectant plotted against molar ratio. Clearly, no interaction between the two molecules is visible.

of the phosphotyrosine residue with the accompanying steric consequences is not compatible with the NF1-SecPH PIP binding region.

4.2.2 Localization studies in life cells

Since protein-lipid overlay assays show that NF1-SecPH binds PIPs, cellular localization experiments were performed to assess if the protein module can associate with membranes in life cells. As outlined previously, the motivation for this experiments is that Ras localizes to distinct subcellular membranes,^{125,126,208,236} which suggests that regulators of Ras might attach to membranes as well in order to interact with their target protein. Both NF1-Sec and Nf1-PH are potential candidates to exert such activities, which can include the binding to lipids, other membrane attached proteins or binding in cooperation with other domains from the same protein.^{206,215,217–219,221–223,237–239}

The localization experiments continue previous studies (PhD thesis, Igor D'Angelo), which did not reveal a specific localization of GFP/YFP (green/yellow fluorescent protein) fused Neurofibromin fragments in monkey fibroblasts, neuroblastoma- or HeLa cells. However, possible complications which can occur in such a setup include the competition of non-labeled endogenous Neurofibromin protein for rare interaction partners or the absence of an appropriate exogenous signal. To circumvent this problems, the localization of some of these constructs was assessed in Schwann cells deficient for Neurofibromin (NF96.2, american type culture collection (ATCC)) and in NIH 3T3 mouse fibroblasts, which can be stimulated with platelet derived growth factor (PDGF) resulting in plasmamembrane localization of some proteins.

One or two days after transient transfection of NF96.2 cells with GFP tagged Neurofibromin fragments including NF1-GRD-SecPH, NF1-SecPH, NF1-Sec and NF1-PH, the localization of the protein was observed in life cells by confocal microscopy under controlled temperature and CO₂ conditions. For all constructs, only a diffuse staining of the whole cell could be observed, similar to control experiments with

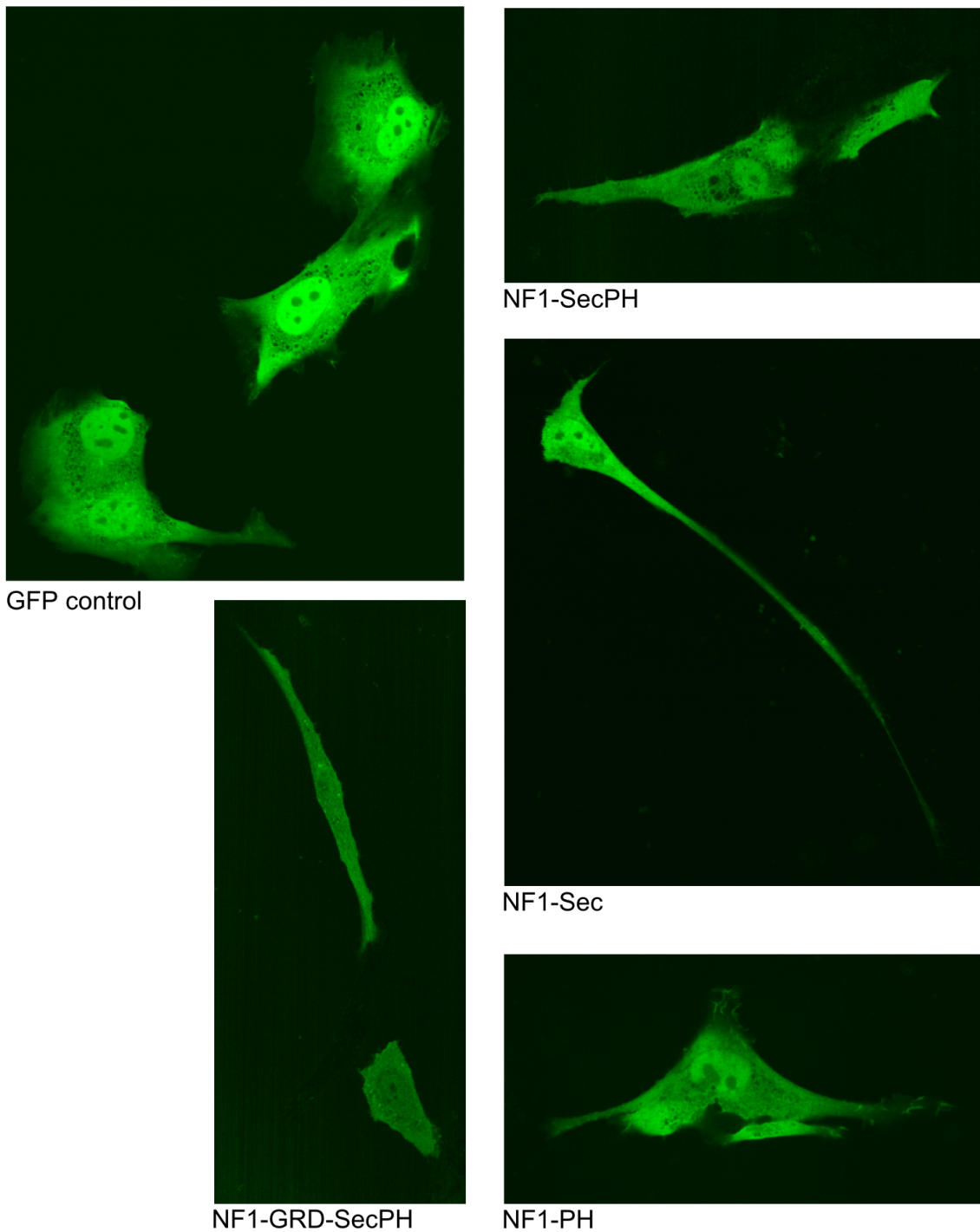


Fig. 4-9: Localization experiments with different neurofibromin constructs including NF1-GRD-SecPH, NF1-SecPH, NF1-Sec and NF1-PH, which are N-terminally fused to GFP. The experiments were done by confocal microscopy (60x magnification) of life cells in a controlled environment (37°C, 5% CO₂) two days after transient transfection of Neurofibromin constructs. For this experiments, the Neurofibromin deficient Schwann cell line NF96.2 from ATCC was used, to prevent competition between the GFP-labeled protein and endogenous Neurofibromin. All constructs as well as the GFP control show a diffuse, uniform staining of the cells, not indicating any specific localization.

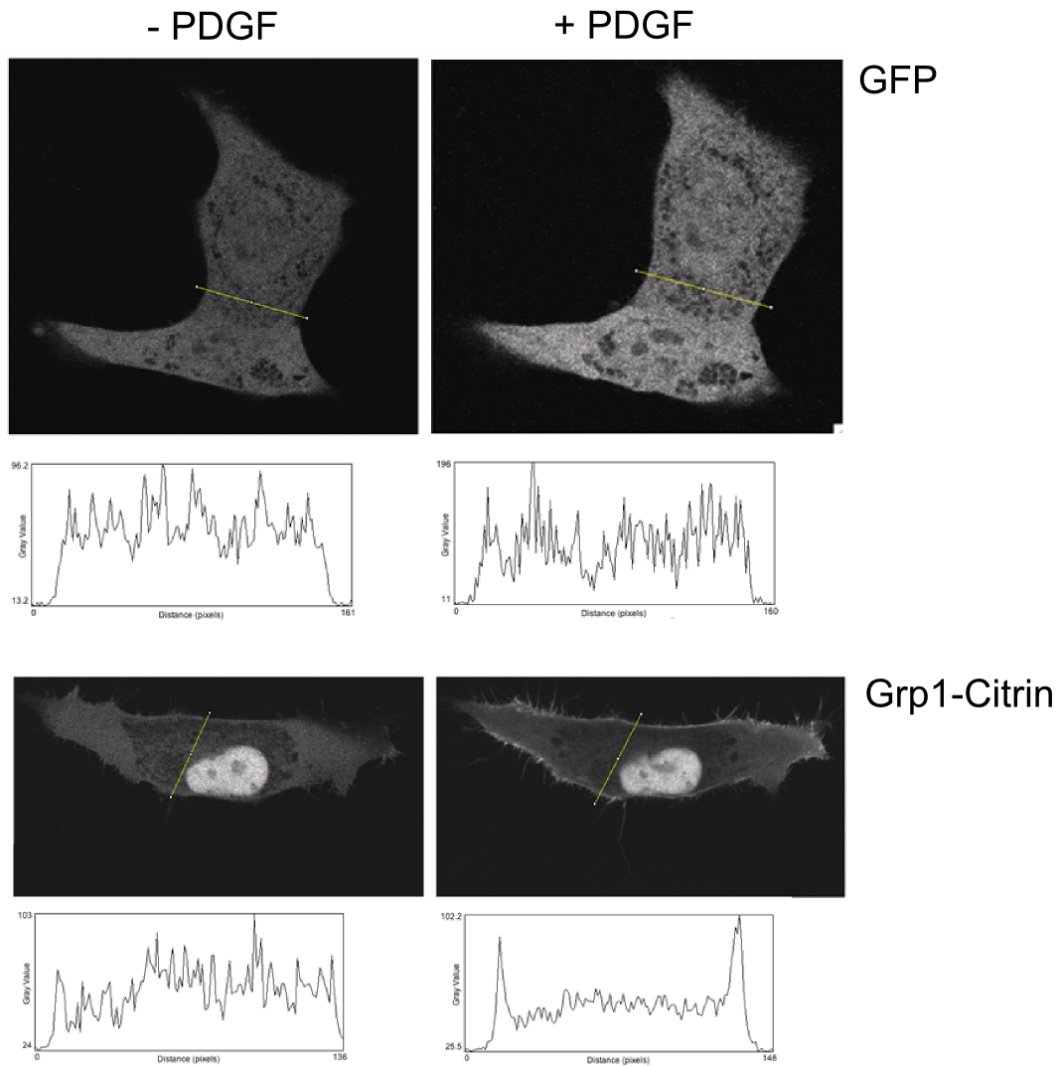


Fig. 4-10: Positive and negative control experiments for PDGF stimulation experiments with NIH 3T3 mouse fibroblast. The upper row shows cells expressing GFP before (left) and after stimulation (right) with PDGF ($100\mu\text{M}$ final concentration). As expected, no differences are visible, also shown by histograms (below) displaying the pixel intensities along the yellow line. In contrast, a clear plasma membrane localization of Grp1 is visible after stimulation (lower row, left image), also indicated by the strong peaks in the histogram (below). Imaging was done by confocal microscopy (60x magnification) with live cells in a controlled environment (37°C , $5\% \text{CO}_2$).

NF96.2 cells expressing GFP alone (fig.4-9).

NIH 3T3 cells were serum starved before imaging and observed before and after stimulation with PDGF, which increases the generation of $\text{PtdIns-(3,4,5)-P}_3$ at the plasmamembrane via activation of PI3K.²⁴⁰ While control experiments with the highly specific and strong PtdIns-3,4,5-P_3 binder GRP1 (general receptor for phosphoinositides isoform 1)²⁴¹ showed immediate localization to the plasmamembrane (fig. 4-10), the NF1-SecPH construct shows a diffuse uniform distri-

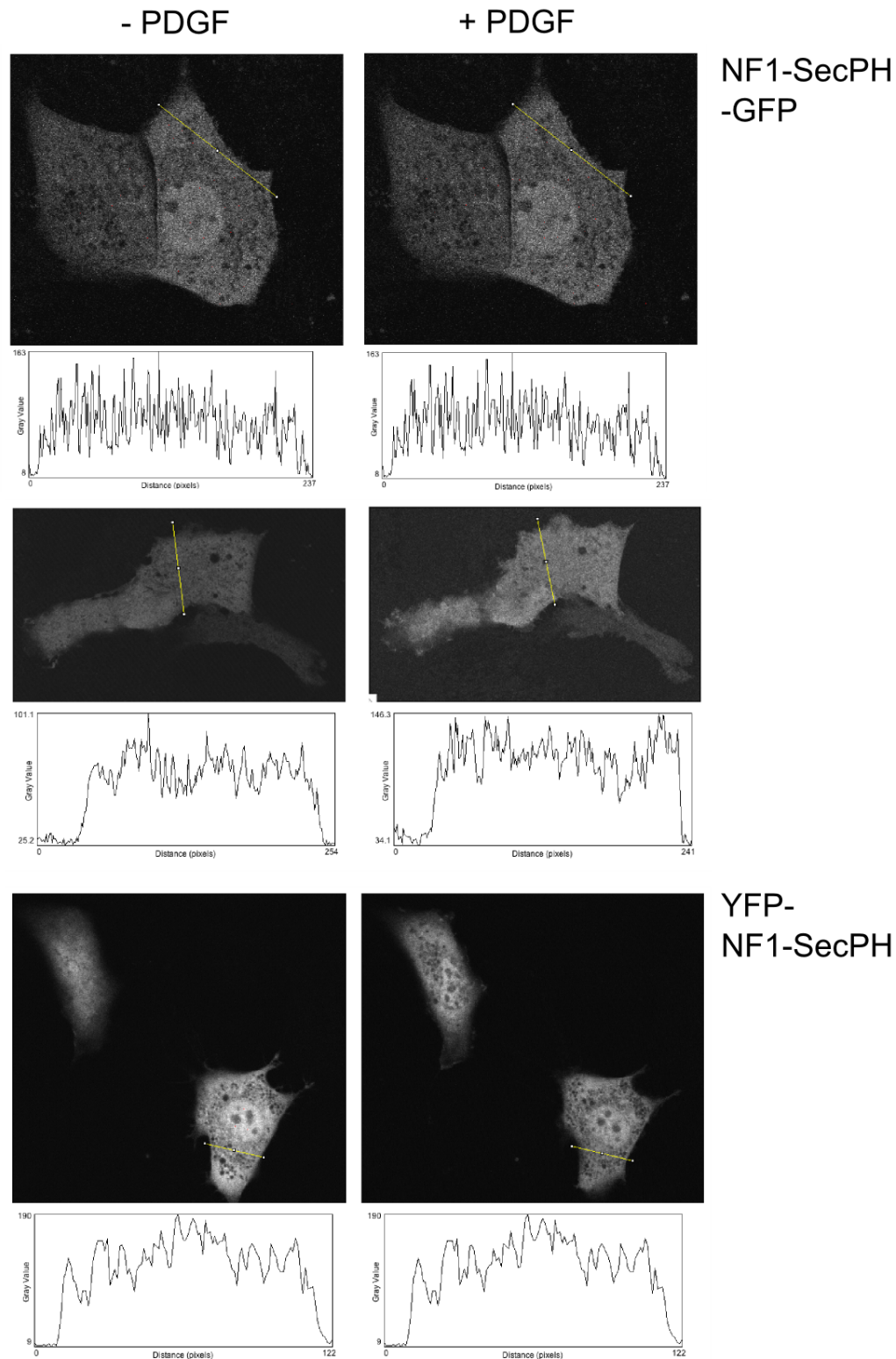


Fig. 4-11: Stimulation experiments in NIH 3T3 cells with NF1-SecPH-GFP and YFP-NF1-SecPH. A similar diffuse uniform stain of the cells can be observed before (left row) and after PDGF stimulation (right row) for both constructs (top two rows and lower row respectively). Histograms (below images) showing the pixel intensities along the yellow lines, display the observations in a quantitative way. Imaging was done by confocal microscopy (60x magnification) with life cells in a controlled environment (37°C, 5% CO₂).

bution before and after stimulation (fig. 4-11), similar to the GFP control.

Although the performed experiments do not show localization of NF1-SecPH, there are still scenarios imaginable where such an activity could have been overlooked. If the tagged fragment is strongly over-expressed and has therefore a much higher abundance than its membrane bound ligand, the few translocated proteins would not stand out against the overall stain. Furthermore, in case of low affinity binding there might be a fast equilibrium between membrane bound and free protein, differences of which would also be difficult to observe. Beside such methodological problems, the question remains whether PDGF is the right choice for stimulation experiments or if other signals are necessary to trigger membrane localization of Neurofibromin. It should be noted that other experiments in our group using full length Neurofibromin showed a diffuse uniform staining of cells, indicating that also the combination of all Neurofibromin domains does not provide a constitutive localization activity (Welti and Seiler, unpublished observation).

4.3 Structural investigation of lipid bound NF1-SecPH

4.3.1 Improved purification procedure for NF1-SecPH

The NF1-SecPH fragment was so far purified by nickel affinity chromatography, cleavage of the His-tag with TEV protease during dialysis and a second nickel affinity chromatography step. While it was possible to crystallize the protein obtained by this procedure, a Triton-X100 detergent molecule was present in the NF1-Sec lipid binding cage, replacing any previously bound cellular ligand. To characterize the interaction of NF1-SecPH with a physiological relevant ligand and analyze the structural consequences of ligand binding, a structure containing such a cellular ligand was highly desired.

To obtain protein without incorporated Triton-X100, cell lysis and

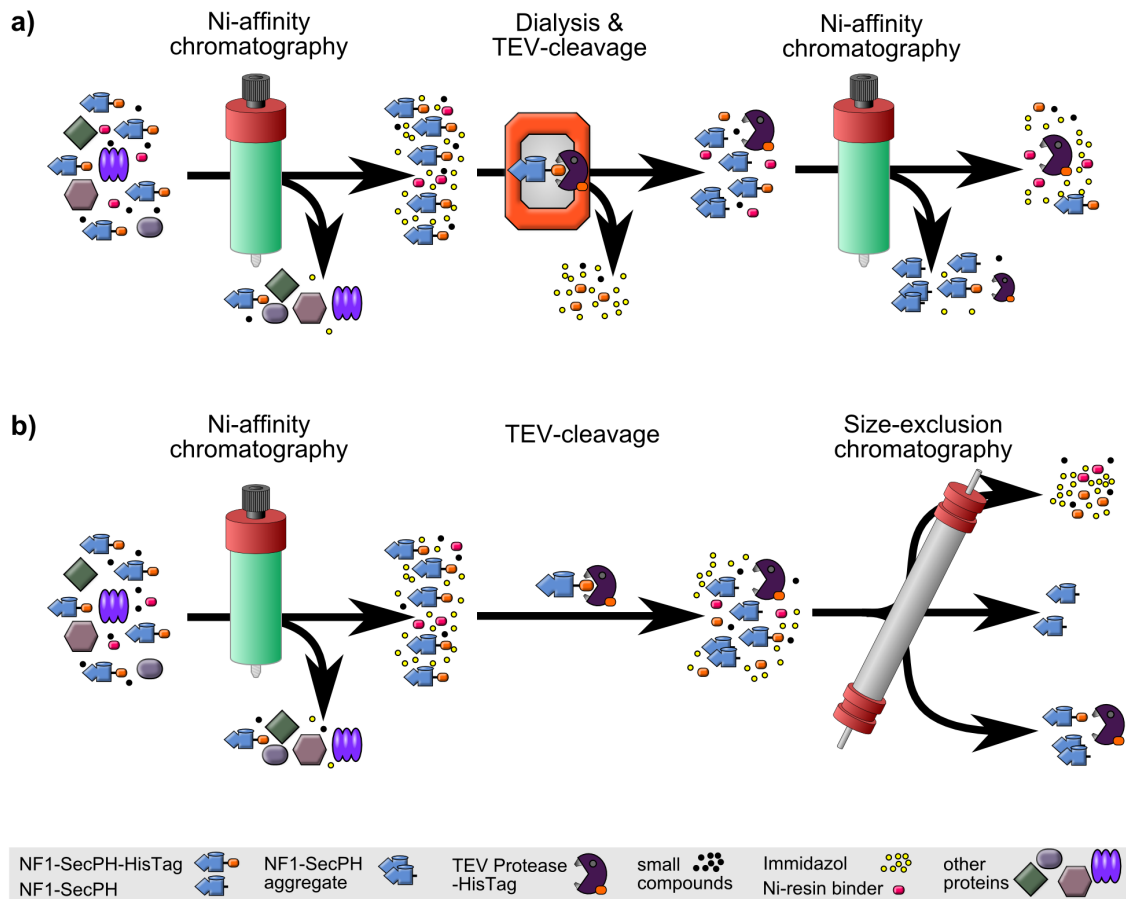


Fig. 4-12: Purification procedures for NF1-SecPH **a)** The protein is purified by Ni-affinity chromatography, cleaved with TEV protease during dialysis and further purified by a second Ni-affinity chromatography step. Traces of TEV-Protease, aggregated and uncleaved protein as well as small compounds can still be present. **b)** New purification procedure. The protein is also purified by Ni-affinity chromatography followed by TEV protease cleavage and size exclusion chromatography. The protein fraction contains usually no aggregates, TEV protease leftovers or small compounds.

all subsequent steps were performed in the absence of detergents. Although the protein purified in this way crystallized, the obtained crystals diffracted only up to 3.5 Å, which is not sufficient for a detailed characterization of a bound ligand molecule. Since already a large number of crystallization trials had been performed, improvement of the purity and homogeneity of the protein sample was considered. Therefore, the second nickel affinity purification step was replaced by preparative size exclusion chromatography, which should remove low molecular weight impurities, traces of aggregated protein and leftovers of TEV protease. Cleavage of the His-tag was carried out for 48h, with a second addition of TEV protease after 24h to obtain full cleavage of

the protein.

With the modified purification protocol, cleaved and detergent free NF1-SecPH protein and mutants could be produced for further crystallization trials with a reasonable yield (about 0.7 mg/g cells) for the wildtype protein. See materials and methods for a detailed description; the analysis of a typical purification is displayed in fig.4-13.

4.3.2 Crystallization of detergent free NF1-SecPH

After establishing the new purification procedure, crystallization of NF1-SecPH was tested in conditions where previous crystallization trials were successful with Triton-X100 bound protein but not detergent free NF1-SecPH. While screens composed of ammonium sulfate / $\text{Na}_4\text{P}_2\text{O}_7 * 10\text{H}_2\text{O}$ or PEG 4000 / $\text{Na}_2\text{Citrate}$ only resulted in protein precipitation, the combination of PEG 4000 and $\text{Na}_4\text{P}_2\text{O}_7 * 10\text{H}_2\text{O}$ lead to large single crystals (fig. 4-14) as observed for Triton-X100 bound protein.

For freezing the crystals in liquid nitrogen, a cryo-solution composed of precipitant solution and 20% ethyleneglycol was used. Diffraction experiments and data collection were performed at the European Synchrotron Radiation Facility (ESRF) in Grenoble at beamline ID14-2 under cryogenic conditions. The crystals belonged to the space group P4_12_12 as confirmed by molecular replacement (see below, Igor D'Angelo) and diffracted to a maximum of 2.5 Å, which was an improvement of about 1Å resolution compared to previous experiments. Processing of the dataset was done with XDS.²⁴² The crystallization conditions of the NF1-SecPH crystals with the best diffraction properties are summarized in table 4-1

compound	amount
$\text{Na}_4\text{P}_2\text{O}_7 * 10\text{H}_2\text{O}$ pH5.4	0.25M
PEG 4k	12.5%
MES pH6	0.10M
1.5µl protein + 0.5µl precipitant, hanging drop, 18°C	

Table 4-1: Crystallization conditions for detergent free NF1-SecPH

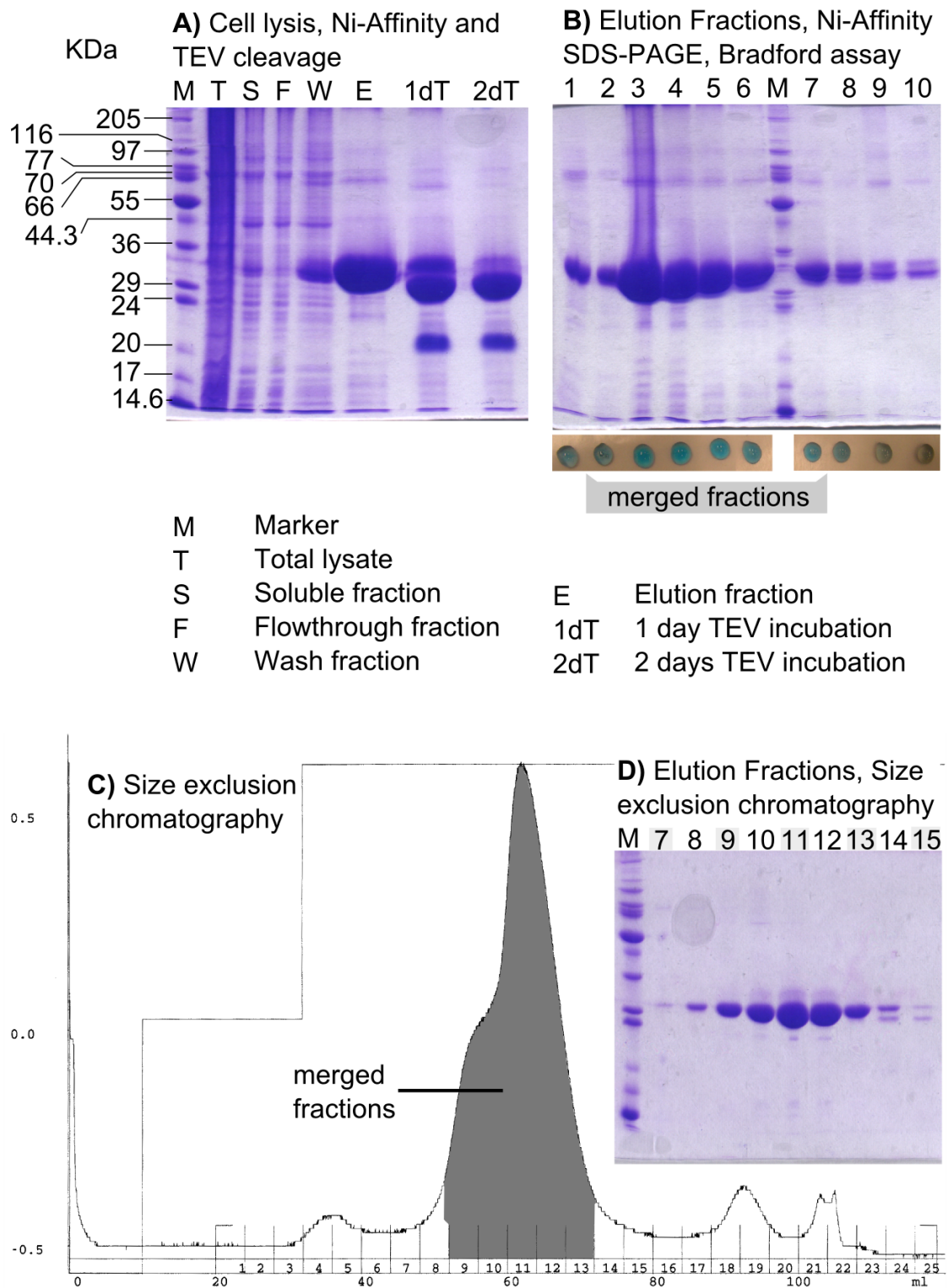


Fig. 4-13: Typical analysis of a NF1-SecPH protein purification. **A)** SDS-PAGE gel showing protein samples after cell lysis (T), ultracentrifugation (S), during Ni-affinity purification (F,W,E) and TEV cleavage (1dT, 2dT). **B)** SDS-PAGE of single elution fractions of the Ni-affinity purification and Bradford assay. **C)** Size exclusion chromatography, OD curve. The merged fractions 9-13 are indicated in gray. **D)** SDS-PAGE gel of fractions 7 - 15 of the size exclusion chromatography.

PEG 4k	Na ₄ P ₂ O ₇ * 10H ₂ O					
	0.20M	0.25M	0.30M	0.20M	0.25M	0.30M
10.0%	m-b **	↓	↓	m-b **	m-b **	s **
11.0%	↓	↓	m *	s-m ***	b *	m ***
12.0%	↓	↓	↓	m **	m-b **	m,b ***
13.0%	b *	↓	s **	↓	m-b **, ↓	s-m *, ↓
<i>1μl Protein + 1μl MS</i>			<i>1.5μl Protein + 0.5μl MS</i>			
<i>0.1M Mes pH6.0</i>						

Fig. 4-14: Crystal screens with detergent free NF1-SecPH (new purification protocol) crystal sizes: tiny (t), small (s), medium (m), large (l), huge (h), amount of crystals: 1-5 (*), 5-20 (**), 20-50(***), 50-200(****), >1000 (*****), precipitation(↓), twinned/multiple (‡), clear drop (-).

In search of crystal forms where the protein might adopt a different conformation, a number of additional robotic (EMBL Crystallization Platform Team (XTP)) and manual screens were carried out. However, despite extensive screening including the variation of surrounding conditions like temperature and experimental setup, suitable crystals could not be obtained until now.

4.3.3 Structure of glycerophospholipid bound NF1-SecPH

The structure of detergent free NF1-SecPH could be solved by molecular replacement with CNS²⁴⁵ (Igor D'Angelo) using the coordinates of the Triton-X100 containing protein module (PDB code 2D4Q) as starting model. From the initial electron density map, the final structure was obtained by alternating structure refinement and manual model building, using CNS and COOT,²⁴⁶ respectively (fig. 4-15, table 4-2). The stereochemistry of the final structure was validated with PROCHECK.²⁴⁷ In difference fourier maps, additional electron density was visible inside the NF1-Sec cage, which could be explained by a bound glycerophospholipid molecule. If superimposed, the detergent

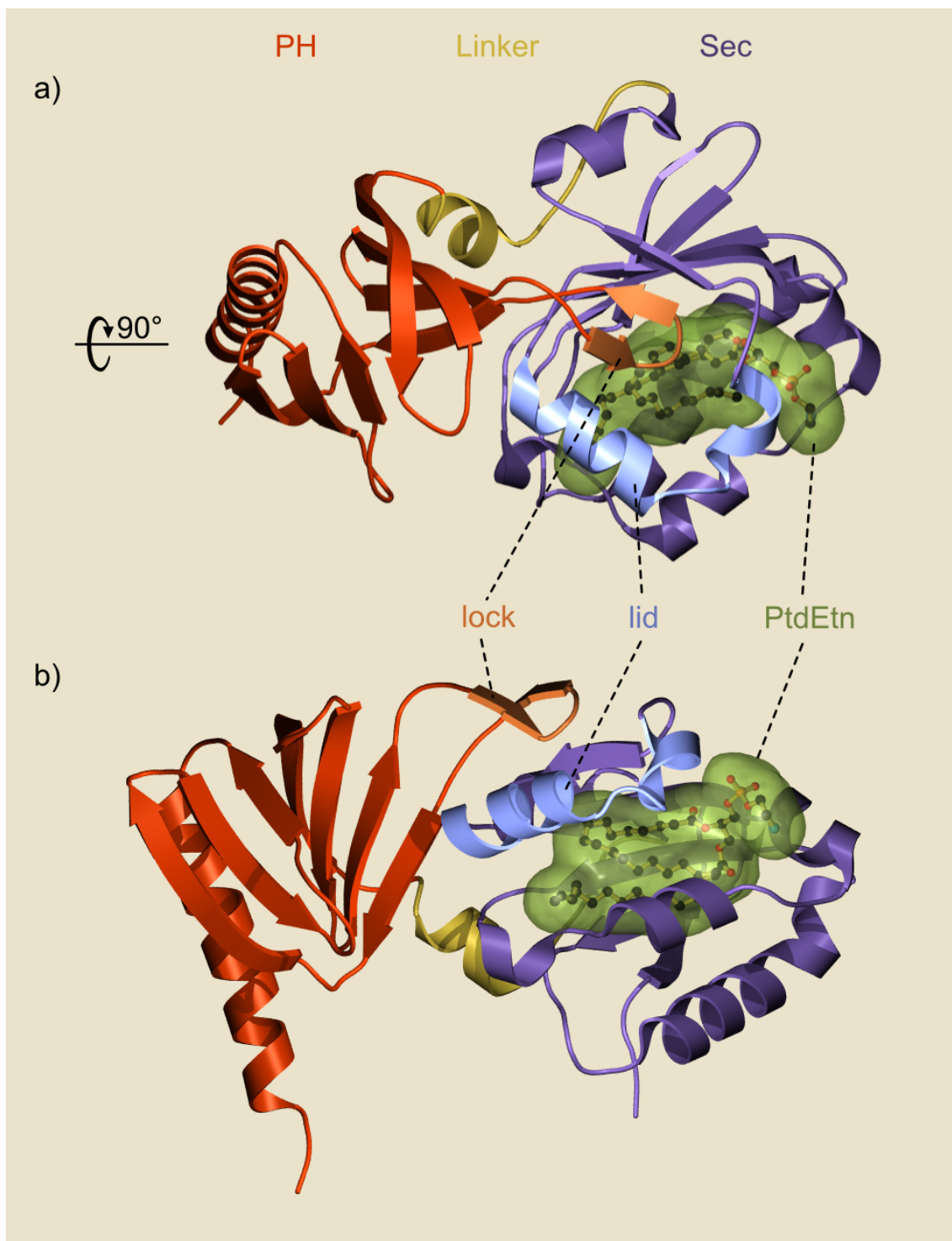


Fig. 4-15: Ribbon representation of the NF1-SecPH module. **a)** Top view, the NF1-PH and NF1-Sec domains are colored in red and violet respectively, connected by the linker region displayed in yellow. The lid-helix of the NF1-Sec domain is highlighted in blue and blocks the entry to the NF1-Sec lipid binding cage. Displayed in orange, the β -protrusion (lock) of the NF1-PH domain is closely interacting with the lid-helix. In green, the calculated surface of the 18:1(9)-16:1-PtdEtn ligand is shown, enwrapping a ball-and-stick model of the lipid (black: carbon, red: oxygen, blue: nitrogen, orange: phosphorus). **b)** Front view. Image created with POVScript+²⁴³ and POV-Ray.²⁴⁴

Table 4-2: Summary of crystallographic analysis of wildtype NF1-SecPH (from Welti et. al.¹¹²).

Data collection:	
X-ray source	ESRF ID14-2
Wavelength (Å)	0.933
Space group	P4 ₁ 2 ₁ 2
Unit cell (Å, deg)	a=b=110.1 c=121.9 $\alpha = \beta = \gamma = 90$
Resolution (Å)	2.5
Highest shell (Å)	2.5-2.6
No. of observations	198'116 (21'650)
Unique reflections	52'887 (5'687)
I/ σ	15.2 (4.1)
R _{sym} (%) ^a	7.0 (33.4)
completeness (%)	97.9 (95.4)
Refinement	
Resolution range (Å)	20-2.5
No. of reflections	49'260
R _{work} /R _{free} ^b	25.4/28.3
No.of atoms Protein	4133
No.of atoms Solvent	78
PtdEtn	2 molecules
Pyrophosphate	2 molecules
Mean B value protein (Å ²)	31.4
Mean B value ligand (Å ²)	47.5
RMSD	
Bond length (Å)	0.011
Bond angle (deg)	1.77
Ramachandran-plot	
Regions (no. residues)	
most favored	394
additional allowed	55
generously allowed	4
disallowed	1

free and the Triton-X100 bound NF1-SecPH structures show a good overlap with an RMSD of 0.8Å for 249C α atoms.^{84,112}

The overall fold of the lipid bound Nf1-SecPH module is very similar to the previous structure, showing the NF1-Sec domain which resembles a typical CRAL-TRIO lipid binding cage and the NF1-PH

domain, consisting of a β -sandwich that is capped by an α -helix. In fig. 4-15, the additional electron density inside the NF1-Sec lipid binding cage is explained with a 18:1(9)-16:1-PtdEtn glycerophospholipid ligand. The bound ligand is stabilized by hydrophobic interactions of its fatty acid tails with the cage interior as well as hydrogen bonds spanning from the lipid head group to main chain atoms of Phe1642 and the side chain of Arg1684. Arg1684 is a conserved residue in Sec14p-like domains^{83,112} and was shown to be essential for the Sec14p PtdIns transfer activity.²⁰⁰ Comparing the bent conformation of the PtdEtn fatty acid tails with alkyl-chains of other ligands found in lipid binding cages, a good agreement can be observed,^{248,249} suggesting altogether that the details of PtdEtn binding as seen in NF1-SecPH are probably a good model for such interactions in related proteins.

The NF1-SecPH module is in a closed conformation as comparisons with related structures show, with the NF1-Sec lid helix obstructing the entry point of the lipid binding cage.^{200,212,213,234} The NF1-PH domain is closely interacting with NF1-Sec, extending a β -protrusion on top of the lid helix. Interestingly, in the observed conformation the lock would block an opening movement of the lid helix due to steric hindrance,^{84,112} pointing towards a regulatory interaction controlling the access to the lipid binding cage.

4.4 Properties of the lipid binding cage

4.4.1 Identification of the bound ligands as PtdEtn and Ptd-Gro

To clarify the identity of the glycerophospholipid observed in the crystal structure, mass spectrometry (MS) analysis was performed with the detergent free NF1-SecPH protein in collaboration with Sven Fraterman (EMBL Heidelberg). By using electrospray ionization time of flight mass spectrometry (ESI-ToF MS), the lipid content of the protein could be analyzed similar to other studies.^{249,250} The result clearly

shows a peak for the protein mass alone and for different protein - lipid complexes, which associate in a 1:1 stoichiometry (fig. 4-16a). For the precise determination of the bound ligands, a lipid extraction was performed and the purified lipids analyzed by nanospray quadrupole time of flight mass spectrometry (Q-ToF MS), unambiguously identifying them as PtdGro and PtdEtn²⁵¹ (fig. 4-16b). The fatty acid part of the lipids varied from unsaturated hexadecanoic (16:0 palmitic acid) to monosaturated cis-9-octadecenoic acid (18:1(9) oleic acid).

Since each molecule has its own ionisation efficiency, the abundance of two compounds can usually not be compared on the basis of the ion intensities in a mass spectrum. Although, the ionisation efficiency of the observed glycerophospholipids is indeed quite different, this is not the case for the NF1-SecPH - lipid complexes, since this parameter depends mainly on the number of charge acceptor sites on the surface of a molecule and its radius. Based on the mass differences of about 85 Da between the observed lipid headgroups, the radii of the protein - lipid complexes can be approximated to vary only about 0.26%.²⁵² Furthermore, the analysis of unprocessed datasets showed no evidence for an influence of positively charged PtdEtn on the surface charge of the protein. The reason for this might be, that the protein engulfs the lipid ligand and isolates it from the surrounding.

Although a quantification of the single lipid species is possible by

compound	R ₁ /R ₂	m/z	compound	R ₁ /R ₂	m/z
PtdGro	18:1/18:1	773	PtdEtn	18:1/18:1	742
	18:1/16:1	745		18:1/16:1	714
	18:1/16:0	747		16:1/16:1	686
	16:1/16:1	717		16:1/16:0	688
	16:1/16:0	719		PtdEtn(² H ₃₁)	18:1/16:0
PtdGro(² H ₃₁)	18:1/16:0	778	PtdCho	18:1/18:1	844
PtdIns	18:1/18:1	861	PtdSer	18:1/18:1	786
	18:1/18:0	863			
	20:4/18:0	885			
	20:3/18:0	887			

Table 4-3: Table with the masses of glycerophospholipids¹¹² observed in the spectra of fig. 4-16.

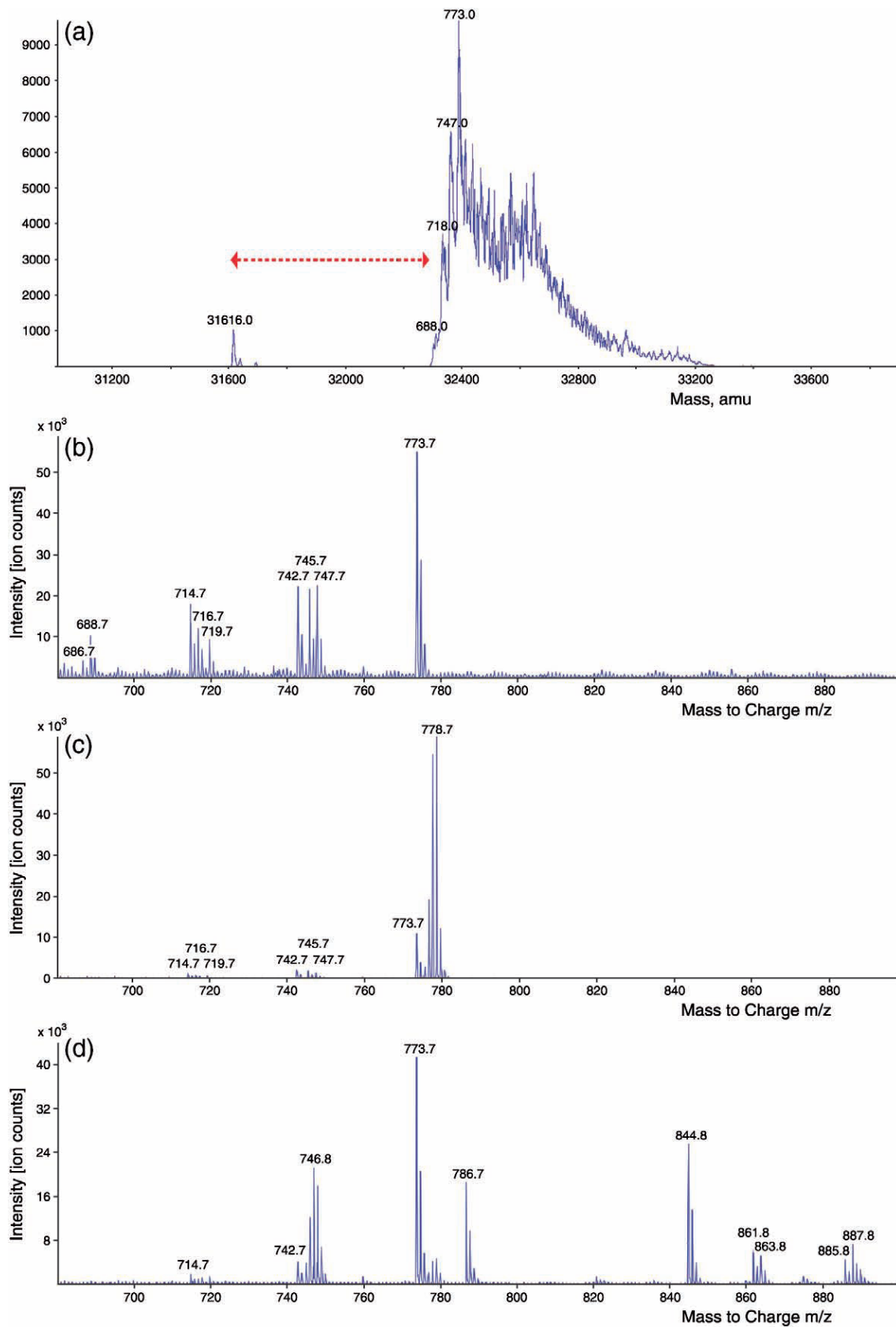


Fig. 4-16: MS analysis of NF1-SecPH.¹¹² See p. 55 for figure legend.

◀ **Fig. 4-16 (p.54): MS analysis of NF1-SecPH.**¹¹² **a)** nanospray ToF-MS spectrum of Nf1-SecPH in complex with lipids. The Protein can be seen alone ($m/z=31616.0$) and in 1:1 complexes with PtdGro (labeled as mass difference to the protein peak; $m/z=\Delta 773.0/ \Delta 747.0/ \Delta 718.0$) and PtdEtn ($m/z=\Delta 688.0$). **b)** Nanospray ToF-MS spectrum (negative mode) of lipids extracted from NF1-SecPH. The protein was expressed in *E.coli* and purified without detergents. Main binders are PtdEtn and PtdGro species (see table 4-3). **c)** Lipid content of NF1-SecPH after exchange reaction with 18:1/16:1-(²H₃₁)-PtdGro liposomes, analyzed by lipid extraction and nanospray ToF-MS (negative mode). Comparing b) and c), the deuterated PtdGro ($m/z=778.7$) has almost completely replaced PtdGro (table 4-3). **d)** Result of lipid exchange reaction with liposomes composed similar to the inner leaflet of Schwann cell plasma membranes, containing 18:1/16:1-(²H₃₁)-PtdEtn, PtdSer, PtdCho, Sphingomyelin and PtdIns. The lipids extracted from Nf1-SecPh were analyzed by nanospray ToF-MS (negative mode), see table 4-3 for peak annotation.

analysis of the complete protein - lipid complexes, this comes at the cost of limited resolution and sensitivity as well as time consuming sample preparation procedures. However, by correlation of low resolution complex spectra with the precise data obtained from lipid extract analysis, both, quantification and precise identification of the bound lipids is possible. Following this approach, the main binder of NF1-SecPH were identified as 36:2-PtdGro followed by 36:2-PtdEtn¹¹² (fig. 4-16).

Intriguingly, in none of the protein - lipid overlay assays binding to PtdEtn or PtdGro was detected, nor were PIPs detected in the mass spectrometry experiments. The reason for this apparent contradiction most probably originates from the different natures of the measurement techniques. MS measurements depend on the ionization of the measured species, which creates an environment where only ligands robustly bound inside the lipid binding cage are detected, but not transient surface binders like PIPs. In contrast, overlay assays work only if the spotted lipids remain attached to the membrane during the assay and immobilize the bound protein. Even if NF1-SecPH extracts spotted PtdEtn or PtdGro from the membrane, no signal would be visible due to the removal of the protein in the subsequent wash steps. Therefore, MS and overlay assays complement each other by addressing different activities rather than producing conflicting results.

4.4.2 NF1-SecPH has lipid exchange activity

To characterize the lipid binding cage in terms of accessibility and specificity, lipid exchange experiments were performed. For this purpose, unilamellar liposomes of various compositions were prepared by extrusion and incubated with the protein. The production of liposomes was monitored with negative stain- and cryo electron microscopy (Simone Prinz, Stephanie Kronenberg), which confirmed the unilamellarity and size of the liposomes (see fig. 4-17). Subsequently, the liposomes were removed by size exclusion chromatography and the lipid content of the protein assessed by lipid extraction and MS analysis, as described above. Control experiments without protein confirmed the complete absence of lipids from the merged fractions after size exclusion chromatography, demonstrating the full removal of liposomes from the sample.

A rapid exchange after 5 min incubation at 291 K, could be observed for the deuterated analogs (1-palmitoyl($^2\text{H}_{31}$)-2-oleoyl-*syn*-glycero-3-PtdEtn / -PtdGro; $^2\text{H}_{31}$ -PtdEtn/ -PtdGro) of the initially bound lipids PtdEtn and PtdGro (fig. 4-16c)). In contrast, PtdCho, PtdSer and PtdIns were only incorporated after extended incubations of 48 h at 291 K or 2 h at 310 K. This results show clearly, that the NF1-SecPH lipid binding cage is accessible in aqueous solutions and able to extract lipids from membranes, preferring PtdEtn and PtdGro *in vitro*. Interestingly, the NF1-Sec derived lock seems not to prevent an opening of the lipid binding cage by default, but is rather flexible or can make way for the lid-helix as part of a concerted movement.

These findings were underlined by competitive experiments with liposomes corresponding in their lipid composition to the inner leaflet of a Schwann cell plasma membrane (41% PtdEtn, 9.3% PtdSer, 17% PtdCho, 21.7% PtdIns and 10% sphingomyelin; molar ratio).²⁵³ Again, the exchange / binding of PtdEtn and PtdGro was clearly favored and could be observed within minutes, while PtdSer, PtdCho and PtdIns was only detected after several hours of incubation (fig. 4-16d)).

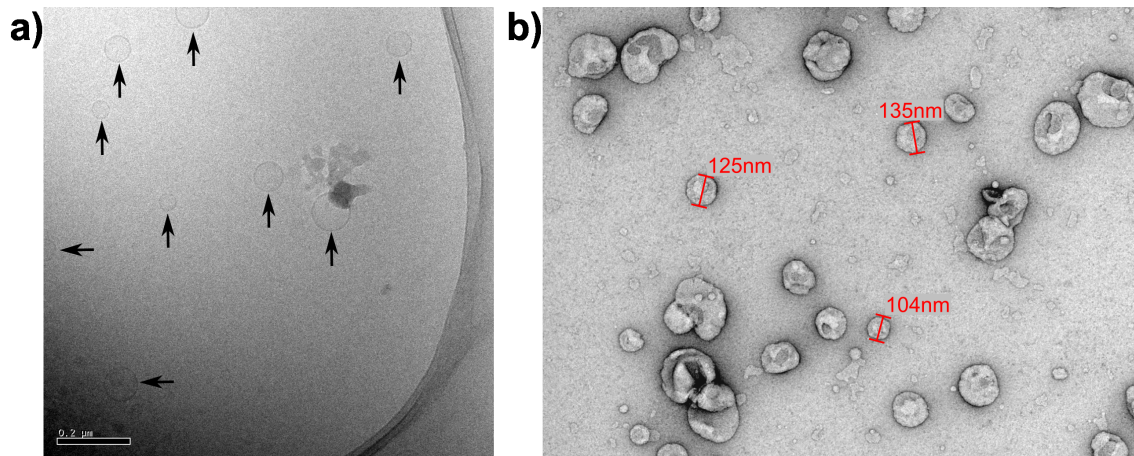


Fig. 4-17: Exemplary electron microscopy images of liposomes to assess size and unilamellarity. **a)** Cryo electron microscopy image of PtdGro liposomes, showing clearly that the liposomes are unilamellar and contain no further membranes. Due to the freezing process, the size distribution of the observed liposomes is not representative, preventing the determination of their average diameter. **b)** Negative stain electron microscopy image of PtdSer liposomes, which have a diameter of roughly 100 - 200 nm and a good homogeneity. This matches well with the 100 nm pore size of the membrane used for extrusion.

Considering that *Escherichia coli* membranes contain 75% PtdEtn and 20% PtdGro,²⁵⁴ it is not surprising that these lipids are bound to NF1-SecPH after purification from this organism. However, in eukaryotic cells, PtdGro is only present in trace amounts, where it is an intermediate of cardiolipin synthesis in mitochondria.²⁵⁵ In contrast, 15% of total phospholipids in neuronal cells are PtdEtn,^{253,256} even increasing to 45% in defined *Drosophila melanogaster* tissues which express a Neurofibromin orthologue.^{67,257-259} Therefore it is suggestive that PtdEtn is a likely physiological ligand of Neurofibromin in neuronal cells.

It should be noted in this context, that colocalization of Neurofibromin and mitochondria could be observed previously¹³⁰ and the Neurofibromin target K-Ras is able to translocate to the outer mitochondrial membrane, where it participates in local signaling events.²⁶⁰ However, further experiments would be necessary to assess if Neurofibromin can bind mitochondrial PtdGro *in vivo* and whether this is physiologically relevant.¹¹²

Mutation	Domain	Location	Reference
I1584V	NF1-Sec	cage backside, protein core	Fahsold 2000 ⁹⁰
R1590W	NF1-Sec	domain contact region	Upadhyaya 1997 ²⁶¹
V1621R	NF1-Sec	cage backside, protein core	Jeong 2006 ⁹⁴
Δ IY1658-59	NF1-Sec	inside cage	Wu 1999 ¹⁰⁵
N1662K	NF1-Sec	interface region	Boyanapalli 2006 ¹⁰⁷
TD1699-1713	Linker	linker	Tassabehji 1993 ¹⁰²
Δ K1750	NF1-PH	interface region	Fahsold 2000 ⁹⁰
A1764S	NF1-PH	protein core	Han 2001 ⁹²
T1787M	NF1-PH	protein surface	Lee 2006 ⁹⁷

Table 4-4: Selected patient derived mutations in NF1-SecPH (see fig. 4-19)

4.5 Patient derived mutations of NF1-SecPH

The structural analysis of patient derived mutations can be used to identify functionally important regions of a protein and characterize the activity in question, thereby advancing the understanding of the related disease and eventually even contribute to the development of therapeutics. For this purpose, the patient derived mutations known in the NF1-SecPH region have been analyzed.

4.5.1 Purification and characterization of NF1-SecPH mutants

In NF1-SecPH, a number of relevant patient derived missense mutations, deletions and even a tandem duplication (TD) have been observed (table 4-4). For biochemical and structural investigations, these mutations were introduced into pETM11 plasmids carrying NF1-SecPH for expression in *E.coli*. While several mutants were already available from our previous investigations, site directed mutagenesis had to be performed to obtain V1621R, Δ IY1658-59 and T1787M.

According to the new protocol for the wildtype protein, all nine mutants listed in table 4-4 were expressed in the E.coli BL21 Codon+ RIL cell strain and purified by Ni-affinity chromatography, His-tag cleavage and size exclusion chromatography.

Although all mutants were purified with the same protocol, considerable differences in the yield, purity and solubility of the proteins

could be observed. While a very good yield was obtained with I1584V and V121R, others including N1662K, Δ IY1658-59 and T1787M were mostly insoluble and prone to degradation as multiple bands on SDS-PAGE gels indicated. Consequently, one can speculate that the pathogenic effect of these mutations is rather caused by the instability of the NF1-SecPH module instead of impaired catalytic or interaction properties. Interestingly both N1662K and Δ IY1658-59 are located near the lid - lock interface region and could hinder interdomain contacts between NF1-Sec and NF1-PH (fig. 4-19).

In order to assess the quality of the purified proteins regarding overall fold, thermal stability and multimerisation, circular dichroism (CD) measurements and analytical size exclusion chromatography were performed (fig. 4-20, 4-21, 4-22). Comparisons between the far UV spectra of wildtype NF1-SecPH and mutants show good consistency, demonstrating that all proteins are folded and have a similar composition of secondary structure elements. Only N1662K deviates from the wildtype curve, which is probably caused by the presence of degradation products in the sample, leading to an overrepresentation of the corresponding protein segments in the CD-Spectrum. Thermal de-

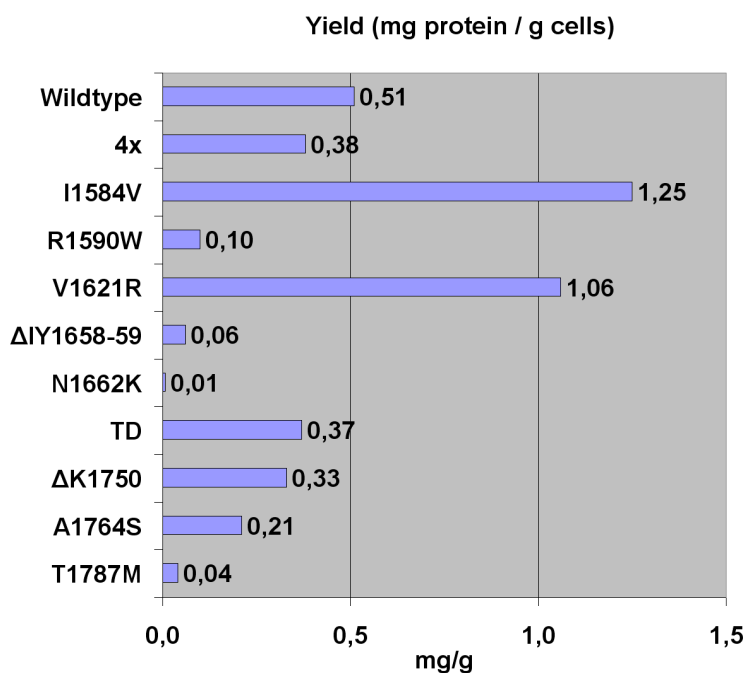


Fig. 4-18: Protein yield of the wildtype protein and the investigated patient derived mutations of NF1-SecPH. Abbreviations: wildtype (WT), tandem duplication 1699-1713 (TD), fourfold mutation K1670A - R1674A - R1748A - K1750A (4x).

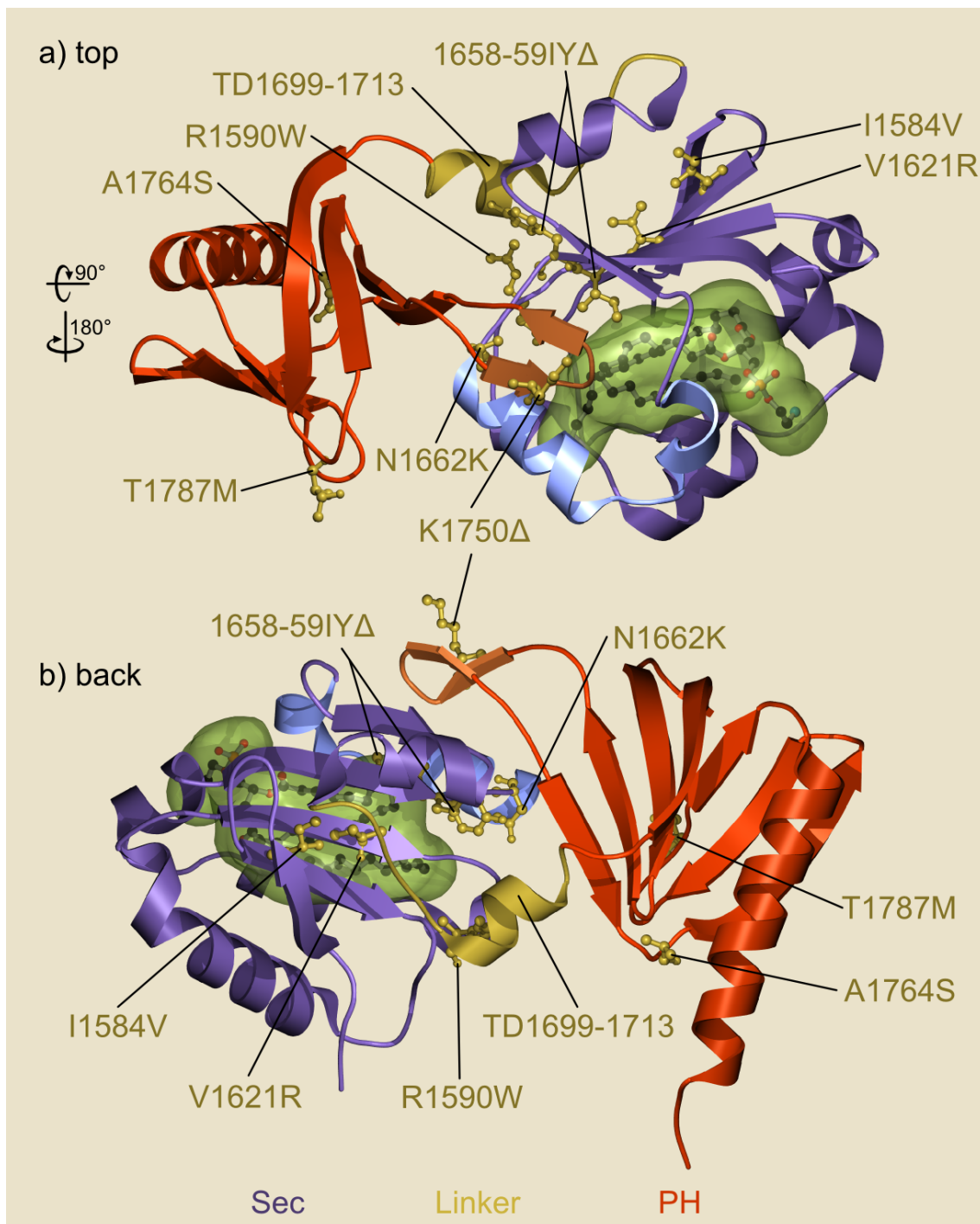


Fig. 4-19: Ribbon representation of NF1-SecPH with known patient derived missense mutations and amino acid deletions, both displayed as ball and stick models. The linker region shown in yellow was found duplicated (TD: tandem duplication) in one patient (see table 4-4). Red: NF1-Sec domain, Violet: NF1-PH. In green, the calculated surface of the 18:1(9)-16:1-PtdEtn ligand is shown, enwrapping a ball-and-stick model of the lipid (black: carbon, red: oxygen, blue: nitrogen, orange: phosphorus) **a)** top view. **b)** back view. Image created with POVScript+²⁴³ and POV-Ray.²⁴⁴

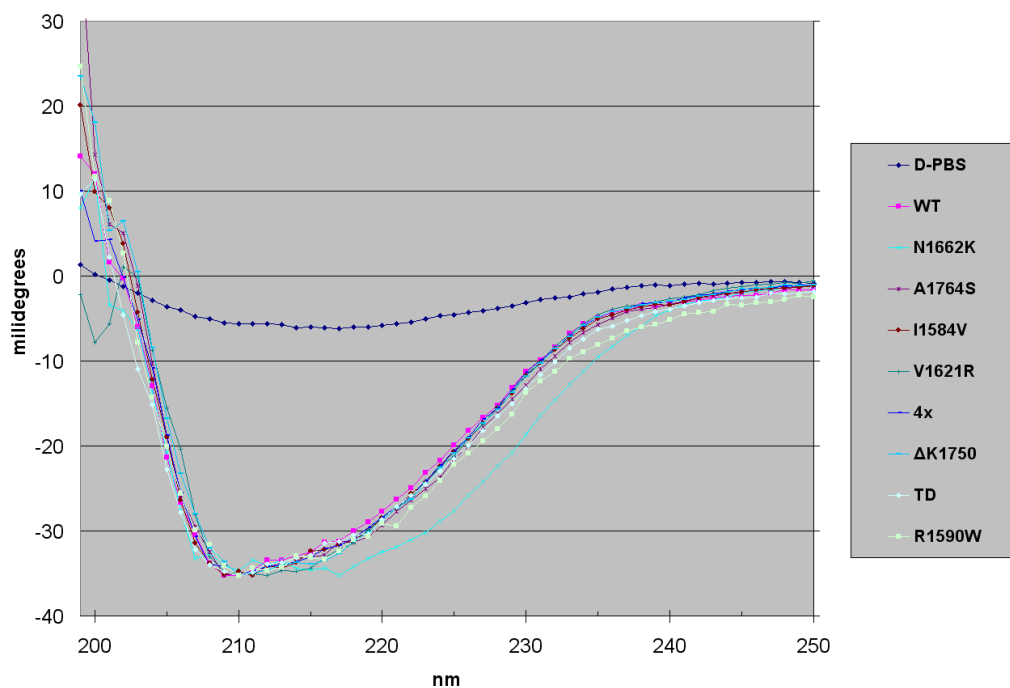


Fig. 4-20: CD-spectra of NF1-SecPH and selected mutants. The spectra were scaled to each other in the y-direction for better comparison. No major variations are visible except for N1662K, showing a slight shift of the spectrum between 215 - 240nm (see text). The recorded data were processed and visualized with Excel (Microsoft).

naturation experiments suggest a melting point of about 60-65°C for most mutants in agreement with the wildtype protein. Interestingly, for Δ K1750 and the TD mutation much lower melting points of about 52.5 and 50°C are observed, indicating an increased protein flexibility. Both, the affected Δ K1750 lock region and the duplicated TD linker are located at the protein surface and could indeed adopt various conformations without disrupting the overall fold of NF1-SecPH. In analytical gel filtration experiments (fig. 4-22), it can be observed that all mutants migrate similar to the wildtype protein. In this buffer conditions, the elution volume of the main peak is about 14 - 14.5 ml corresponding to a monomer (about 31 KDa) as estimated with a logarithmic plot of the size standard (not shown). A second peak can be observed mainly for V1621R (12 ml), where a tetramer would be expected (about 124 KDa). In agreement with the CD-spectroscopy data, also the similarity of the hydrodynamic radii suggests that the analyzed proteins are structurally related.

MS analysis of the NF1-SecPH mutants was carried out in col-

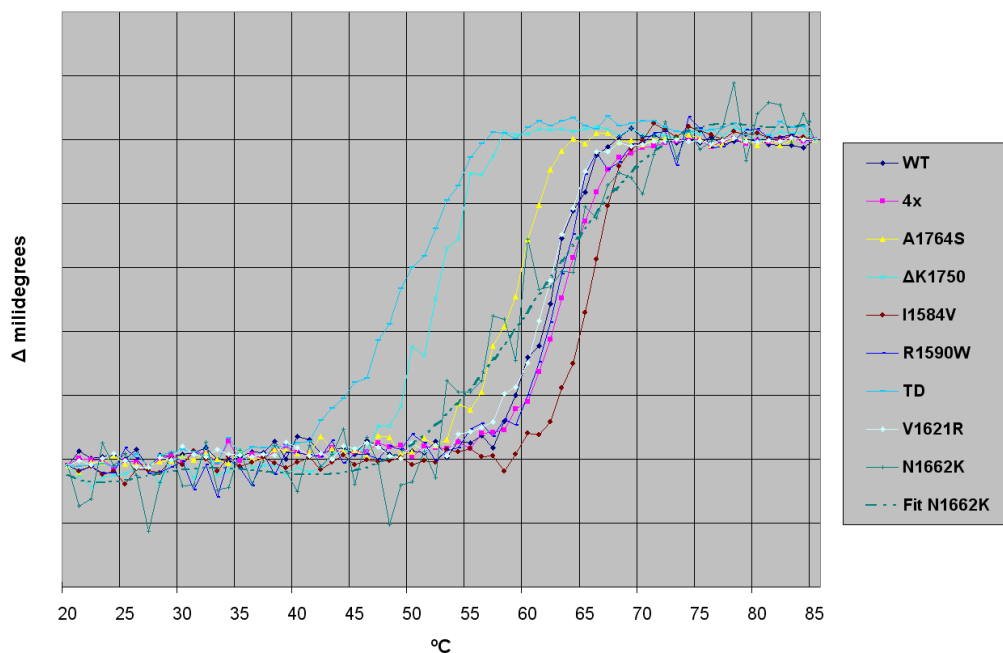


Fig. 4-21: Thermal denaturation of NF1-SecPH and selected mutants. Single wavelength measurements at 220 nm were performed while the temperature was increased from 20 to 85°C. The melting points of most mutants conform with the wildtype protein, with values between 60 - 65°C. In contrast, the measurements for TD and Δ K1750 indicate a lower melting point of about 50 and 52.5°C respectively. The recorded data was visualized and scaled in y-direction with Excel (Microsoft).

laboration with Sven Fraterman (EMBL Heidelberg), showing for a selected range that they are also bound to PtdEtn and PtdGro like the wildtype protein. Also this results suggest, that the different mutations do not seem to have a major influence on the overall conformation of the lipid binding cage. The analyzed mutations included A1764S (NF1-PH), R1590W (NF1-Sec), Δ K1750 and K1670A - R1674A - R1748A - K1750A (4x, lid - lock interface region) as well as TD (duplication of the linker regions), covering all structural regions of NF1-SecPH. Also exchange experiments comparing the wildtype protein and the mutation 4x, which affects the entrance to the lipid binding cage, did not show any differences.

4.5.2 Structure of the Δ K1750 mutant

To investigate the differences between wildtype and mutant proteins on the structural level, crystallization trials were done with all patient derived mutants. As starting point, the crystallization conditions of

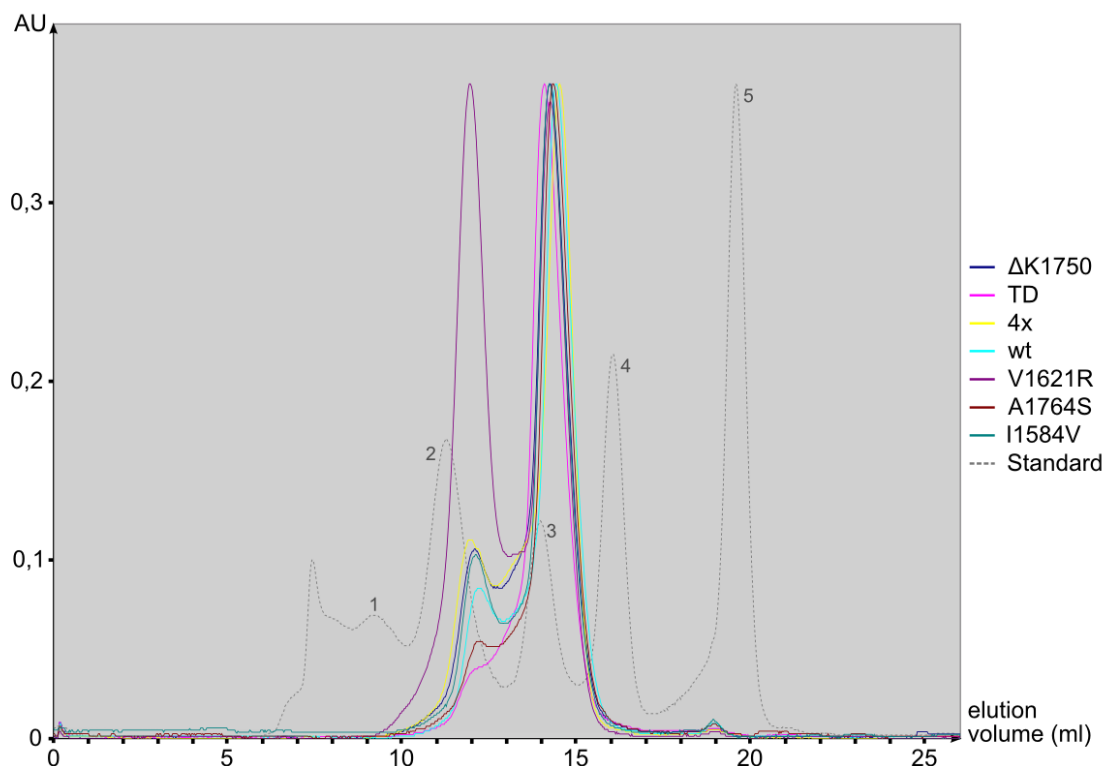


Fig. 4-22: Analytical size exclusion chromatography curves for NF1-SecPH and patient derived mutants. The main peak at 14 - 14.5 ml corresponds to a monomeric protein (about 31 KDa) while a second peak mainly visible for V1621R at 12 ml could be explained with a tetramer (about 124 KDa). The peaks of the standard curve (BioRad, Gelfiltration standard) correspond to 1) 670 KDa, 2) 185 KDa, 3) 44 KDa, 4) 17 KDa and 5) 1.35 KDa. A Superdex 200 column from GE Healthcare with a column volume of 25 ml and a resolution of 10 - 600 KDa was used.

the triton free wildtype protein were used, but extended to robotic screens (EMBL Crystallization Platform Team (XTP)) if necessary. Similar to the wildtype protein, also several of the mutants could be crystallized successfully due to the improved purification protocol. In the course of a laboratory practical, the Δ K1750 mutant could be crystallize by utilizing the same crystallization screen (p. 49) that was used previously for the wildtype protein (Uli Karst, trainee). The most suited crystals could be obtained in a hanging drop setup with following conditions:

compound	amount
MES pH6.0	0.1M
PEG 4000	12%
$\text{Na}_4\text{P}_2\text{O}_7 \cdot 10\text{H}_2\text{O}$	0.3M
<hr/>	
0.1 μ l mother solution + 1.5 μ l protein	

Table 4-5: Summary of crystallographic analysis of the NF1-SecPH Δ K1750 mutant (Igor D'Angelo, unpublished results)

Data collection	
X-ray source	ESRF ID14-1
Wavelength (Å)	1.000
Space group	P4 ₁ 2 ₁ 2
Unit cell (Å, deg)	a=b=114.33 c=125.33 $\alpha = \beta = \gamma = 90$
Resolution (Å)	2.23
Highest shell (Å)	2.23-2.3
No. of observations	287'397 (20'611)
Unique reflections	76'273 (5484)
I/ σ	13.8 (3.5)
R _{sym} (%) ^a	5.0 (35.7)
completeness (%)	97.8 (99)
Refinement	
Resolution range (Å)	20-2.23
No. of reflections	34'675
R _{work} /R _{free} ^b	21/26
No.of atoms Protein	693
No.of atoms Solvent	58
Mean B value protein (Å ²)	44.3
RMSD	
Bond length (Å)	0.018
Bond angle (deg)	1.9
Ramachandran-plot	
Regions (%)	
most favored	87.7
additional allowed	10.6
generously allowed	1.5
disallowed	0.2

a) as defined in XDS,²⁴² b) as defined in CNS²⁴⁵

A dataset with a resolution of 2.5Å was collected at the European Synchrotron Radiation Facility (ESRF) Grenoble at beamline ID14-1. Structure determination was done by Igor D'Angelo (table 4-5, using the wildtype structure to generate an initial model from the integrated data (XDS,²⁴² CNS²⁴⁵), followed by manual and automated refinement (CNS, COOT²⁴⁶). The final model is nearly identical to

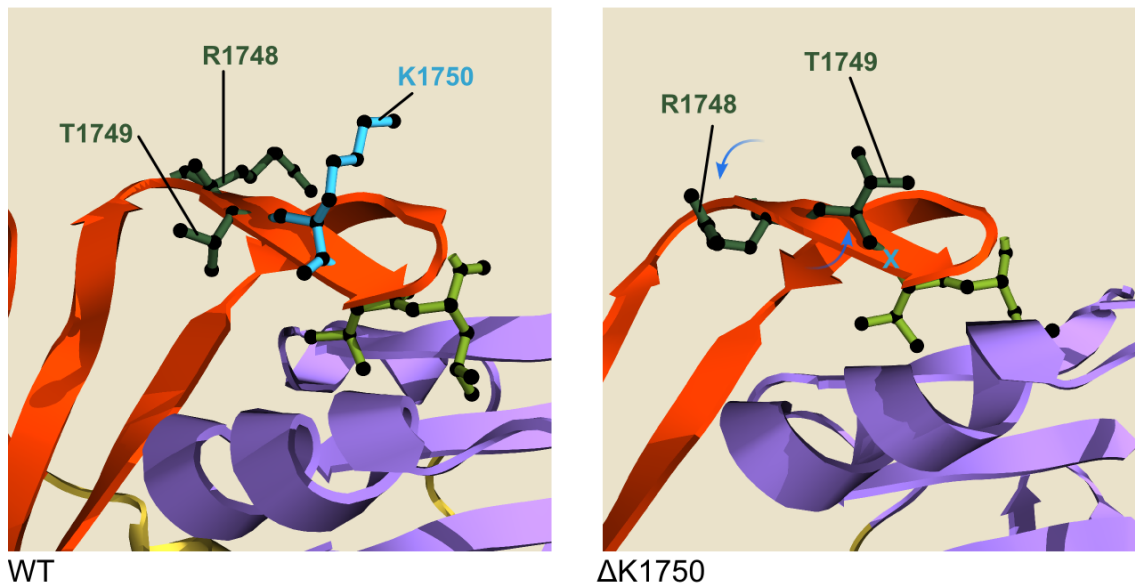


Fig. 4-23: Structural comparison between the lid - lock interface region of wildtype NF1-SecPH and Δ K1750. In the wildtype structure the residues K1750 and R1748 are in an upward orientation, which probably permits participation in PIP binding. In contrast, the peptide backbone of Δ K1750 adopts an switched conformation leading to a rearrangement of R1748 and T1749 as indicated with blue arrows. A blue cross marks the position where K1750 is missing. Protein - lipid overlay assays with Δ K1750 show a decrease of PIP binding similar to the results obtained with double mutant constructs (p. 35), suggesting that not only K1750 is missing, but R1748 is no longer able to participate in PIP binding as well.

the wildtype structure, showing only differences in the lock region of NF1-PH, were the mutation is located. Apparently, removal of K1750 induced a local flip of the protein backbone, leading to an inversed orientation of the R1748 and T1749 side chains (fig. 4-23). This rearrangement is compatible with the weakened PIP binding activity of Δ K1750. Similar to the weakly binding double mutations (K1670A - R1674A, R1748A - K1750A and R1666A - K1670A), two residues contributing to the PIP binding platform are missing: K1750 is deleted while R1748 adopts a conformation incompatible with ligand binding. Since the rest of the protein is unchanged, this findings could suggest a connection between the function of the lipid binding cage and the observed phenotype.

4.5.3 Structure of the TD mutant

The TD mutant could be crystallized and its structure determined in the course of a diploma thesis by Sonja Kühn. Although the TD mutation affects Neurofibromin, the related phenotype is rather indicative for Noonan-syndrome, which shares a number of clinical manifestations with NF1.^{262,263} A large number of Noonan-syndrome cases are associated with gain-of-function alterations in the SHP-2 protein, which acts, besides other functions, as positive regulator of the Ras-Raf-MEK-Erk signaling cascade.^{264,265} Suggestive explanations for this observation would include the possibility that TD affects the GAP activity of Neurofibromin and causes an equivalent perturbation of Ras signaling like SHP-2 alterations. Also imaginable is that the TD alteration disrupts an interaction of neurofibromin with a protein to be identified, leading to an indirect effect on SHP-2 activity.

Crystals of TD could only be obtained after extensive robotic and manual screening (diploma thesis, Sonja Kühn) and optimization of crystallization conditions. The crystals with the best diffraction properties were obtained in a hanging drop experiment with following conditions:

compound	amount
HEPES pH7.0	0.05M
PEG 400	39%
(NH ₄) ₂ SO ₄	0.2M

The crystals diffracted to 2.5 Å at ID14-3 at the ESRF Grenoble and were solved by molecular replacement (Sonja Kühn) with CNSsolve²⁴⁵ using the PtdEtn bound wildtype structure (PDB code 2E2X)¹¹² as search model. Refinement was done in various steps using CNSsolve, REFMAC 5 (CCP4 suite)²⁶⁶ and COOT for model building (table 4-6). Comparing the final structure with the wildtype protein, again no major changes are visible besides a slightly different orientation of the single domains towards each other. No electron density for the linker region including the tandem duplication is visible, indicating this re-

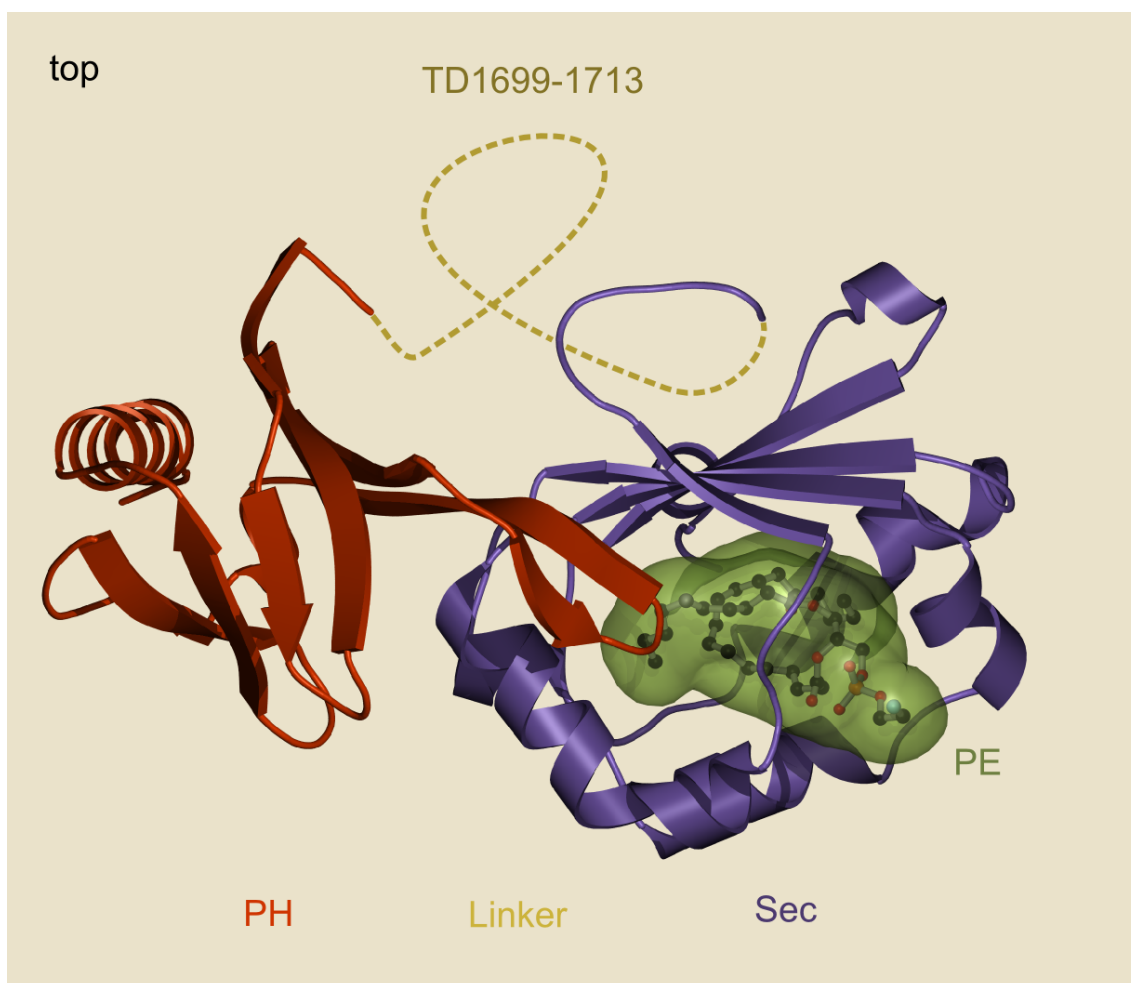


Fig. 4-24: Structure of the NF1-SecPH tandem duplication (TD) mutant in ribbon representation. Similar to $\Delta K1750$, the overall structure of NF1-SecPH TD is unchanged compared to the wildtype protein. The linker region including the duplicated residues 1699 - 1713 is not visible in the electron density map, therefore depicted here symbolically as dashed yellow line. This observation indicates that the linker is flexible, in consistency with thermal denaturation experiments (p. 61).

gion to be unordered and flexible. This finding is compatible with the lower melting point observed in CD measurements in comparison to the wildtype protein. A difference to the wildtype protein is the orientation of the PtdEtn ligand, which is positioned more toward the outside of the lipid binding cage and forms a crystal contact with the next protein molecule via H-bonds to a solvent molecule. Therefore, the lipid head group is also not interacting with the residues R1684 and F1642 as observed in the wildtype structure. The fatty acid chains of the lipid are as well in a different orientated than their counterparts in the wildtype structure, demonstrating that the conformation of the

Table 4-6: Summary of crystallographic analysis of the NF1-SecPH tandem duplication mutant (from Sonja Kühn, diploma thesis)

Data collection	
X-ray source	ESRF ID14-3
Wavelength (Å)	0.931
Space group	P6 ₄ 22
Unit cell (Å, deg)	a=b=104.6 c=116.3 $\alpha = \beta = 90$ $\gamma = 120$
Resolution (Å)	2.52
Highest shell (Å)	2.52-2.67
No. of observations	300'107 (10519)
Unique reflections	12'507 (1532)
I/ σ	21.78 (2.49)
R _{sym} (%) ^a	11.2 (78.4)
completeness (%)	94.5 (75.4)
Refinement	
Resolution range (Å)	19.77-2.52
No. of reflections	12'506
R _{work} /R _{free} ^b	24.11 / 31.09
No. of atoms Protein	1969
No. of atoms Solvent	15
PtdEtn	1 molecule
Presumable metal atoms	4
Mean B value protein (Å ²)	54.47
Ramachandran-plot	
Regions (% of residues)	
most favored	77.7
additional allowed	17.3
generously allowed	4.1
disallowed	0.9

a) as defined in XDS,²⁴² b) as defined in CNS²⁴⁵

lipid tails does rather not depend on defined interactions with the hydrophobic cage, but the availability of space.

The question remains how the TD alteration exerts its pathogenic effect. Although the duplicated linker region is not visible in the electron density, it can be ruled out that the geometry of the NF1-SecPH module is somehow distorted by to the TD alteration. It is more

likely that due to its enlarged size, the duplicated linker prevents an intramolecular contact within Neurofibromin or masks a binding site for interaction partners. This might lead to an improperly folded protein or disturb the information flow between Neurofibromin and other signal regulatory proteins.

4.6 Access to the lipid binding cage can be inhibited with PIPs

In order to address the question if PIPs can regulate the access to the lipid binding cage via stabilization of the lid - lock interaction, the effect of soluble PIP headgroups on lipid exchange assays was investigated. Therefore, exchange experiments with NF1-SecPH and $^2\text{H}_{31}$ -PtdGro liposomes were performed in the presence of increasing amounts of 1D-*myo*-Inositol-3-phosphate (Ins-3-P) or *myo*-Inositol-1,2,3,4,5,6-hexakisphosphate (InsP₆). The results indicate an inhibition of the lipid exchange reaction in the presence of Ins-Ps (fig. 4-25).

For Ins-3-P and InsP₆ IC₅₀ values of 271 and 49 μM could be calculated, indicating that the number of phosphate groups influences the inhibitory power of the compound via their negative charge. The single measuring points of the inhibition curves (fig. 4-25a)) represent the ratio between the summed intensities of the initial and exchanged ligands. Data processing and analysis was done with Excel (Microsoft) and Igor Pro 5.0 (Wavemetrics) by Sven Fraterman. Further experiments showed, that *myo*-Inositol is not able to inhibit the exchange reaction in contrast to Ins-3-P and in agreement with the observed charge dependence of the inhibitory power of these compounds (fig. 4-25b)). Underlining the findings of the mutational analysis, the four-fold NF1-SecPH mutant (R1748A-K1750A-K1670A-R1674A) cannot be inhibited by Ins-3-P, since the compound is unable to bind to the protein (fig. 4-25b)).

Although the performed experiments cannot clarify the identity of

a physiological inhibitory compound or protein, they strongly support a mechanistic view in which the interface region plays a significant role in regulating access to the lipid binding cage. In the current model, the lipid binding cage can adopt an open conformation either directly by a combined movement of lock and lid, or by sequential conformational changes (fig. 4-26,1-3). Once in an open conformation, the protein module can exchange the incorporated ligand against a lipid extracted from a membrane (fig. 4-26,4). Alternatively, an inhibitor molecule

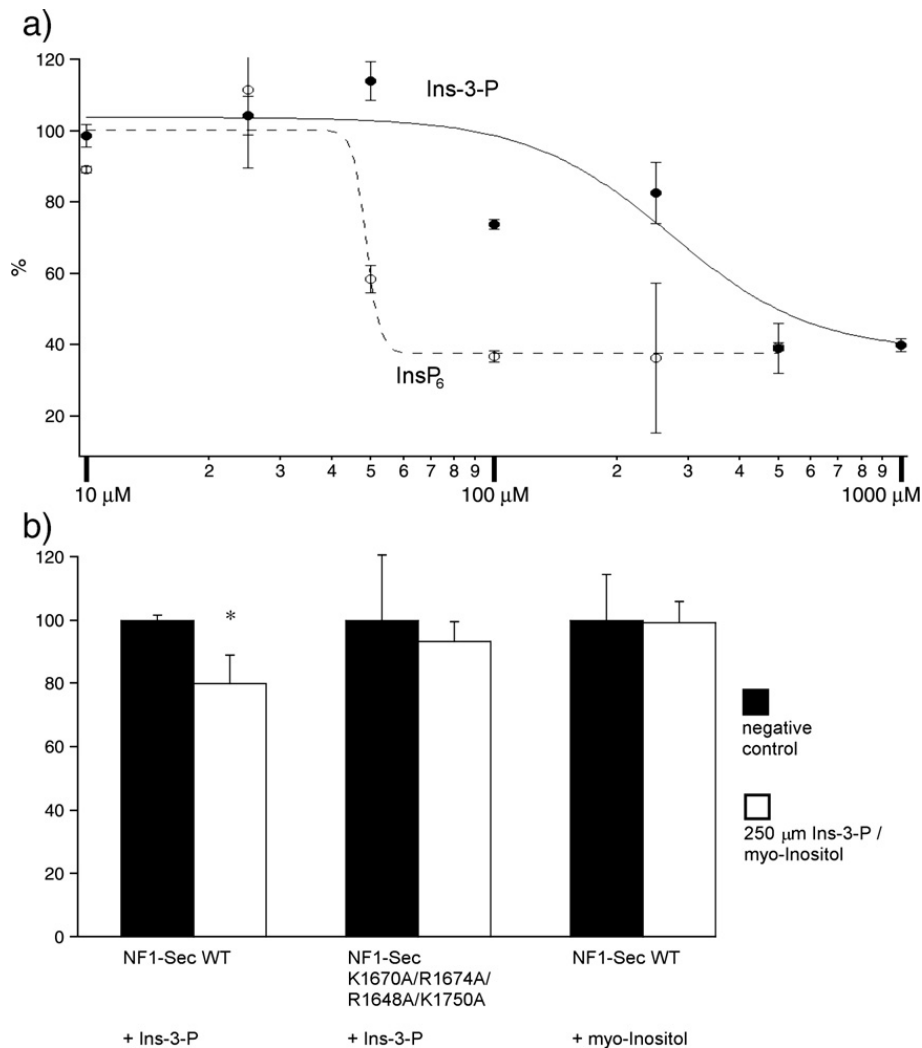


Fig. 4-25: Inhibition of lipid exchange reactions with NF1-SecPH and $^2\text{H}_{31}$ -PtdGro liposomes by InsPs.¹¹² **a)** Inhibition curves, the single measure points represent the ratio between the summed intensities of the initial and the exchanged ligands. **b)** While the exchange reaction with wildtype NF1-SecPH protein can be inhibited by InsPs, this is not observed for the four fold mutant (R1748A-K1750A-K1670A-R1674A) since the inhibitors are not able to bind the protein. Consistent with protein - lipid overlay assays, myo-Inositol is not able to inhibit the exchange reaction, because it lacks a negatively charged group for protein binding.

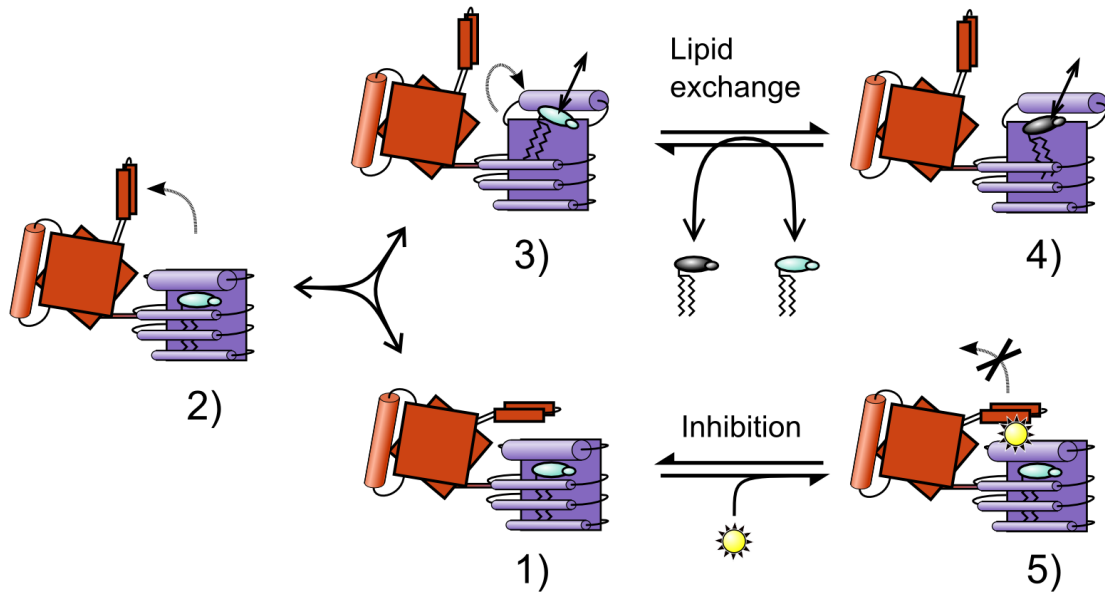


Fig. 4-26: Model of NF1-SecPH lipid exchange and inhibition of exchange. Starting from 1) the closed cage can become open either by a concerted 1)→3) or stepwise movement of lid and lock 1)→2)→3) as indicated with black arrows. Once open, the bound lipid can be exchanged 4). Alternatively, a negative regulator can bind to the lid - lock interface region and stabilize the closed conformation of the cage 5), inhibiting the exchange reaction.

binds the lock - lid region of the closed lipid binding cage and prevents the lock from making way for an opening movement of the lid-helix (fig. 4-26,1;5)).

4.7 Conclusions and outlook

Background: In the course of this thesis work, the Sec14- and PH-like domains of the RasGAP Neurofibromin were structurally and biochemically investigated. A suggestive question in this context is whether the NF1-SecPH module can regulate or influence the GAP activity of Neurofibromin. This might occur directly in response to a specific interaction or indirectly by affecting the subcellular localization of Neurofibromin and therewith its possibility to interact with Ras. In previous studies we established the basis for such investigations by solving the structure of the NF1-SecPH module and showed an interaction with PIPs.⁸⁴

Ras proteins usually control a number of different signal transduction pathways by direct interaction. However, incoming signals

are not relayed to all subordinate pathways at once but only to a signal-specific subset, depending on the subcellular localization of the activated Ras proteins.²³⁶ The localization of Ras is a dynamic process which is spatio-temporally regulated and maintained by a steady cycle of de- and re-acylation of the Ras C-terminus.¹²⁵ To maintain the selective regulation of specific Ras pathways, it therefore seems necessary that the related GEF and GAP proteins can also associate with defined endomembrane compartments and affect distinct populations of membrane bound Ras. A number of signal regulatory proteins including PTPases, RhoGAPs and RhoGEFs were indeed shown to be able to associate with membranes depending on their Sec14-like domains. In the case of the proto-oncogenic RhoGEF Dbs the subcellular localization is further influenced by a regulatory intramolecular interaction of the Sec14-like domain with a PH domain located at the opposite terminus of the protein.^{237-239,267,268}

Localization experiments: To address this topic experimentally, localization experiments were performed in our group, expressing GFP/YFP-fused Neurofibromin fragments in mammalian cells. Based on these studies, localization was examined after stimulation with PDGF²⁴¹ and in a Neurofibromin deficient Schwann cell line, excluding competition with endogenous protein for rare interaction partners. In all experiments, only a diffuse unspecific staining could be observed which was also seen with a full length Neurofibromin construct (Welti and Seiler, unpublished observation), suggesting that there is no constitutive, specific localization of Neurofibromin. Given the biological background of Ras, we suspect that Neurofibromin has a membrane association activity either by itself or via mediating proteins. As suggested by the experiments performed, a specific signal or stimulus, which we could not yet identify, might be necessary to trigger this activity.

Since localization of a protein can also depend on the simultaneous cooperation of more than one activity,²¹⁶ localization experiments

might give false negative results if the investigated fragments do not contain all domains necessary. Also analysis of the full length protein might be difficult, if one of these domains is subject to an autoinhibitory mechanism or is missing an activating signal or interaction. An approach to this problem is the biochemical assessment of protein fragments, which was applied to NF1-SecPH since this module is one of the few Neurofibromin segments that can be recombinantly produced in a satisfactory way.

Interaction with PIPs: In previous experiments we could show binding of NF1-SecPH to different immobilized lipids with protein-lipid overlay assays. The quality of these assays could be improved by the usage of purified anti-NF1-SecPH antibodies and an optimization of the detection procedure. This revealed binding to PtdEtn and PtdSer as false positive results, while the interactions with PIPs and Sulfatide could be confirmed as well as the mutational analysis which identified the PIP interaction region. The investigation of patient derived mutations showed a weakened ligand binding of Δ K1750, suggesting an involvement of this region in physiological relevant interactions. However, whether PIPs are physiological relevant ligands of Neurofibromin remains questionable, since NF1-SecPH does not show specificity for distinct PIP species, and this lack of specificity was also observed for the full length protein (Anabell Parret, unpublished).

Ligand bound NF1-SecPH Structure: Since in the previous structure of NF1-SecPH a detergent molecule from the purification process was bound,⁸⁴ a structure disclosing the mode of interaction with a physiological ligand was highly desirable. While this problem could not be solved with extended crystallization screens, crystallization and structure determination of ligand-bound wildtype NF1-SecPH as well as the patient derived mutations Δ K1750 and TD were possible after improvement of the protein purification procedure.

In the structure of the wildtype protein, electron density compat-

ible with a glycerophospholipid was visible, showing for the first time the mode of interaction between such a ligand and a CRAL_TRIO lipid binding cage.¹¹² Mass spectrometry analysis showed a 1:1 stoichiometry of the NF1-SecPH:lipid complex and unambiguously identified the bound ligands as PtdEtn and PtdGro. While in eucaryotic cells PtdGro is only present in mitochondria as an intermediate of cardiolipin synthesis, PtdEtn is an abundant membrane lipid that we propose to be a likely physiological ligand in neuronal cells.^{253,255,256}

By utilizing liposomes, it could be shown that NF1-SecPH can adopt an open conformation, interact with membranes and can exchange the bound lipid against a membrane derived one, favoring PtdEtn and PtdGro. Furthermore, soluble PIP headgroups are able to inhibit the exchange of lipids, apparently by stabilizing parts of NF1-PH in a way that prevents NF1-Sec from adopting an open conformation.¹¹²

The consequences of lipid incorporation for Neurofibromin's overall function are rather unclear and difficult to estimate, given the unusual interaction of the two domains. However, some scenarios seem more likely including a membrane association activity or a lipid sensing function, which might modulate the GAP activity.²⁶⁹ Although kinetic experiments in the presence of lipids did not show an altered activity of GRD (Vladimir Pena, unpublished), it should be noted that the specificity of several RhoGAPs can vary and depends on the prenylation state of their target GTPases.²⁷⁰ This suggests that farnesyl- and/or palmitoylation of Ras might be necessary to observe a lipid dependent regulation of Neurofibromin's GAP activity in such experiments. Although the idea that NF1-Sec might be able to incorporate the farnesyl/palmitoyl chains of Ras should also be considered, it seems rather unlikely that Neurofibromin has a quantitative lipid transport activity.²⁶⁹

Analysis of patient derived Mutants: The structure of the Δ K1750 mutation shows an alteration of the NF1-SecPH interface

region, which is in agreement with its weakened PIP binding activity, and matches with protein/PIP binding sites of other PH domains.^{214,215,271,272} The second crystallized mutation TD contains a duplication of the linker region between NF1-Sec and NF1-PH, however this only marginally changes the orientation of the two domains towards each other. In the electron density the linker region itself is not visible, indicating a high flexibility which is compatible with the lower melting point of the protein. Since the biochemical analysis of patient derived mutations did not show large differences when compared to the wildtype protein, the NF1-SecPH module might have a further, yet undiscovered function.

The structural changes in the mutant proteins suggest that such an activity could be located at the top/back of NF1. In this region is not only K1750 located, but also the elongated linker region present in TD could reach there and mask, for example, a protein binding site. Furthermore, the I1584V and V1621R alterations are located nearby, which rather seem to cause a functional impairment instead of a destabilization of the protein. A protein ligand docking to this region of Nf1-Sec might additionally regulate access to the lipid binding cage, similar to the effect observed with PIPs.

In the case of Nf1-PH it is difficult to estimate further possible functions, since the lack of sequence homology to other domain complicates a precise classification to any subgroup of PH-like domains (see p.28). It is noteworthy that other similar cases are known, including BEACH domain containing proteins, TFIIH, Pob3 and Ran-BD domains,^{233,273-275} most of which are involved in protein - protein interactions. However, since the individual activities of these proteins are completely unrelated, it is not possible to further restrict the spectrum of probable NF1-PH functions from these observations. Furthermore, some PH-like domains can also bind to two different ligands simultaneously like PLC- β 2,^{276,277} further complicating the identification of a related activity of NF1-PH even more.

Outlook: This work describes the structural and biochemical basis of glycerophospholipid binding to NF1-SecPH as well as the properties of the lipid binding cage and patient derived mutations. Future studies could be performed to investigate the effect of lipid incorporation on other Neurofibromin domains including GRD, and the role it serves *in vivo*. For further localization studies, the experiments performed give direction, suggesting that a localization activity is probably regulated and triggered by defined signaling events. Identification of such events by further stimulation experiments with life cells could clarify, which signals are recognized by Neurofibromin and how they might lead to the regulation of Ras and/or other targets. The investigation of patient derived mutations suggests that there might be another binding activity hosted by NF1-SecPH, encouraging further interaction screens like TAP-TAG purifications, pull down assays and yeast two hybrid screens. Identification of further ligands could reveal additional cellular processes connected to Neurofibromin function.

5 Materials and methods

5.1 Common Methods

Common molecular biology methods have been done due to standard laboratory protocols^{278,279} or according to manufacturers Protocols, like dialysis, glycerol stocks, SDS-PAGE- and agarose gels.

Purification of plasmid DNA in mini and midi scale as well as recovery of DNA fragments from agarose gels was done with kits from Qiagen. Analytical and preparative restriction digests were performed with restriction enzymes from New England Biolabs (NEB) and ligations with T4 DNA Ligase (Roche) or the rapid DNA dephos and ligation kit (Roche). For the production of plasmid DNA, the DH5 α *E.coli* cell line was used (Life technologies).

Protein concentrations were determined by absorbance measurements at 280 and 320 nm using a GeneQuant pro (Amersham Biosciences) photospectrometer and UVettes (Eppendorf) according to the formula:

$$c(\text{protein})[\text{mg/ml}] = (\text{OD}_{280} - \text{OD}_{320}) * \frac{M_w[\text{Da}] * \text{dilutionFactor}}{\epsilon}$$

with the protein concentration in mg/ml ($c(\text{protein})[\text{mg/ml}]$), the absorbance at 280 and 320 nm (OD_{280} , OD_{320}), the molecular weight in daltons ($M_w[\text{Da}]$) and the extinction coefficient (ϵ). The protein in question was denatured and diluted in 8M guanidinium hydrochlorid (Pierce) prior to the measurement. Both M_w and ϵ were calculated with the ExPASy ProtParam tool.²⁸⁰

Western blot protein transfer was done with a BioRad Transblot cassette (BioRad) and Imobilontm-fl membrane (Milipore) for 1 - 2 h with a current of 80 - 100 mA (35V). The detection procedure was similar as described for protein lipid overlay assays (see below, p.80), except for the use of less pure BSA (Serva, albumin bovine fraction V) and skipping of the incubation step with protein after blocking of the membrane.

5.2 Expression and purification of NF1-SecPH

The NF1-SecPH module (aa 1545-1816) or patient derived missense mutations were expressed in BL21 CodonPlus(DE)-RIL *E. coli* cells (Stratagene), with a pETM-11 vector (Gunther Stier, EMBL) in the presence of Kanamycin (34 μ g/ml) and Chloramphenicol (20 μ g/ml). From an over night starter culture (LB medium, EMBL media kitchen), 500 ml cultures (TB-FB medium, EMBL media kitchen) were inoculated and incubated (37°C, 200rpm) until an OD of 0.8 - 1.0 was reached. The cultures were then induced with 100 μ l of 1M IPTG (isopropyl β -D-1-thiogalactopyranoside), cooled for 5 min on ice and incubated over night (20h, 15°C 200rpm). After harvesting the cells by centrifugation (appropriate buckets, max speed), the pellet was resuspended in lysis buffer (LyB, 20 mM Tris, 0.5 M NaCl, 40mM Imidazol, 1mM β -Mercaptoethanol (β -ME), pH8.1) and lysed by 15 min of incubation in the presence of Lysozym (1 μ g/ml, Sigma) and DNaseI (1 μ g/ml, Roche), followed by sonication (2x 5min, duty cycle 50%, power 5; Branson W-250, Heinemann). The cell lysate was then cleared of cell debris and particles by ultracentrifugation (1h, 40.000 rpm, 4°C; Beckmann L-70), and applied to a preequilibrated HisTrap column (1ml nickel containing resin, GE healthcare) for 2h (4°C) in a circulatory way with a peristaltic pump. The column was then washed with 10 ml of LyB and slowly eluted with 10 ml of elution buffer (ElB, 20 mM Tris, 0.5 M NaCl, 125 mM imidazol, 1 mM β -ME, pH8.1) in 1 ml fractions. Protein containing fractions were merged after visual inspection of protein content by drop-scale bradford assays. The His-tag was then removed by cleavage with TEV (Tobacco etch virus) protease (48h, 5 μ g / mg protein, 4°C, second addition after 24h) and the eluat concentrated to a total volume of 2 ml (Amicon[®] Ultra-15 10K MWCO, Milipore). For further purification of the sample including the removal of compounds, cleaved His-tag and TEV protease, a preparative size exclusion chromatography was performed (GE healthcare, Superdex 200 HiLoad 16/60)) using buffer GF (20

mM Tris, 150 mM NaCl, 1 mM β -ME, 1 mM EDTA, pH8.0) and the appropriate fractions merged after analysis of protein purity by SDS-PAGE. Finally the protein sample was concentrated (see above) to 10 - 15 mg/ml and stored at -80°C after snap freezing in liquid nitrogen. All steps of the purification were routinely inspected by SDS-PAGE to monitor the sample quality and identify error sources in case of protein loss.

5.3 Protein - lipid overlay assays

5.3.1 Generation of α NF1-SecPH antibodies

Since the detection of NF1-SecPH via expression tags was giving false positive signals in some assays, α NF1-SecPH antibodies were raised and purified for a direct detection of the protein. Removal of the fusion tag can furthermore eliminate false negative signals which might occur due to the masking of a binding site by the tag or the impairment of a catalytic activity.

The antibodies were raised in rabbits (*Oryctolagus cuniculus*) by usage of the RIBI adjuvant system (Corixa) and purified NF1-SecPH protein according to manufacturers protocols and guidelines of the EMBL Laboratory Animal Resources (LAR) facility, which also performed all animal handling. Obtained blood was incubated 1 h for 37°C and the blood clotting removed by centrifugation (30 min, 4000 rpm, 4°C). Remaining clots were removed with a further centrifugation step (10 min, 4000 rpm, 4°C) and the resulting serum flash frozen in liquid nitrogen before storage at -80°C .

To purify the antibodies from the serum, an affinity column was prepared by coupling NF1-SecPH to a sepharose matrix (CNBr-activated sepharose 4B, GE Healthcare) due to manufacturers instructions. Loading of 5 ml serum to the resin was done by batch incubation for 12 h in the presence of 5 mM EDTA and 0.2 mM PMFS at 4°C . After the column was washed with 5x 10 ml PBS + 0.05% Tween-20 the antibodies were eluted with 5 ml elution buffer (0.2M Glycine,

0.15M NaCl) pH2.7 followed by 5ml elution buffer pH2.3 to detach high affinity binders. The eluate was immediately neutralized with an appropriate amount of 2M Tris pH9.0, to prevent permanent denaturation of the antibodies and concentrated to 0.5 - 1.0 mg/ml protein with a spin concentrator (Amicon[®] Ultra-15 10K MWCO, Milipore). Finally, the concentrated sample was dialyzed (Slide-A-Lyser[®] 10'000 MWCO, Pierce) over night at 4°C to PBS and subsequently flash frozen in liquid nitrogen for storage at -80°C. Typically 0.7 mg of pure antibody could be obtained from 5 ml of serum. The purified antibodies from different batches were tested by western blot analysis for functionality and specificity towards NF1-SecPH, showing also that the different mutants are recognized (fig. 4-1, p. 31). Usually the NF1-SecPH affinity matrix was reusable after extended washing with PBS.

5.3.2 Protein lipid overlay assays

To assess the lipid binding properties of Nf1-SecPH and mutants, lipid overlay assays were done, using PIP-Strips[™], PIP-Arrays and Sphingo-Strips from Echelon biosciences as well as custom made lipid arrays from Oriol Galego (EMBL). All strips and arrays consists of a nylon membrane where an assortment of lipids is spotted onto. In a simplistic model, the lipids are thought to stick to the nylon membrane by interactions with their hydrophobic fatty acid tails and expose their headgroup to the surrounding environment. Proteins which can bind the lipid head groups are therefore immobilized and remain on the membrane during subsequent wash steps, in contrast to non-binders that are removed. Similar to a western blot, the protein was detected with Rabbit α NF1-SecPH antibodies, secondary Goat α Rabbit-HRP antibodies (Sigma-Aldrich), the enhanced chemiluminescence (ECL) plus kit and autoradiography film (GE Healthcare).

To reduce the background of the assay, the whole procedure was carried out at 4°C and the exchange of solutions was done as quick as possible to prevent prolonged exposure of the membrane to air. After

the blocking of the membrane for 1 h with PBS/Tween/BSA (PBS (media kitchen EMBL) with 0.1% v/v Tween 20 (Sigma-Aldrich) and 3% w/v fatty acid free BSA (Sigma-Aldrich)), 10 μ g of protein were added and incubated for 3 h with panning. Following 10 times 5 min washing with PBS/Tween (as above without BSA), rabbit α NF1-SecPH antibody (1:1000) was applied in PBS/Tween/BSA and incubated for 1 h. Subsequently, the membrane was rinsed two times and incubated once for 1 h and 3 times for 10 min with PBS/Tween to remove surplus antibody. The secondary Goat α Rabbit-HRP antibody (1:10'000) was incubated for 30 min in PBA/Tween/BSA, followed by three times rinsing and once 1 h and four times 5 min incubation with PBS/Tween. Directly thereafter, the ECL plus kit and autoradiography film was used according to manufacturers instructions for visualization.

As positive control PIP-GripTM (Echelon biosciences) was used in the first experiments but replaced later by wildtype NF1-SecPH protein, which at the same time was used as reference for the evaluation of signal intensities of mutant proteins, since exposure times always vary slightly. A negative control is included on most membranes and also the absence of signal outside of spot areas shows that protein and antibody is not binding unspecifically to the membrane.

5.3.3 Site directed mutagenesis

Site directed mutagenesis was done with the QuikChange[®] site directed mutagenesis kit (Stratagene) according to manufacturers instructions, with the wildtype NF1-SecPH DNA in the pETM-11 vector which was available from earlier experiments. Δ IY1658-59 was generated stepwise via Δ IY1659. For the PCR reaction, Pfu Turbo DNA polymerase and a RoboCycler (Gradient 96) with heated lid were used (both Stratagene), nucleotides and primers were obtained from Sigma-Aldrich.

primer sequences 5'-3' forward/reverse complementary

V1621R

gcaaagccatatgaaattCGTgtggaccttaccataccgg
ccggtatgggtaaggtccacACGaatttcatatggctttgc

ΔY1659

cgacaacgtctccgcagtctatatac<>aactgtaactcctggg
cccaggagttacagtt<>gatatagactgcgagacgttgctcg

ΔIY1658-59

gcttacgacaacgtctccgcagtctat<>aactgtaactcctggggtcaggg
ccctgaccaggagttacagtt<>atagactgcgagacgttgctgtaage

T1787M

ccattgcaaaccagggcATGccgctcaccttcatgc
gcatgaaggtgagcggCATgccttggttgcaatgg

changed codons are in uppercase, <> indicates skipped aa

5.4 Crystallographic techniques

5.4.1 Crystallization

X-ray crystallography is a method to determine the structure of a molecule at atomic resolution. In order to obtain a diffraction pattern strong enough to be recorded, it is necessary that the material in question is available as single crystal of an appropriate size. Proteins can be crystallized by various techniques, of which two prominent ones are the hanging- and sitting drop method.

In brief, the protein solution is mixed with precipitant and sealed airtight in a small chamber together with a reservoir of the precipitant solution. Inside this chamber, the drop is either hanging on the bottom of a coverslide (hanging drop), which also seals the chamber or positioned on top of a small pedestal (sitting drop). In this setup, the protein drop starts to loose solvent molecules to the reservoir solution due to their higher ionic strength, until an equilibrium is reached. Thereby, the effective protein concentration in the drop increases and can reach the phases in which nucleation or precipitation occurs (fig. 5-1). In the optimal case, only a few nucleation events occur before the

drop enters the metastable phase where no further nucleation occurs, but existing crystals continue to grow.

For initial screening, all available commercial (Hampton Research, Emerald BioSystems) and home-made robotic screens were performed (EMBL Crystallization Platform Team (XTP), Mosquito Robot, Molecular Dimensions) and manually monitored for crystallization. Usually drops were prepared by the robot in a 100 nl protein + 100 nl precipitant fashion. Initial hits were then further optimized by hand in 24-well plates with drop volumes of 0.5 - 2 μ l in different ratios of 1:4 or 1:1 with protein concentrations ranging from 10 - 15 mg/ml.

5.4.2 X-ray data collection

During this step of structure determination, the actual diffraction experiment is performed and the resulting data recorded. The protein crystal is therefore kept under cryogenic conditions while exposed to a monochromatic X-ray beam with a wavelength of about 1 Å, which interacts with the electron clouds of the crystallized proteins and is diffracted according to Bragg's Law. This can be viewed as a Fourier analysis of the crystalline object, resulting in a diffraction pattern where each spot represents a basis function. Once a sufficient number of maxima are recorded by rotation of the crystal in the X-ray beam, the protein structure can be reconstructed by Fourier synthesis from the collected data. This can not be done directly however, since it is not possible to record the phase information due to technical limitations. Ways to circumvent the phase problem include the estimation of phases from the structure of a very similar, known molecule (molecular replacement) or to compare a heavy-atom derivatized version to the original protein crystal, leading also to an estimate for initial phases (isomorphous replacement). Although, X-ray crystallography is a powerful method to analyze even the largest protein complexes at atomic resolution, flexible regions can not be monitored due to their varying conformations in the crystal and are absent in the final electron density map.

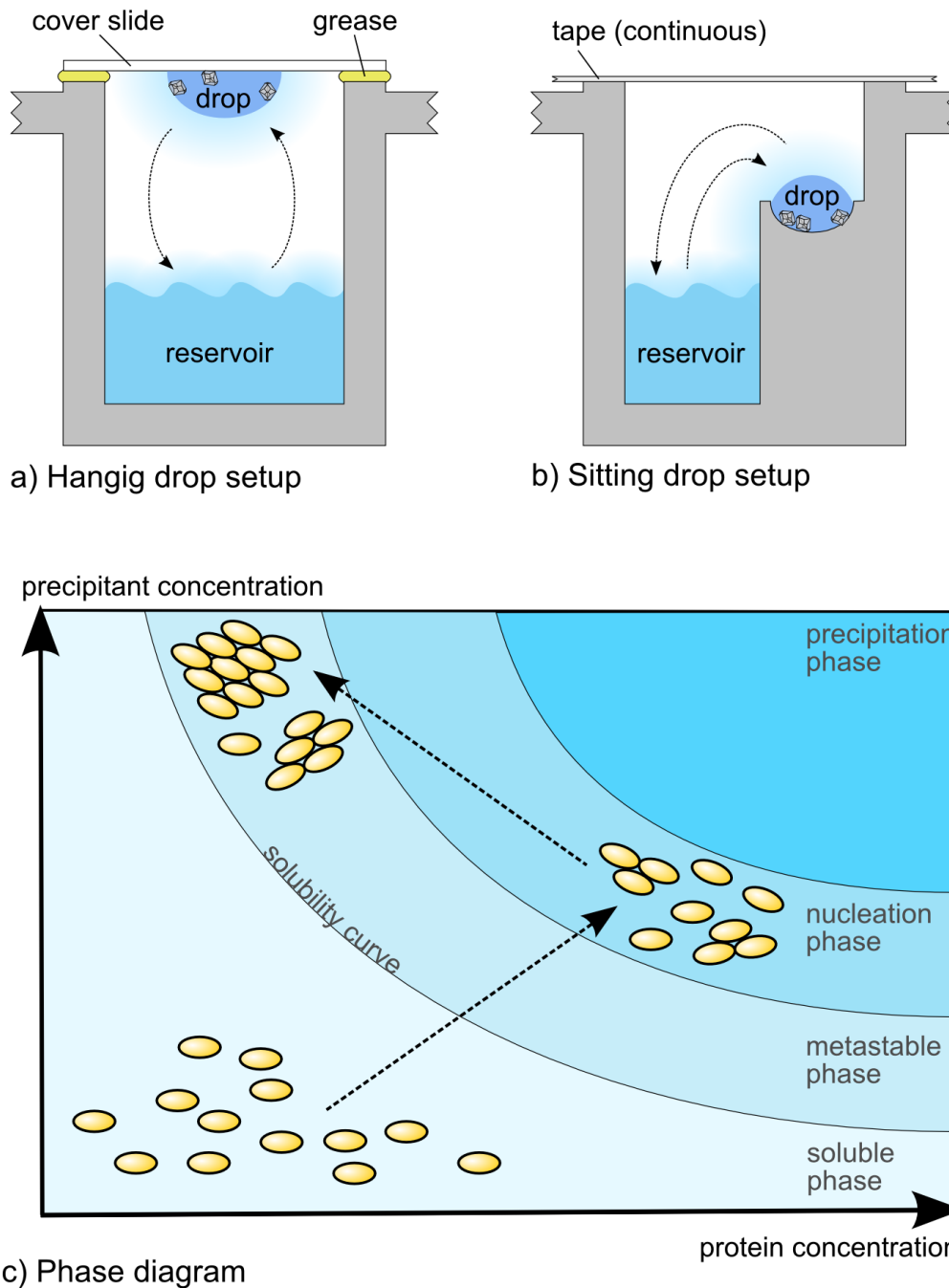


Fig. 5-1: Crystallization setup for Proteins. **a)** Hanging drop setup; the protein drop is attached on the bottom of a cover slide which seals the well containing reservoir solution. Broken arrows indicate the diffusion of solvent molecules. The drop loses solvent molecules until an equilibrium is reached. **b)** Sitting drop setup; here the protein drop sits on top of a pedestal and the well is sealed (together with neighboring wells) by continuous tape. From the principle similar to hanging drop experiments, this setup can be pipetted by robots. **c)** Phase diagram; the protein and precipitant concentration increase slowly due to the loss of solvent molecules by vapor diffusion. Once the nucleation phase is reached, protein crystals nucleate and start to grow. The precipitant concentration continues to increase due to the ongoing dehydration of the drop, while crystal growth depletes the soluble protein until an equilibrium between dissolving and growth of the crystal is reached.

To prepare the crystal for data collection, it is transferred to a drop with cryosolution and then frozen and stored in liquid nitrogen. During data collection, the low temperature helps to enhance the ordered state of the crystal by reducing molecular thermal vibrations and conformational disorder, improving resolution and signal to noise ratio of the data. In addition, the diffusion speed of free radicals generated during exposure to the X-ray is decreased, prolonging the lifespan of the protein crystal. Beside cryoprotectant like 20% ethyleneglycol or PEG, the used cryosolution is usually composed according to the crystallization conditions in question. This prevents dissolving as well as ice formation, which could damage the crystal and interferes with the diffraction experiment.

Crystals were usually tested for diffraction quality at the rotating anode setup at EMBL Heidelberg and then brought to the european synchrotron radiation facility (ESRF, Grenoble) for complete data collection. After the collection of about 10 rotation images, the space-group was determined and a data collection strategy calculated with XDS, according to which a complete high- and low-resolution dataset was acquired.

5.4.3 Structure determination by molecular replacement

The structures of the discussed proteins were determined by molecular replacement, using previously obtained NF1-SecPH coordinates as starting models. Recorded datasets were processed and integrated with XDS,²⁴² while CNS²⁴⁵ was used for the molecular replacement (MR) procedures.

To use the phase information of the known protein for the recorded dataset, it is necessary to find the right orientation and position of the model structure in the unit cell. For comparison and evaluation of a given orientation, the patterson functions of model and recorded dataset are calculated and superpositioned. Once a good match is found, a patterson correlation refinement is done, where the orientation of domains or rigid secondary structure elements against each

other is optimized. Finally, the right position of the optimized model is determined with a translational search, which is evaluated by comparison of the observed reflexes with structure factors calculated for each investigated location.²⁸¹

With such a starting model, initial electron density maps could be calculated and final structures obtained by alternating model building and structure refinement using COOT²⁴⁶ and CNSsolve or REFMAC 5 (CCP4 suite),²⁶⁶ respectively.

5.5 Analysis of the NF1-SecPH - glycerophospholipid interaction

5.5.1 Lipid extraction

To analyze the lipids bound to the NF1-SecPH module after purification or exchange reactions, an isolation with the method described by Folch^{112,251} was done and subjected to mass spectrometry. The method takes advantage of the different solubility of lipids in aqueous and organic solvents. In brief, a sample with a volume of 100 μl and 15 mg/ml of protein is added to 375 μl of methanol (MeOH) and vortexed for 10 min. Afterwards, 750 μl of chloroform (CHCl_3) is added and again vortexed for 10 min. Finally 225 μl of water are added and the sample stirred or inverted for another 10 min, spun down (5 min, 500 rpm) and the lower, organic phase collected. For an increase of purity, the organic phase is mixed with 400 μl of $\text{CHCl}_3/\text{MeOH}/\text{H}_2\text{O}$ 3:48:47 and inverted 5 times. The sample is again centrifuged (5 min, 500 rpm) and the lower, organic phase collected. For mass spectrometry analysis, the sample is completely dried in a vacuum centrifuge, redissolved in 19 μl of $\text{CHCl}_3/\text{MeOH}$ 1:2 (v/v), and briefly vortexed. After the addition of 1 μl of 100 mM ammonium acetate (in MeOH), the sample is directly injected into the mass spectrometer and analyzed.

5.5.2 Preparation of liposomes

Liposomes were prepared to investigate the interaction of NF1-SecPH with membranes of a defined lipid composition. The preparation of the liposomes was done with an extruder following published protocols.^{282,283} To protect the lipids during preparation against oxidation, the solutions were overlaid with argon whenever possible and contact time to air was kept short. Furthermore, the temperature was kept above the highest phase transition temperature T_m of the lipids during the complete procedure, to ensure a uniform mixture. If the temperature is too low, lipid bilayers are present in a tightly packed and rigid gel phase, while above T_m the liquid crystal phase is adopted, where lipid movement and flexibility is increased. Values of T_m vary largely and are strongly dependent on the type of fatty acid chains in the lipid, ranging from -16°C for PtdEtn (18:1) to 70°C for unsaturated PtdEtn (18:0), as taken from the website of Avanti polar lipids inc. or the CRC Handbook of lipid bilayers.²⁸⁴ To decrease the loss of lipids at surfaces, glass ware or siliconized pipette tips and sample tubes (Biozym, no longer produced) were used during the preparation.

For the preparation of Liposome solutions with 10 mM total lipid, 2 μmol of appropriate lipids (obtained from Avanti polar lipids inc.) were mixed together and completely dried in a vacuum centrifuge (Uniequip, univapo 150H). Afterwards they were resuspended by vortexing in 200 μl of liposome buffer (100 mM KCl, 1 mM MOPS, pH7.0) and incubated above the highest T_m for 1 h with vigorous shaking. This causes the lipids to dissolve in the aqueous solution as multilamellar liposomes of various sizes. To be able to estimate the amount of accessible lipid, the liposomes need to be converted to unilamellar vesicles, preferentially with a uniform and defined size. Therefore the liposome solution is subjected to five freeze/thaw cycles (liquid nitrogen / 37°C) for an initial reduction of size. Afterwards they were extruded 20 times through two stacked 100 nm pore size polycarbonate membranes with an extruder (Avanti polar lipids inc.) leading to

unilamellar liposomes of about 100 - 200 nm (fig. 4-17, p. 57). Finally the liposome solution was overlaid with argon, stored at 4°C and used within 3 to 4 days.

5.5.3 Lipid exchange reactions and inhibition

With lipid exchange experiments, the accessibility of the NF1-SecPH lipid binding cage was assessed as well as its specificity and the amount of exchange. Therefore, 5 μ l of liposomes (10 mM total lipid) with a given composition were incubated with 20 μ l of protein (10 - 15mg/ml) and incubated for 5 min at room temperature. For inhibition experiments, the compounds of question were added before the incubation and then proceeded as described. Afterwards, the liposomes were removed by analytical size exclusion chromatography (GE Healthcare, Superdex 200, 25ml column volume, buffer GF p.79), the protein containing fractions merged and concentrated (Amicon[®] Ultra-15 10K MWCO, Milipore) to the minimal volume of about 250 μ l. The lipid content was analyzed by lipid extraction and subsequent mass spectrometry. Control experiments with liposomes only showed that the collected fractions from the size exclusion chromatography did not contain any lipids.

5.5.4 Mass spectrometry analysis

To identify the composition of extracted lipids (p. 86), the samples were analyzed by nanospray Q-ToF MS (quadrupol - time of flight mass spectrometry) in negative ion mode collecting data over a range of 650-1000 m/z . In addition to mass determination, the identity of the lipids was also examined by fragmentation of the respective precursor ions, followed by data collection over a range of 50-900 m/z . Data were collected with an electrospray ionization (ESI)- ToF spectrometer (QStar Pulsar i, Applied Biosystems) and processed with the Arcade software tool (Matthias Wilm, EMBL Heidelberg, unpublished). All MS experiments were performed by Sven Fraterman (EMBL Hei-

delberg).

For analysis, the sample is transferred into a volatile solvent (see above) and enters the spectrometer via a small conductive capillary. By applying a strong electric field, a Taylor cone with a steady cone jet forms at the tip of the capillary, leading to the continuous formation of small charged droplets. By several rounds of a not completely understood process called Coulombic fission, the droplets break down to lone ions. During this process, the droplets shrink due to evaporation of the volatile solvent and burst as soon as the repelling force between the charged analytes becomes too strong.

The mass of the generated ions is then calculated from the time they need to travel a given distance after acceleration by a defined high-voltage pulse. The accuracy of the measurement is usually increased by an inserted electrostatic reflector field, which changes the flight direction of the ions by 180 degrees and compensates thereby for differences between the initial positions and velocities of the ions.

In the Q-ToF setup, the ions pass through a quadrupole before mass determination, which can be used as mass filter permitting only the passage of ions with a specific mass-to-charge (m/z) value. Therefore, a high frequency electrical field is generated between the rods of the quadrupole, which forces all ions without the corresponding m/z value onto unstable trajectories, resulting in a collision with the rods. By the subsequent use of a collision chamber, a characteristic set of fragments can be generated from the selected precursor ion, allowing its unambiguous identification in the ToF section.²⁸⁵⁻²⁸⁷

For the mass determination of native proteins, the buffer of the sample was exchanged against 80mM ammonium bicarbonate (80mM, pH6.5) by dialysis for 2h. Afterwards, the sample was diluted 1:20 in 80mM ammonium bicarbonate(pH6.5)/5% methanol and applied to nanospray Q-ToF MS analysis in positive ion mode, collecting data over a range of 1000-6000 m/z .

The inhibitory effect of soluble PIP headgroups on lipid exchange reactions was assessed by calculating the ratios between the summed

peak intensities of the exchanged lipid D₃₁-PtdGro and the initial ligands (PtdEtn and PtdGro). The ratios were processed, compared (Microsoft Excel, Wavemetrics Igor Pro5.0) and differences tested for significance with the Student's T-Test, with $p < 0.05$ considered as significant.¹¹²

5.6 Protein characterization

5.6.1 Analytical size exclusion chromatography

With this technique, the approximate molecular weight and the multimeric state of a compound can be estimated. The porous matrix of the column offers smaller molecules a large number of holes and channels to enter, increasing the time to pass through the whole column. Although the retention time in the column depends not directly on the molecular weight but the hydrodynamic radius of a compound, for most proteins a good estimate can be made with a protein standard. This technique can also be used to separate proteins of different size and remove small compounds or high molecular weight impurities. Usually, a Superdex 200 column from GE Healthcare with a column volume of 25 ml was used with buffer GF (see above).

5.6.2 Circular dichroism spectroscopy

Circular dichroism (CD) spectroscopy can be used to estimate the overall ratio of α -helical, β -sheet and coiled-coil secondary structure elements of a protein. Thereby, also the structural similarity of mutants or the thermal stability of a protein can be investigated. For the measurement, the difference between the absorption of right and left circular polarized light by the chiral peptide bonds of the protein is recorded for a range of wavelengths. In consequence, the overall signal intensity is also dependent on the protein concentration and the pathlength of the used cuvette. The obtained curve can be interpreted as linear combination of reference spectra for the different secondary structure elements, revealing the overall secondary structure composi-

tion of the protein. To determine the thermal stability of a protein, the signal change at a fixed wavelength can be observed while constantly increasing the temperature of the sample. Upon denaturation of the protein, the conformation of the peptide backbone changes strongly, which leads to a notable change of the CD signal.

For the performed measurements, 200 - 600 μ l of protein (0.2 mg/ml, in PBS) were transferred to a quartz precision cuvette (Helmann, 100-QS, 110-QS) and analyzed with a Jasco-710 spectropolarimeter. CD spectra were recorded with 1 nm resolution from 199 - 250 nm with a sensitivity of 20 mdeg and 10 accumulations at 20°C. The thermal denaturation of proteins was observed at 205 nm from 20 - 80°C.

5.6.3 Isothermal titration calorimetry

With isothermal titration calorimetry (ITC) the thermodynamic parameters of molecular interactions can be determined. By recording the evolving or absorbed heat during the titration of a molecule to its binding partner over time, the binding affinity (K_a ; equilibrium constant K), the enthalpy change (ΔH) and the binding stoichiometry (n) of the reaction are measured. With the Gibbs-Helmholtz equation $\Delta G = \Delta H - T\Delta S$ and $\Delta G = -RT\ln K$,²⁸⁸ also the Gibbs free energy change ΔG and the entropy change ΔS can be calculated.

The experimental setup consists of a measuring cell with injection system and an identical reference cell, both shielded by an adiabatic jacket and made from an efficient thermal conducting material. Between the two cells, the temperature difference is continuously measured and corrected for by feedback driven heating of the measuring cell. During the titration experiment, the reference cell is constantly heated with low power and the energy uptake for the adjustment of the measuring cell recorded. Is the association of molecule and binding partner exotherm, less energy is needed to adjust the measurement cell and vice versa for an endotherm reaction.

ITC measurements were performed with a VP-ITC calorimeter (MicroCal) at 25°C, by titrating a 2 mM phosphotyrosine (Fluka)

solution to 222 μM of NF1-SecPH. The protein was prior to the experiment dialyzed (Slide-A-Lyser[®] 10'000 MWCO, Pierce) to ITC buffer (20 mM Tris, 150 mM NaCl, 1 mM EDTA, pH8.0). With the buffer used during dialysis, the phosphotyrosine sample was prepared and the pH value carefully adjusted.

5.7 Mammalian cell culture and microscopy

To investigate the subcellular localization of Neurofibromin fragments in life cells, NIH 3T3 mouse fibroblasts (ATCC, American Type Culture Collection) and the NF1^{-/-} human Schwann cell line sNF96.2 (ATCC, CRL-2884) were cultivated. The cells were grown in appropriate condition (37°C, 5% CO₂, media see table 5-1) and splitted regularly in a 1:2 or 1:3 ratio to prevent the formation of a confluent monolayer of cells. For splitting, the cells were detached from the culture flasks by 10 min of incubation with Trypsin-EDTA (Invitrogen) at 37°C, gently pelleted and resuspended in a sufficient amount of fresh medium.

From previous experiments, different Neurofibromin fragments were available (Fabien Bonneau, EMBL Heidelberg) in pEGFP and pEYFP plasmids (Clontech), which can drive the expression of the inserted fragment as N-terminal GFP- or C-terminal YFP-fusion in mammalian cells. Transfection of the plasmids was done according to man-

<i>cell type</i>	<i>compound</i>	<i>final amount</i>	<i>provider</i>
NIH 3T3	DMEM L-glutamine penicillin streptomycin Fetal bovine serum	- 4mM 100 U/ml 100 $\mu\text{g}/\text{ml}$ 10%	EMBL media kitchen Gibco Gibco Gibco PAA
sNF96.2	DMEM complete Fetal bovine serum	- 10%	ATCC (30-2002) ATCC (ATCC-30-2021)

Table 5-1: Growth media for the NIH 3T3 and sNF96.2 cell lines

manufacturers instructions, either with FuGENE6 (Roche) for sNF96.2 cells or Lipofectamin 2000TM (Invitrogen) in case of NIH 3T3 cultures. Prior to transfection, the cells were transferred to a 35 mm glass bottom culture dish (MatTek corporation, Part No.:p35G-1.5-10-C) and in case of NIH 3T3 cells serum starved for 12 h in OptiMEM-I[®] medium (Invitrogen), to ensure a good response to PDGF. One day after transfection, the cells were visualized by confocal microscopy (Olympus FluoView FV1000 system) at regulated environmental conditions (Olympus evotec, 37°C, 5% CO₂) with a magnification of 60x. For stimulation experiments, PDGF (Sigma, P8147) was directly added to live cells during visualization, with a final concentration of 100 μM. Recorded images were processed with the FV1000 software (Olympus) and the Olympus FLUOVIEW Ver.1.6a Viewer.

6 Appendix

6.1 Publication list

Stefan Welti, Igor D'Angelo and Klaus Scheffzek "Structure and Function of Neurofibromin" *Monogr Hum Genet*, vol. 16, pp. 113-128, 2008

Stefan Welti, Sven Fraterman, Igor D'Angelo, Matthias Wilm and Klaus Scheffzek, "The Sec14 homology module of neurofibromin binds cellular glycerophospholipids: mass spectrometry and structure of a lipid complex." *J Mol Biol*, vol. 366, no. 2, pp. 551-562, Feb 2007, PMID: 17187824

Igor D'Angelo, Stefan Welti, Fabien Bonneau and Klaus Scheffzek, "A novel bipartite phospholipid-binding module in the neurofibromatosis type I protein" *EMBO Rep*, vol. 7, no. 2, pp. 174-179, Feb 2006, PMID: 16397625.

Fabien Bonneau, Igor D'Angelo, Stefan Welti, Gunter Stier, Jari Ylännä and Klaus Scheffzek, "Expression, purification and preliminary crystallographic characterization of a novel segment from the neurofibromatosis type I protein." *Acta Crystallogr D Biol Crystallogr*, vol. 60, no. Pt 12 Pt 2, pp. 2364-2367, Dec 2004, PMID: 15583390.

6.2 Abbreviations used in Fig. 3-4 (p.24)

AC	Adenylyl cyclase
Akt/PKB	protein kinase B
AMPK	AMP activated kinase
aPKC	atypical protein kinase C
BAD	Bcl-2 antagonist of cell death
BRaf	B rapidly growing fibrosarcoma
Cdc42	cell division cycle 42
Cdc42GEF	cell division cycle 42 GTPase exchange factor
CRMP-2	Collapsin response mediator protein-2
c-Fos	FBJ (Finkel-Biskis-Jinkins) osteosarcoma, v-Fos FBJ murine osteosarcoma viral oncogene homolog
c-Jun	ju-nana (jap. for 17), v-Jun avian sarcoma virus 17 oncogene homolog
c-myc	myelocytomatosis, v-Myc avian myelocytomatosis viral oncogene homolog
DAG	diacylglycerol
Dock180	dedicator of cytokinesis 180
eIF4B	eukaryotic initiation factor 4B
eIF4E	eukaryotic initiation factor 4E
ECM	extracellular matrix
ELMO	engulfment and cell motility
Ena/VASP	enabled / vasodilator-stimulated phosphoprotein
ER	endoplasmatic reticulum
Erk	extracellular signal-regulated kinase
ETS	erythroblastosis, v-ETS erythroblastosis virus E26 oncogene homolog (avian)
FOXO	forkhead box O1
Gab1	GRB2(growth factor receptor-bound)-associated binding protein 1
GF	growth factor
GPCR	G-protein coupled receptor
GRB2	growth factor receptor-bound 2
Gsk3	glycogen synthase kinase 3
G _{αi}	guanine nucleotide-binding protein α-inhibiting activity polypeptide
G _{αq}	guanine nucleotide-binding protein α q polypeptide
G _{αs}	guanine nucleotide-binding protein α-stimulatory activity polypeptide
HIF1	hypoxia-inducible factor-1
IP145P ₃	1D- <i>myo</i> -inositol 1,4,5-tris(phosphate)
IRS1	insulin receptor substrate 1
KSR	kinase suppressor of Ras
LKB1	renamed to STK 11, serine/threonine protein kinase 11
Mek	mitogen-activated protein kinase kinase 1
mLST8	mammalian lethal with sec thirteen 8, GβL
mTOR	mammalian target of rapamycin
Par3	partitioning defective 3

Par6	partitioning defective 6
PDK1	pyruvate dehydrogenase kinase, isozyme 1
PI3K	phosphatidylinositol 3-kinase
PI34P ₂	1-(3- <i>sn</i> -Phosphatidyl)-D- <i>myo</i> -inositol 3,4-bis(phosphate)
PI345P ₃	1-(3- <i>sn</i> -Phosphatidyl)-D- <i>myo</i> -inositol 3,4,5-tris(phosphate)
PI45P ₂	1-(3- <i>sn</i> -Phosphatidyl)-D- <i>myo</i> -inositol 4,5-bis(phosphate)
PKA	protein kinase A
PKC α	protein kinase C α
PKD	protein kinase D
PLC	phospholipase C
Pol-II	polymerase II
PTEN	phosphatase and tensin homolog
P-Rex1	phosphatidylinositol-3,4,5-trisphosphate-dependent Rac exchanger 1
Pyk2	proline-rich tyrosine kinase 2, = PTK2B
Rac	Ras related C3 botulinum toxin substrate 1
Raf	replication-defective acutely transforming, v-Raf-1 murine leukemia viral oncogene homolog 1
Ral	Ras-like protein
Rap1	Ras-related protein 1
Raptor	regulatory associated protein of mTOR
Ras	rat sarcoma viral oncogene homolog
REDD1	Regulated in development and DNA damage response 1
Rheb	Ras homolog enriched in brain
RhoA	Ras homology A
Rictor	rapamycin-insensitive companion of mTOR
Rock	Rho-associated, coiled-coil containing protein kinase
Rsk	ribosomal protein S6 kinase
RTK	receptor tyrosine kinase
SHC	Src homology 2 domain containing
SHIP1	SH2-containing inositol phosphatase
SKAR	S6K1 ALY/REF-like target
SOS	son of sevenles
Src	v-Src avian sarcoma (Schmidt-Ruppin A-2) viral oncogene
STAT3	signal transducer and activator of transcription 3
STEF	= Tiam2, T-cell lymphoma invasion and metastasis protein-2
S6	surface antigen 6
S6K1/2	ribosomal protein S6 kinase
Tiam1	T-cell lymphoma invasion and metastasis protein-1
TSC1	tuberous sclerosis complex 1, hamartin
TSC2	tuberous sclerosis complex 2, tuberin
VPS34	phosphatidylinositol 3-kinase class 3, PIK3C3
4E-BP1	4E binding protein 1, EIF4EBP1

6.3 Key to the lipid arrays

The lipid arrays were custom made by Oriol Galego (EMBL Heidelberg).

A 1	NBD-PG	G 1	Chl:MeOH 1:1
2	PtdIns	2	Palmitoyl-CoA
3	PtdIns 3-phosphate	3	α -hydroxy stearoyl Coenzyme A, (NH ₄ ⁺) ₃ salt)
4	PtdIns 4-phosphate	4	Hexadecanoic acid
5	PtdIns 4,5-bisphosphate	5	(9Z)-Octadecenoic acid
6	PtdIns 3,4,5-trisphosphate	6	(9Z,12Z)-Octadecadienoic acid
B 1	PtdSer	H 1	15(S)-HETE
2	PtdCho	2	Acylglycerol
3	PtdGro M	3	Diacylglycerol
4	Phosphatidate	4	Triacylglycerol
5	Cardiolipin M	5	1,2-Diacyl-3- β - D-galactosyl-sn-glycerol
6	NBD-PG	6	Chl:MeOH:H ₂ O 1:1:0.2
C 1	PtdEtn	I 1	Digalactosyl-diacylglycerol
2	Phosphatidyl-N-methylethanolamine	2	Diacylglycerol pyrophosphate
3	Phosphatidyl-N-dimethylethanolamine	3	1-Alkyl-2-acetyl-sn-glycero- 3-phosphocholine
4	Ethanolamine phosphate, O-Phosphorylethanolamine	4	1-Acyl-sn-glycerol 3-phosphate
5	CDP-diacylglycerol	5	Geranyl diphosphate
6	CDP-choline	6	Farnesyl diphosphate
D 1	NBD-PG	J 1	Geranylgeranyl diphosphate
2	CDP ethanolamine	2	Squalene
3	3-Dehydrosphinganine, 3-keto-dihydrosphingosine	3	Coenzyme Q
4	Sphinganine, D-erythro-Dihydrosphingosine	4	Dolichol
5	Sphinganine 1-phosphate	5	Lanosterol
6	Phytosphingosine	6	Ergosterol
E 1	Phytosphingosine 1-phosphate	K 1	Desmosterol
2	N-Acylsphinganine, Dihydroceramide	2	Ergocalciferol
3	Ceramide, N-Acylsphingosine	3	S-Adenosyl-L-methionine
4	N-Acyl Phytosphingosine C8 Phytoceramide	4	L-Serine
5	N-acyl-phytosphingosine	5	Chloroform
6	NBD-PG	6	NBD-PG
F 1	Sphingosine		
2	Sphingosine 1-phosphate		
3	CoA		
4	Acetyl CoA		
5	Acetoacetyl-CoA		
6	(S)-3-Hydroxy-3-methylglutaryl-CoA		

6.4 Units, amino acids and prefixes

Abbreviated units	
A	ampere
Å	Ångström = $1 \times 10^{-10} \text{m}$
cal	calorie, 1cal ca. 4.184 kJ
Da	dalton
°C	degree Celsius, $K = ^\circ\text{C} + 273.14$
deg	degrees
g	gramm
h	hour
J	joule
K	degree Kelvin
l	liter
M	mol / l
m	meter
min	minute
rpm	rotations per minute
V	volt

Abbreviations of amino acids (aa)					
Alanine	Ala	A	Methionine	Met	M
Cysteine	Cys	C	Asparagine	Asn	N
Aspartic Acid	Asp	D	Proline	Pro	P
Glutamic Acid	Glu	E	Glutamine	Gln	Q
Phenylalanine	Phe	F	Arginine	Arg	R
Glycine	Gly	G	Serine	Ser	S
Histidine	His	H	Threonine	Thr	T
Isoleucine	Ile	I	Valine	Val	V
Lysine	Lys	K	Tryptophan	Trp	W
Leucine	Leu	L	Tyrosine	Tyr	Y

Prefixes		
G	giga	10^9
M	mega	10^6
K	kilo	10^3
m	mili	10^{-3}
μ	micro	10^{-6}
n	nano	10^{-9}
p	pico	10^{-12}
f	femto	10^{-15}

References

- [1] Rosalie E Ferner, “Neurofibromatosis 1.” *Eur J Hum Genet*, vol. 15, no. 2, pp. 131–138, Feb 2007, PMID: 16957683.
- [2] Amy Theos, Bruce R Korf, American College of Physicians, and American Physiological Society, “Pathophysiology of neurofibromatosis type 1.” *Ann Intern Med*, vol. 144, no. 11, pp. 842–849, Jun 2006, PMID: 16754926.
- [3] Online Mendelian Inheritance in Man; OMIMTM, “Neurofibromatosis type I” (162200) McKusick-Nathans Institute of Genetic Medicine, Johns Hopkins University (Baltimore, MD) and National Center for Biotechnology Information, National Library of Medicine (Bethesda, MD); <http://www.ncbi.nlm.nih.gov/omim/>.
- [4] International Classification of Diseases (ICD), “Neurofibromatosis (nonmalignant)” (ICD-10 Q85.0) World Health Organization; <http://www.who.int/classifications/icd/en/>.
- [5] Friedrich Daniel von Recklinghausen, *Über die multiplen Fibrome der Haut und ihre Beziehung zu den multiplen Neuromen*, Verlag Hirschwald, Berlin, 1882.
- [6] C. Lázaro, A. Ravella, A. Gaona, V. Volpini, and X. Estivill, “Neurofibromatosis type 1 due to germ-line mosaicism in a clinically normal father.” *N Engl J Med*, vol. 331, no. 21, pp. 1403–1407, Nov 1994, PMID: 7969279.
- [7] S. M. Huson, D. A. Compston, P. Clark, and P. S. Harper, “A genetic study of von recklinghausen neurofibromatosis in south east wales. i. prevalence, fitness, mutation rate, and effect of parental transmission on severity.” *J Med Genet*, vol. 26, no. 11, pp. 704–711, Nov 1989, PMID: 2511318.
- [8] D. Viskochil, R. White, and R. Cawthon, “The neurofibromatosis type 1 gene.” *Annu Rev Neurosci*, vol. 16, pp. 183–205, 1993, PMID: 8460890.
- [9] Rosalie E Ferner, “Neurofibromatosis 1 and neurofibromatosis 2: a twenty first century perspective.” *Lancet Neurol*, vol. 6, no. 4, pp. 340–351, Apr 2007, PMID: 17362838.
- [10] Ming-Jen Lee and Dennis A Stephenson, “Recent developments in neurofibromatosis type 1.” *Curr Opin Neurol*, vol. 20, no. 2, pp. 135–141, Apr 2007, PMID: 17351482.
- [11] Oren N Gottfried, David H Viskochil, Daniel W Fults, and William T Couldwell, “Molecular, genetic, and cellular pathogenesis of neurofibromas and surgical implications.” *Neurosurgery*, vol. 58, no. 1, pp. 1–16; discussion 1–16, Jan 2006, PMID: 16385324.
- [12] Yuan Zhu and Luis F Parada, “The molecular and genetic basis of neurological tumours.” *Nat Rev Cancer*, vol. 2, no. 8, pp. 616–626, Aug 2002, PMID: 12154354.
- [13] Yuan Zhu, Pritam Ghosh, Patrick Charnay, Dennis K Burns, and Luis F Parada, “Neurofibromas in nf1: Schwann cell origin and role of tumor environment.” *Science*, vol. 296, no. 5569, pp. 920–922, May 2002, PMID: 11988578.

- [14] Michael G Vitale, Abhijit Guha, and David L Skaggs, “Orthopaedic manifestations of neurofibromatosis in children: an update.” *Clin Orthop Relat Res*, , no. 401, pp. 107–118, Aug 2002, PMID: 12151887.
- [15] Shelley L Hyman, E. Arthur Shores, and Kathryn N North, “Learning disabilities in children with neurofibromatosis type 1: subtypes, cognitive profile, and attention-deficit-hyperactivity disorder.” *Dev Med Child Neurol*, vol. 48, no. 12, pp. 973–977, Dec 2006, PMID: 17109785.
- [16] A. B. Trovó-Marqui, E. M. Goloni-Bertollo, N. I. Valério, E. C. Pavarino-Bertelli, M. P. Muniz, M. F. Teixeira, J. R. Antonio, and E. H. Tajara, “High frequencies of plexiform neurofibromas, mental retardation, learning difficulties, and scoliosis in brazilian patients with neurofibromatosis type 1.” *Braz J Med Biol Res*, vol. 38, no. 9, pp. 1441–1447, Sep 2005, PMID: 16138229.
- [17] Rossella Vivarelli, Salvatore Grosso, Fulvia Calabrese, MariaAngela Farnetani, Rosanna Di Bartolo, Guido Morgese, and Paolo Balestri, “Epilepsy in neurofibromatosis 1.” *J Child Neurol*, vol. 18, no. 5, pp. 338–342, May 2003, PMID: 12822818.
- [18] Evangelia Zapanti and Ioannis Ilias, “Pheochromocytoma: physiopathologic implications and diagnostic evaluation.” *Ann N Y Acad Sci*, vol. 1088, pp. 346–360, Nov 2006, PMID: 17192579.
- [19] Robert Listernick, Rosalie E Ferner, Grant T Liu, and David H Gutmann, “Optic pathway gliomas in neurofibromatosis-1: controversies and recommendations.” *Ann Neurol*, vol. 61, no. 3, pp. 189–198, Mar 2007, PMID: 17387725.
- [20] Christopher J Stasik and Ossama Tawfik, “Malignant peripheral nerve sheath tumor with rhabdomyosarcomatous differentiation (malignant triton tumor).” *Arch Pathol Lab Med*, vol. 130, no. 12, pp. 1878–1881, Dec 2006, PMID: 17149968.
- [21] Shujuan J Xia, Joseph G Pressey, and Frederic G Barr, “Molecular pathogenesis of rhabdomyosarcoma.” *Cancer Biol Ther*, vol. 1, no. 2, pp. 97–104, 2002, PMID: 12170781.
- [22] Ayalew Tefferi and D. Gary Gilliland, “Oncogenes in myeloproliferative disorders.” *Cell Cycle*, vol. 6, no. 5, pp. 550–566, Mar 2007, PMID: 17351342.
- [23] Sofie De Schepper, Joachim Boucneau, Jo Lambert, Ludwine Messiaen, and Jean-Marie Naeyaert, “Pigment cell-related manifestations in neurofibromatosis type 1: an overview.” *Pigment Cell Res*, vol. 18, no. 1, pp. 13–24, Feb 2005, PMID: 15649148.
- [24] A. Richetta, S. Giustini, S. M. Recupero, M. Pezza, V. Carlomagno, G. Amoroso, and S. Calvieri, “Lisch nodules of the iris in neurofibromatosis type 1.” *J Eur Acad Dermatol Venereol*, vol. 18, no. 3, pp. 342–344, May 2004, PMID: 15096151.
- [25] M. R. Wallace, D. A. Marchuk, L. B. Andersen, R. Letcher, H. M. Odeh, A. M. Saulino, J. W. Fountain, A. Brereton, J. Nicholson, and A. L. Mitchell, “Type 1 neurofibromatosis gene: identification of a large transcript disrupted in three nfl patients.” *Science*, vol. 249, no. 4965, pp. 181–186, Jul 1990, PMID: 2134734.

- [26] R. M. Cawthon, R. Weiss, G. F. Xu, D. Viskochil, M. Culver, J. Stevens, M. Robertson, D. Dunn, R. Gesteland, and P. O'Connell, "A major segment of the neurofibromatosis type 1 gene: cDNA sequence, genomic structure, and point mutations." *Cell*, vol. 62, no. 1, pp. 193–201, Jul 1990, PMID: 2114220.
- [27] D. Viskochil, A. M. Buchberg, G. Xu, R. M. Cawthon, J. Stevens, R. K. Wolff, M. Culver, J. C. Carey, N. G. Copeland, and N. A. Jenkins, "Deletions and a translocation interrupt a cloned gene at the neurofibromatosis type 1 locus." *Cell*, vol. 62, no. 1, pp. 187–192, Jul 1990, PMID: 1694727.
- [28] D. A. Marchuk, A. M. Saulino, R. Tavakkol, M. Swaroop, M. R. Wallace, L. B. Andersen, A. L. Mitchell, D. H. Gutmann, M. Boguski, and F. S. Collins, "cDNA cloning of the type 1 neurofibromatosis gene: complete sequence of the *nf1* gene product." *Genomics*, vol. 11, no. 4, pp. 931–940, Dec 1991, PMID: 1783401.
- [29] Vertebrate Genome Annotation database (VEGA),
"NF1" (VEGA v.28; Locus ID: OTTHUMG00000132871)
Wellcome Trust Sanger Institute, Hinxton, Cambridge, UK and EMBL-EBI,
Hinxton, Cambridge, UK; <http://vega.sanger.ac.uk/index.html>.
- [30] T. Hubbard, D. Barker, E. Birney, G. Cameron, Y. Chen, L. Clark, T. Cox, J. Cuff, V. Curwen, T. Down, R. Durbin, E. Eyra, J. Gilbert, M. Hammond, L. Huminiecki, A. Kasprzyk, H. Lehvaslaiho, P. Lijnzaad, C. Melsopp, E. Mongin, R. Pettett, M. Pocock, S. Potter, A. Rust, E. Schmidt, S. Searle, G. Slater, J. Smith, W. Spooner, A. Stabenau, J. Stalker, E. Stupka, A. Ureta-Vidal, I. Vastrik, and M. Clamp, "The ensembl genome database project." *Nucleic Acids Res*, vol. 30, no. 1, pp. 38–41, Jan 2002, PMID: 11752248.
- [31] P. Flicek, B. L. Aken, K. Beal, B. Ballester, M. Caccamo, Y. Chen, L. Clarke, G. Coates, F. Cunningham, T. Cutts, T. Down, S. C. Dyer, T. Eyre, S. Fitzgerald, J. Fernandez-Banet, S. Grf, S. Haider, M. Hammond, R. Holland, K. L. Howe, K. Howe, N. Johnson, A. Jenkinson, A. Khri, D. Keefe, F. Kokocinski, E. Kulesha, D. Lawson, I. Longden, K. Megy, P. Meidl, B. Overduin, A. Parker, B. Pritchard, A. Prlic, S. Rice, D. Rios, M. Schuster, I. Sealy, G. Slater, D. Smedley, G. Spudich, S. Trevanion, A. J. Vilella, J. Vogel, S. White, M. Wood, E. Birney, T. Cox, V. Curwen, R. Durbin, X. M. Fernandez-Suarez, J. Herrero, T. J P Hubbard, A. Kasprzyk, G. Proctor, J. Smith, A. Ureta-Vidal, and S. Searle, "Ensembl 2008." *Nucleic Acids Res*, Nov 2007, PMID: 18000006.
- [32] J. L. Ashurst, C-K. Chen, J. G R Gilbert, K. Jekosch, S. Keenan, P. Meidl, S. M. Searle, J. Stalker, R. Storey, S. Trevanion, L. Wilming, and T. Hubbard, "The vertebrate genome annotation (vega) database." *Nucleic Acids Res*, vol. 33, no. Database issue, pp. D459–D465, Jan 2005, PMID: 15608237.
- [33] Ina Vandenbroucke, Tom Callens, Anne De Paepe, and Ludwine Messiaen, "Complex splicing pattern generates great diversity in human *nf1* transcripts." *BMC Genomics*, vol. 3, no. 1, pp. 13, May 2002, PMID: 12057013.
- [34] Ina Vandenbroucke, Jo Vandesompele, Anne De Paepe, and Ludwine Messiaen, "Quantification of *nf1* transcripts reveals novel highly expressed splice variants." *FEBS Lett*, vol. 522, no. 1-3, pp. 71–76, Jul 2002, PMID: 12095621.
- [35] D. H. Gutmann, L. B. Andersen, J. L. Cole, M. Swaroop, and F. S. Collins, "An alternatively-spliced mRNA in the carboxy terminus of the

- neurofibromatosis type 1 (nf1) gene is expressed in muscle.” *Hum Mol Genet*, vol. 2, no. 7, pp. 989–992, Jul 1993, PMID: 8364582.
- [36] D. H. Gutmann, R. T. Geist, K. Rose, and D. E. Wright, “Expression of two new protein isoforms of the neurofibromatosis type 1 gene product, neurofibromin, in muscle tissues.” *Dev Dyn*, vol. 202, no. 3, pp. 302–311, Mar 1995, PMID: 7780179.
- [37] G. Danglot, V. Rgnier, D. Fauvet, G. Vassal, M. Kujas, and A. Bernheim, “Neurofibromatosis 1 (nf1) mrnas expressed in the central nervous system are differentially spliced in the 5’ part of the gene.” *Hum Mol Genet*, vol. 4, no. 5, pp. 915–920, May 1995, PMID: 7633452.
- [38] G. R. Skuse and A. J. Cappione, “Rna processing and clinical variability in neurofibromatosis type i (nf1).” *Hum Mol Genet*, vol. 6, no. 10, pp. 1707–1712, 1997, PMID: 9300663.
- [39] G. R. Skuse, A. J. Cappione, M. Sowden, L. J. Metheny, and H. C. Smith, “The neurofibromatosis type i messenger rna undergoes base-modification rna editing.” *Nucleic Acids Res*, vol. 24, no. 3, pp. 478–485, Feb 1996, PMID: 8602361.
- [40] A. J. Cappione, B. L. French, and G. R. Skuse, “A potential role for nf1 mrna editing in the pathogenesis of nf1 tumors.” *Am J Hum Genet*, vol. 60, no. 2, pp. 305–312, Feb 1997, PMID: 9012403.
- [41] T. Nishi, P. S. Lee, K. Oka, V. A. Levin, S. Tanase, Y. Morino, and H. Saya, “Differential expression of two types of the neurofibromatosis type 1 (nf1) gene transcripts related to neuronal differentiation.” *Oncogene*, vol. 6, no. 9, pp. 1555–1559, Sep 1991, PMID: 1923522.
- [42] H. Suzuki, K. Takahashi, K. Yasumoto, N. Fuse, and S. Shibahara, “Differential tissue-specific expression of neurofibromin isoform mrnas in rat.” *J Biochem (Tokyo)*, vol. 120, no. 5, pp. 1048–1054, Nov 1996, PMID: 8982875.
- [43] D. P. Huynh, T. Nechiporuk, and S. M. Pulst, “Differential expression and tissue distribution of type i and type ii neurofibromins during mouse fetal development.” *Dev Biol*, vol. 161, no. 2, pp. 538–551, Feb 1994, PMID: 8314000.
- [44] D. H. Gutmann, R. T. Geist, D. E. Wright, and W. D. Snider, “Expression of the neurofibromatosis 1 (nf1) isoforms in developing and adult rat tissues.” *Cell Growth Differ*, vol. 6, no. 3, pp. 315–323, Mar 1995, PMID: 7794799.
- [45] D. H. Gutmann, Y. Zhang, and A. Hirbe, “Developmental regulation of a neuron-specific neurofibromatosis 1 isoform.” *Ann Neurol*, vol. 46, no. 5, pp. 777–782, Nov 1999, PMID: 10553997.
- [46] M. H. Shen, P. S. Harper, and M. Upadhyaya, “Molecular genetics of neurofibromatosis type 1 (nf1).” *J Med Genet*, vol. 33, no. 1, pp. 2–17, Jan 1996, PMID: 8825042.
- [47] Upadhyaya and Cooper, *Neurofibromatosis type 1 - from genotype to phenotype*, Human Molecular Genetics Series. Bios Scientific Publishers, Oxford, Washington DC, 1998.

- [48] M. M. Daston, H. Scrabble, M. Nordlund, A. K. Sturbaum, L. M. Nissen, and N. Ratner, "The protein product of the neurofibromatosis type 1 gene is expressed at highest abundance in neurons, schwann cells, and oligodendrocytes." *Neuron*, vol. 8, no. 3, pp. 415–428, Mar 1992, PMID: 1550670.
- [49] M. M. Daston and N. Ratner, "Neurofibromin, a predominantly neuronal gtpase activating protein in the adult, is ubiquitously expressed during development." *Dev Dyn*, vol. 195, no. 3, pp. 216–226, Nov 1992, PMID: 1301085.
- [50] C. Teinturier, G. Danglot, R. Slim, D. Pruliere, J. M. Launay, and A. Bernheim, "The neurofibromatosis 1 gene transcripts expressed in peripheral nerve and neurofibromas bear the additional exon located in the gap domain." *Biochem Biophys Res Commun*, vol. 188, no. 2, pp. 851–857, Oct 1992, PMID: 1280127.
- [51] K. Takahashi, H. Suzuki, T. Kayama, Y. Suzuki, T. Yoshimoto, H. Sasano, and S. Shibahara, "Multiple transcripts of the neurofibromatosis type 1 gene in human brain and in brain tumours." *Clin Sci (Lond)*, vol. 87, no. 5, pp. 481–485, Nov 1994, PMID: 7874833.
- [52] G. Danglot, C. Teinturier, A. Duverger, and A. Bernheim, "Tissue-specific alternative splicing of neurofibromatosis 1 (nf1) mrna." *Biomed Pharmacother*, vol. 48, no. 8-9, pp. 365–372, 1994, PMID: 7858173.
- [53] A. B. Trovó-Marqui and E. H. Tajara, "Neurofibromin: a general outlook." *Clin Genet*, vol. 70, no. 1, pp. 1–13, Jul 2006, PMID: 16813595.
- [54] Patrick Vourc'h and Christian Andres, "Oligodendrocyte myelin glycoprotein (omgp): evolution, structure and function." *Brain Res Brain Res Rev*, vol. 45, no. 2, pp. 115–124, May 2004, PMID: 15145622.
- [55] R. M. Cawthon, L. B. Andersen, A. M. Buchberg, G. F. Xu, P. O'Connell, D. Viskochil, R. B. Weiss, M. R. Wallace, D. A. Marchuk, and M. Culver, "cdna sequence and genomic structure of ev12b, a gene lying within an intron of the neurofibromatosis type 1 gene." *Genomics*, vol. 9, no. 3, pp. 446–460, Mar 1991, PMID: 1903357.
- [56] D. Viskochil, R. Cawthon, P. O'Connell, G. F. Xu, J. Stevens, M. Culver, J. Carey, and R. White, "The gene encoding the oligodendrocyte-myelin glycoprotein is embedded within the neurofibromatosis type 1 gene." *Mol Cell Biol*, vol. 11, no. 2, pp. 906–912, Feb 1991, PMID: 1899288.
- [57] Rui M Costa and Alcino J Silva, "Mouse models of neurofibromatosis type i: bridging the gap." *Trends Mol Med*, vol. 9, no. 1, pp. 19–23, Jan 2003, PMID: 12524206.
- [58] Biplab Dasgupta and David H Gutmann, "Neurofibromatosis 1: closing the gap between mice and men." *Curr Opin Genet Dev*, vol. 13, no. 1, pp. 20–27, Feb 2003, PMID: 12573431.
- [59] A. I. McClatchey and K. Cichowski, "Mouse models of neurofibromatosis." *Biochim Biophys Acta*, vol. 1471, no. 2, pp. M73–M80, 2001, PMID: 11342186.
- [60] L. F. Parada, "Neurofibromatosis type 1." *Biochim Biophys Acta*, vol. 1471, no. 1, pp. M13–M19, Jul 2000, PMID: 10967421.

- [61] L. Q. Le and L. F. Parada, “Tumor microenvironment and neurofibromatosis type i: connecting the gaps.” *Oncogene*, vol. 26, no. 32, pp. 4609–4616, Jul 2007, PMID: 17297459.
- [62] K. Cichowski, T. S. Shih, E. Schmitt, S. Santiago, K. Reilly, M. E. McLaughlin, R. T. Bronson, and T. Jacks, “Mouse models of tumor development in neurofibromatosis type 1.” *Science*, vol. 286, no. 5447, pp. 2172–2176, Dec 1999, PMID: 10591652.
- [63] Feng-Chun Yang, Shi Chen, Travis Clegg, Xiaohong Li, Trent Morgan, Selina A Estwick, Jin Yuan, Waleed Khalaf, Sarah Burgin, Jeff Travers, Luis F Parada, David A Ingram, and D. Wade Clapp, “Nf1+/- mast cells induce neurofibroma like phenotypes through secreted tgf-beta signaling.” *Hum Mol Genet*, vol. 15, no. 16, pp. 2421–2437, Aug 2006, PMID: 16835260.
- [64] Feng-Chun Yang, David A Ingram, Shi Chen, Cynthia M Hingtgen, Nancy Ratner, Kelly R Monk, Travis Clegg, Hilary White, Laura Mead, Mary Jo Wenning, David A Williams, Reuben Kapur, Simon J Atkinson, and D. Wade Clapp, “Neurofibromin-deficient schwann cells secrete a potent migratory stimulus for nf1+/- mast cells.” *J Clin Invest*, vol. 112, no. 12, pp. 1851–1861, Dec 2003, PMID: 14679180.
- [65] Theoharis C Theoharides and Pio Conti, “Mast cells: the jekyll and hyde of tumor growth.” *Trends Immunol*, vol. 25, no. 5, pp. 235–241, May 2004, PMID: 15099563.
- [66] Rui M Costa, Nikolai B Federov, Jeff H Kogan, Geoffrey G Murphy, Joel Stern, Masuo Ohno, Raju Kucherlapati, Tyler Jacks, and Alcino J Silva, “Mechanism for the learning deficits in a mouse model of neurofibromatosis type 1.” *Nature*, vol. 415, no. 6871, pp. 526–530, Jan 2002, PMID: 11793011.
- [67] I. The, G. E. Hannigan, G. S. Cowley, S. Reginald, Y. Zhong, J. F. Gusella, I. K. Hariharan, and A. Bernards, “Rescue of a drosophila nf1 mutant phenotype by protein kinase a.” *Science*, vol. 276, no. 5313, pp. 791–794, May 1997, PMID: 9115203.
- [68] R. L. Davis, “Neurofibromin progress on the fly.” *Nature*, vol. 403, no. 6772, pp. 846–847, Feb 2000, PMID: 10706269.
- [69] J. A. Williams, H. S. Su, A. Bernards, J. Field, and A. Sehgal, “A circadian output in drosophila mediated by neurofibromatosis-1 and ras/mapk.” *Science*, vol. 293, no. 5538, pp. 2251–2256, Sep 2001, PMID: 11567138.
- [70] H. F. Guo, J. Tong, F. Hannan, L. Luo, and Y. Zhong, “A neurofibromatosis-1-regulated pathway is required for learning in drosophila.” *Nature*, vol. 403, no. 6772, pp. 895–898, Feb 2000, PMID: 10706287.
- [71] Ivan Shun Ho, Frances Hannan, Hui-Fu Guo, Inessa Hakker, and Yi Zhong, “Distinct functional domains of neurofibromatosis type 1 regulate immediate versus long-term memory formation.” *J Neurosci*, vol. 27, no. 25, pp. 6852–6857, Jun 2007, PMID: 17581973.
- [72] Jiayuan Tong, Frances Hannan, Yinghua Zhu, Andre Bernards, and Yi Zhong, “Neurofibromin regulates g protein-stimulated adenylyl cyclase activity.” *Nat Neurosci*, vol. 5, no. 2, pp. 95–96, Feb 2002, PMID: 11788835.

- [73] James A Walker, Anna V Tchoudakova, Peter T McKenney, Suzanne Brill, Dongyun Wu, Glenn S Cowley, Iswar K Hariharan, and Andr Bernardts, “Reduced growth of drosophila neurofibromatosis 1 mutants reflects a non-cell-autonomous requirement for gtpase-activating protein activity in larval neurons.” *Genes Dev*, vol. 20, no. 23, pp. 3311–3323, Dec 2006, PMID: 17114577.
- [74] James Jiayuan Tong, Samuel E Schriener, David McCleary, Brian J Day, and Douglas C Wallace, “Life extension through neurofibromin mitochondrial regulation and antioxidant therapy for neurofibromatosis-1 in drosophila melanogaster.” *Nat Genet*, vol. 39, no. 4, pp. 476–485, Apr 2007, PMID: 17369827.
- [75] Vertebrate Genome Anotation database (VEGA), “OMPG” (VEGA v.28; Locus ID:OTTHUMG00000132871) Wellcome Trust Sanger Institute, Hinxton, Cambridge, UK and EMBL-EBI, Hinxton, Cambridge, UK; <http://vega.sanger.ac.uk/index.html>.
- [76] Vertebrate Genome Anotation database (VEGA), “EVI2A” (VEGA v.28; Locus ID:OTTHUMT00000281525) Wellcome Trust Sanger Institute, Hinxton, Cambridge, UK and EMBL-EBI, Hinxton, Cambridge, UK; <http://vega.sanger.ac.uk/index.html>.
- [77] Vertebrate Genome Anotation database (VEGA), “EVI2B” (VEGA v.28; Locus ID:OTTHUMT00000256349) Wellcome Trust Sanger Institute, Hinxton, Cambridge, UK and EMBL-EBI, Hinxton, Cambridge, UK; <http://vega.sanger.ac.uk/index.html>.
- [78] I. Izawa, N. Tamaki, and H. Saya, “Phosphorylation of neurofibromatosis type 1 gene product (neurofibromin) by camp-dependent protein kinase.” *FEBS Lett*, vol. 382, no. 1-2, pp. 53–59, Mar 1996, PMID: 8612763.
- [79] G. Bollag, F. McCormick, and R. Clark, “Characterization of full-length neurofibromin: tubulin inhibits ras gap activity.” *EMBO J*, vol. 12, no. 5, pp. 1923–1927, May 1993, PMID: 8491185.
- [80] G. F. Xu, P. O’Connell, D. Viskochil, R. Cawthon, M. Robertson, M. Culver, D. Dunn, J. Stevens, R. Gesteland, and R. White, “The neurofibromatosis type 1 gene encodes a protein related to gap.” *Cell*, vol. 62, no. 3, pp. 599–608, Aug 1990, PMID: 2116237.
- [81] K. Scheffzek, M. R. Ahmadian, L. Wiesmller, W. Kabsch, P. Stege, F. Schmitz, and A. Wittinghofer, “Structural analysis of the gap-related domain from neurofibromin and its implications.” *EMBO J*, vol. 17, no. 15, pp. 4313–4327, Aug 1998, PMID: 9687500.
- [82] M. R. Ahmadian, L. Wiesmller, A. Lautwein, F. R. Bischoff, and A. Wittinghofer, “Structural differences in the minimal catalytic domains of the gtpase-activating proteins p120gap and neurofibromin.” *J Biol Chem*, vol. 271, no. 27, pp. 16409–16415, Jul 1996, PMID: 8663212.
- [83] L. Aravind, A. F. Neuwald, and C. P. Ponting, “Sec14p-like domains in nf1 and dbl-like proteins indicate lipid regulation of ras and rho signaling.” *Curr Biol*, vol. 9, no. 6, pp. R195–R197, Mar 1999, PMID: 10209105.

- [84] Igor D'Angelo, Stefan Welti, Fabien Bonneau, and Klaus Scheffzek, "A novel bipartite phospholipid-binding module in the neurofibromatosis type 1 protein." *EMBO Rep*, vol. 7, no. 2, pp. 174–179, Feb 2006, PMID: 16397625.
- [85] Y. P. Hsueh, A. M. Roberts, M. Volta, M. Sheng, and R. G. Roberts, "Bipartite interaction between neurofibromatosis type i protein (neurofibromin) and syndecan transmembrane heparan sulfate proteoglycans." *J Neurosci*, vol. 21, no. 11, pp. 3764–3770, Jun 2001, PMID: 11356864.
- [86] D. Mangoura, Y. Sun, C. Li, D. Singh, D. H. Gutmann, A. Flores, M. Ahmed, and G. Vallianatos, "Phosphorylation of neurofibromin by pkc is a possible molecular switch in egf receptor signaling in neural cells." *Oncogene*, vol. 25, no. 5, pp. 735–745, Feb 2006, PMID: 16314845.
- [87] E. Ars, H. Kruyer, M. Morell, E. Pros, E. Serra, A. Ravella, X. Estivill, and C. Lzaro, "Recurrent mutations in the nf1 gene are common among neurofibromatosis type 1 patients." *J Med Genet*, vol. 40, no. 6, pp. e82, Jun 2003, PMID: 12807981.
- [88] Birke Bausch, Wiktor Borozdin, Victor F Mautner, Michael M Hoffmann, Detlef Boehm, Mercedes Robledo, Alberto Cascon, Tomas Harenberg, Francesca Schiavi, Christian Pawlu, Mariola Peczkowska, Claudio Letizia, Stefano Calvieri, Giorgio Arnaldi, Rolf D Klingenberg-Noftz, Nicole Reisch, Ambrogio Fassina, Laurent Brunaud, Martin A Walter, Massimo Mannelli, Graham Macgregor, F. Fausto Palazzo, Marta Barontini, Martin K Walz, Bernhard Kremens, Georg Brabant, Roland Pffle, Ann-Cathrin Koschker, Felix Lohofner, Markus Mohaupt, Oliver Gimm, Barbara Jarzab, Sarah R McWhinney, Giuseppe Opocher, Andrzej Januzewicz, Jrgen Kohlhase, Charis Eng, and Hartmut P H Neumann, "Germline nf1 mutational spectra and loss-of-heterozygosity analyses in patients with pheochromocytoma and neurofibromatosis type 1." *J Clin Endocrinol Metab*, Apr 2007, PMID: 17426081.
- [89] Alessandro De Luca, Anna Buccino, Debora Gianni, Massimo Mangino, Sandra Giustini, Antonio Richetta, Luigina Divona, Stefano Calvieri, Rita Mingarelli, and Bruno Dallapiccola, "Nf1 gene analysis based on dhplc." *Hum Mutat*, vol. 21, no. 2, pp. 171–172, Feb 2003, PMID: 12552569.
- [90] R. Fahsold, S. Hoffmeyer, C. Mischung, C. Gille, C. Ehlers, N. Kückceylan, M. Abdel-Nour, A. Gewies, H. Peters, D. Kaufmann, A. Buske, S. Tinschert, and P. Nürnberg, "Minor lesion mutational spectrum of the entire nf1 gene does not explain its high mutability but points to a functional domain upstream of the gap-related domain." *Am J Hum Genet*, vol. 66, no. 3, pp. 790–818, Mar 2000, PMID: 10712197.
- [91] Siân Griffiths, Peter Thompson, Ian Frayling, and Meena Upadhyaya, "Molecular diagnosis of neurofibromatosis type 1: 2 years experience." *Fam Cancer*, vol. 6, pp. 21–34, Aug 2006, PMID: 16944272.
- [92] S. S. Han, D. N. Cooper, and M. N. Upadhyaya, "Evaluation of denaturing high performance liquid chromatography (dhplc) for the mutational analysis of the neurofibromatosis type 1 (nf1) gene." *Hum Genet*, vol. 109, no. 5, pp. 487–497, Nov 2001, PMID: 11735023.
- [93] J. Hudson, C. L. Wu, M. Tassabehji, E. M. Summers, S. Simon, M. Super, D. Donnai, and N. Thakker, "Novel and recurrent mutations in the

- neurofibromatosis type 1 (nf1) gene.” *Hum Mutat*, vol. 9, no. 4, pp. 366–367, 1997, PMID: 9101300.
- [94] Seon-Yong Jeong, Sang-Jin Park, and Hyon J Kim, “The spectrum of nf1 mutations in korean patients with neurofibromatosis type 1.” *J Korean Med Sci*, vol. 21, no. 1, pp. 107–112, Feb 2006, PMID: 16479075.
- [95] Lan Kluwe, Reinhard E Friedrich, Bruce Korf, Raimund Fahsold, and Victor-F. Mautner, “Nf1 mutations in neurofibromatosis 1 patients with plexiform neurofibromas.” *Hum Mutat*, vol. 19, no. 3, pp. 309, Mar 2002, PMID: 11857752.
- [96] S. Krkljus, C. R. Abernathy, J. S. Johnson, C. A. Williams, D. J. Driscoll, R. Zori, H. J. Stalker, S. A. Rasmussen, F. S. Collins, B. G. Kousseff, L. Baumbach, and M. R. Wallace, “Analysis of cpg c-to-t mutations in neurofibromatosis type 1. mutations in brief no. 129. online.” *Hum Mutat*, vol. 11, no. 5, pp. 411, 1998, PMID: 10336779.
- [97] Ming-Jen Lee, Yi-Ning Su, Huey-Ling You, Shinn-Chong Chiou, Li-Chu Lin, Chih-Chao Yang, Wang-Chao Lee, Wu-Liang Hwu, Fon-Jou Hsieh, Dennis A Stephenson, and Chia-Li Yu, “Identification of forty-five novel and twenty-three known nf1 mutations in chinese patients with neurofibromatosis type 1.” *Hum Mutat*, vol. 27, no. 8, pp. 832, Aug 2006, PMID: 16835897.
- [98] C. Mattocks, D. Baralle, P. Tarpey, C. french Constant, M. Bobrow, and J. Whittaker, “Automated comparative sequence analysis identifies mutations in 89of nf1 patients and confirms a mutation cluster in exons 11-17 distinct from the gap related domain.” *J Med Genet*, vol. 41, no. 4, pp. e48, Apr 2004, PMID: 15060124.
- [99] L. M. Messiaen, T. Callens, G. Mortier, D. Beysen, I. Vandenbroucke, N. Van Roy, F. Speleman, and A. D. Paepe, “Exhaustive mutation analysis of the nf1 gene allows identification of 95defects.” *Hum Mutat*, vol. 15, no. 6, pp. 541–555, 2000, PMID: 10862084.
- [100] H. Peters, D. Hess, R. Fahsold, and M. Schlke, “A novel mutation 11425p in the gap-region of the nf1 gene detected by temperature gradient gel electrophoresis (tgge). mutation in brief no. 230. online.” *Hum Mutat*, vol. 13, no. 4, pp. 337, 1999, PMID: 10220149.
- [101] S. M. Purandare, W. G. Lanyon, and J. M. Connor, “Characterisation of inherited and sporadic mutations in neurofibromatosis type-1.” *Hum Mol Genet*, vol. 3, no. 7, pp. 1109–1115, Jul 1994, PMID: 7981679.
- [102] M. Tassabehji, T. Strachan, M. Sharland, A. Colley, D. Donnai, R. Harris, and N. Thakker, “Tandem duplication within a neurofibromatosis type 1 (nf1) gene exon in a family with features of watson syndrome and noonan syndrome.” *Am J Hum Genet*, vol. 53, no. 1, pp. 90–95, Jul 1993, PMID: 8317503.
- [103] M. Upadhyaya, M. J. Osborn, J. Maynard, M. R. Kim, F. Tamanoi, and D. N. Cooper, “Mutational and functional analysis of the neurofibromatosis type 1 (nf1) gene.” *Hum Genet*, vol. 99, no. 1, pp. 88–92, Jan 1997, PMID: 9003501.
- [104] M. Upadhyaya, M. Ruggieri, J. Maynard, M. Osborn, C. Hartog, S. Mudd, M. Penttinen, I. Cordeiro, M. Ponder, B. A. Ponder, M. Krawczak, and D. N. Cooper, “Gross deletions of the neurofibromatosis type 1 (nf1) gene are

- predominantly of maternal origin and commonly associated with a learning disability, dysmorphic features and developmental delay.” *Hum Genet*, vol. 102, no. 5, pp. 591–597, May 1998, PMID: 9654211.
- [105] R. Wu, C. López-Correa, J. L. Rutkowski, L. L. Baumbach, T. W. Glover, and E. Legius, “Germline mutations in *nf1* patients with malignancies.” *Genes Chromosomes Cancer*, vol. 26, no. 4, pp. 376–380, Dec 1999, PMID: 10534774.
- [106] Ina Vandenbroucke, Patrick Van Oostveldt, Elisabeth Coene, Anne De Paepe, and Ludwine Messiaen, “Neurofibromin is actively transported to the nucleus.” *FEBS Lett*, vol. 560, no. 1-3, pp. 98–102, Feb 2004, PMID: 14988005.
- [107] Madanamohan Boyanapalli, Oscar B Lahoud, Ludwine Messiaen, Bhumsoo Kim, Marianna S Anderle de Saylor, Sara J Duckett, Sita Somara, and Daniel D Mikol, “Neurofibromin binds to caveolin-1 and regulates ras, fak, and akt.” *Biochem Biophys Res Commun*, vol. 340, no. 4, pp. 1200–1208, Feb 2006, PMID: 16405917.
- [108] Mohamed-Ali Hakimi, David W Speicher, and Ramin Shiekhattar, “The motor protein kinesin-1 links neurofibromin and merlin in a common cellular pathway of neurofibromatosis.” *J Biol Chem*, vol. 277, no. 40, pp. 36909–36912, Oct 2002, PMID: 12191989.
- [109] C. Li, Y. Cheng, D. A. Gutmann, and D. Mangoura, “Differential localization of the neurofibromatosis 1 (*nf1*) gene product, neurofibromin, with the f-actin or microtubule cytoskeleton during differentiation of telencephalic neurons.” *Brain Res Dev Brain Res*, vol. 130, no. 2, pp. 231–248, Oct 2001, PMID: 11675125.
- [110] Sofie De Schepper, Joachim M A Boucneau, Wendy Westbroek, Mieke Mommaas, Jos Onderwater, Ludwine Messiaen, Jean-Marie A D Naeyaert, and Jo L W Lambert, “Neurofibromatosis type 1 protein and amyloid precursor protein interact in normal human melanocytes and colocalize with melanosomes.” *J Invest Dermatol*, vol. 126, no. 3, pp. 653–659, Mar 2006, PMID: 16374483.
- [111] G. A. Martin, D. Viskochil, G. Bollag, P. C. McCabe, W. J. Crosier, H. Haubruck, L. Conroy, R. Clark, P. O’Connell, and R. M. Cawthon, “The gap-related domain of the neurofibromatosis type 1 gene product interacts with ras p21.” *Cell*, vol. 63, no. 4, pp. 843–849, Nov 1990, PMID: 2121370.
- [112] Stefan Welti, Sven Fraterman, Igor D’Angelo, Matthias Wilm, and Klaus Scheffzek, “The sec14 homology module of neurofibromin binds cellular glycerophospholipids: mass spectrometry and structure of a lipid complex.” *J Mol Biol*, vol. 366, no. 2, pp. 551–562, Feb 2007, PMID: 17187824.
- [113] Siriporn Patrakitkomjorn, Daiki Kobayashi, Takashi Morikawa, Masayo Morifuji Wilson, Nobuyuki Tsubota, Atsushi Irie, Tatsuya Ozawa, Masashi Aoki, Nariko Arimura, Kozo Kaibuchi, Hideyuki Saya, and Norie Araki, “Nf1 tumor suppressor, neurofibromin, regulates the neuronal differentiation of pc12 cells via its associating protein, collapsin response mediator protein-2.” *J Biol Chem*, Jan 2008, PMID: 18218617.
- [114] Liping Feng, Shunji Yunoue, Hiroshi Tokuo, Tatsuya Ozawa, Dongwei Zhang, Siriporn Patrakitkomjorn, Toru Ichimura, Hideyuki Saya, and Norie Araki, “Pka phosphorylation and 14-3-3 interaction regulate the function of neurofibromatosis type i tumor suppressor, neurofibromin.” *FEBS Lett*, vol. 557, no. 1-3, pp. 275–282, Jan 2004, PMID: 14741381.

- [115] R. Ballester, D. Marchuk, M. Boguski, A. Saulino, R. Letcher, M. Wigler, and F. Collins, “The *nfl* locus encodes a protein functionally related to mammalian gap and yeast *ira* proteins.” *Cell*, vol. 63, no. 4, pp. 851–859, Nov 1990, PMID: 2121371.
- [116] K. Cichowski and T. Jacks, “Nf1 tumor suppressor gene function: narrowing the gap.” *Cell*, vol. 104, no. 4, pp. 593–604, Feb 2001, PMID: 11239415.
- [117] E. Legius, D. A. Marchuk, F. S. Collins, and T. W. Glover, “Somatic deletion of the neurofibromatosis type 1 gene in a neurofibrosarcoma supports a tumour suppressor gene hypothesis.” *Nat Genet*, vol. 3, no. 2, pp. 122–126, Feb 1993, PMID: 8499945.
- [118] S. D. Colman, C. A. Williams, and M. R. Wallace, “Benign neurofibromas in type 1 neurofibromatosis (*nfl*) show somatic deletions of the *nfl* gene.” *Nat Genet*, vol. 11, no. 1, pp. 90–92, Sep 1995, PMID: 7550323.
- [119] E. Serra, S. Puig, D. Otero, A. Gaona, H. Kruyer, E. Ars, X. Estivill, and C. Lzaro, “Confirmation of a double-hit model for the *nfl* gene in benign neurofibromas.” *Am J Hum Genet*, vol. 61, no. 3, pp. 512–519, Sep 1997, PMID: 9326316.
- [120] G. Bollag, D. W. Clapp, S. Shih, F. Adler, Y. Y. Zhang, P. Thompson, B. J. Lange, M. H. Freedman, F. McCormick, T. Jacks, and K. Shannon, “Loss of *nfl* results in activation of the ras signaling pathway and leads to aberrant growth in haematopoietic cells.” *Nat Genet*, vol. 12, no. 2, pp. 144–148, Feb 1996, PMID: 8563751.
- [121] J. E. DeClue, S. Heffelfinger, G. Benvenuto, B. Ling, S. Li, W. Rui, W. C. Vass, D. Viskochil, and N. Ratner, “Epidermal growth factor receptor expression in neurofibromatosis type 1-related tumors and *nfl* animal models.” *J Clin Invest*, vol. 105, no. 9, pp. 1233–1241, May 2000, PMID: 10791998.
- [122] T. N. Basu, D. H. Gutmann, J. A. Fletcher, T. W. Glover, F. S. Collins, and J. Downward, “Aberrant regulation of ras proteins in malignant tumour cells from type 1 neurofibromatosis patients.” *Nature*, vol. 356, no. 6371, pp. 713–715, Apr 1992, PMID: 1570015.
- [123] A. Guha, N. Lau, I. Huvar, D. Gutmann, J. Provias, T. Pawson, and G. Boss, “Ras-gtp levels are elevated in human *nfl* peripheral nerve tumors.” *Oncogene*, vol. 12, no. 3, pp. 507–513, Feb 1996, PMID: 8637706.
- [124] Biplab Dasgupta and David H Gutmann, “Neurofibromin regulates neural stem cell proliferation, survival, and astroglial differentiation in vitro and in vivo.” *J Neurosci*, vol. 25, no. 23, pp. 5584–5594, Jun 2005, PMID: 15944386.
- [125] Oliver Rocks, Anna Peyker, and Philippe I H Bastiaens, “Spatio-temporal segregation of ras signals: one ship, three anchors, many harbors.” *Curr Opin Cell Biol*, vol. 18, no. 4, pp. 351–357, Aug 2006, PMID: 16781855.
- [126] Oliver Rocks, Anna Peyker, Martin Kahms, Peter J Verveer, Carolin Koerner, Maria Lumbierres, Jrgen Kuhlmann, Herbert Waldmann, Alfred Wittinghofer, and Philippe I H Bastiaens, “An acylation cycle regulates localization and activity of palmitoylated ras isoforms.” *Science*, vol. 307, no. 5716, pp. 1746–1752, Mar 2005, PMID: 15705808.

- [127] Panagiotis A Konstantinopoulos, Michalis V Karamouzis, and Athanasios G Papavassiliou, "Post-translational modifications and regulation of the ras superfamily of gtpases as anticancer targets." *Nat Rev Drug Discov*, vol. 6, no. 7, pp. 541–555, Jul 2007, PMID: 17585331.
- [128] R. Malhotra and N. Ratner, "Localization of neurofibromin to keratinocytes and melanocytes in developing rat and human skin." *J Invest Dermatol*, vol. 102, no. 5, pp. 812–818, May 1994, PMID: 8176268.
- [129] M. Nordlund, X. Gu, M. T. Shipley, and N. Ratner, "Neurofibromin is enriched in the endoplasmic reticulum of cns neurons." *J Neurosci*, vol. 13, no. 4, pp. 1588–1600, Apr 1993, PMID: 8463837.
- [130] M. Roudebush, T. Slabe, V. Sundaram, C. L. Hoppel, M. Golubic, and D. W. Stacey, "Neurofibromin colocalizes with mitochondria in cultured cells." *Exp Cell Res*, vol. 236, no. 1, pp. 161–172, Oct 1997, PMID: 9344596.
- [131] P. E. Gregory, D. H. Gutmann, A. Mitchell, S. Park, M. Boguski, T. Jacks, D. L. Wood, R. Jove, and F. S. Collins, "Neurofibromatosis type 1 gene product (neurofibromin) associates with microtubules." *Somat Cell Mol Genet*, vol. 19, no. 3, pp. 265–274, May 1993, PMID: 8332934.
- [132] I. R. Vetter and A. Wittinghofer, "The guanine nucleotide-binding switch in three dimensions." *Science*, vol. 294, no. 5545, pp. 1299–1304, Nov 2001, PMID: 11701921.
- [133] K. Scheffzek, M. R. Ahmadian, W. Kabsch, L. Wiesmller, A. Lautwein, F. Schmitz, and A. Wittinghofer, "The ras-rasgap complex: structural basis for gtpase activation and its loss in oncogenic ras mutants." *Science*, vol. 277, no. 5324, pp. 333–338, Jul 1997, PMID: 9219684.
- [134] K. A. Maegley, S. J. Admiraal, and D. Herschlag, "Ras-catalyzed hydrolysis of gtp: a new perspective from model studies." *Proc Natl Acad Sci U S A*, vol. 93, no. 16, pp. 8160–8166, Aug 1996, PMID: 8710841.
- [135] A. Klose, M. R. Ahmadian, M. Schuelke, K. Scheffzek, S. Hoffmeyer, A. Gewies, F. Schmitz, D. Kaufmann, H. Peters, A. Wittinghofer, and P. Nrnberg, "Selective disactivation of neurofibromin gap activity in neurofibromatosis type 1." *Hum Mol Genet*, vol. 7, no. 8, pp. 1261–1268, Aug 1998, PMID: 9668168.
- [136] K. Scheffzek, A. Lautwein, W. Kabsch, M. R. Ahmadian, and A. Wittinghofer, "Crystal structure of the gtpase-activating domain of human p120gap and implications for the interaction with ras." *Nature*, vol. 384, no. 6609, pp. 591–596, Dec 1996, PMID: 8955277.
- [137] Mohammad Reza Ahmadian, Christina Kiel, Patricia Stege, and Klaus Scheffzek, "Structural fingerprints of the ras-gtpase activating proteins neurofibromin and p120gap." *J Mol Biol*, vol. 329, no. 4, pp. 699–710, Jun 2003, PMID: 12787671.
- [138] B. A. Sermon, J. F. Eccleston, R. H. Skinner, and P. N. Lowe, "Mechanism of inhibition by arachidonic acid of the catalytic activity of ras gtpase-activating proteins." *J Biol Chem*, vol. 271, no. 3, pp. 1566–1572, Jan 1996, PMID: 8576154.

- [139] M. Golubić, K. Tanaka, S. Dobrowolski, D. Wood, M. H. Tsai, M. Marshall, F. Tamanoi, and D. W. Stacey, “The gtpase stimulatory activities of the neurofibromatosis type 1 and the yeast *ira2* proteins are inhibited by arachidonic acid.” *EMBO J*, vol. 10, no. 10, pp. 2897–2903, Oct 1991, PMID: 1915269.
- [140] M. Golubić, J. A. Harwalkar, S. S. Bryant, V. Sundaram, R. Jove, and J. H. Lee, “Differential regulation of neurofibromin and p120 gtpase-activating protein by nutritionally relevant fatty acids.” *Nutr Cancer*, vol. 30, no. 2, pp. 97–107, 1998, PMID: 9589427.
- [141] Maurizio Scaltriti and Jos Baselga, “The epidermal growth factor receptor pathway: a model for targeted therapy.” *Clin Cancer Res*, vol. 12, no. 18, pp. 5268–5272, Sep 2006, PMID: 17000658.
- [142] M. M. McKay and D. K. Morrison, “Integrating signals from rtk to erk/mapk.” *Oncogene*, vol. 26, no. 22, pp. 3113–3121, May 2007, PMID: 17496910.
- [143] G. Carpenter and Q. Ji, “Phospholipase c-gamma as a signal-transducing element.” *Exp Cell Res*, vol. 253, no. 1, pp. 15–24, Nov 1999, PMID: 10579907.
- [144] Walter Kolch, “Coordinating erk/mapk signalling through scaffolds and inhibitors.” *Nat Rev Mol Cell Biol*, vol. 6, no. 11, pp. 827–837, Nov 2005, PMID: 16227978.
- [145] Masuko Katoh and Masaru Katoh, “Cross-talk of wnt and fgf signaling pathways at gsk3beta to regulate beta-catenin and snail signaling cascades.” *Cancer Biol Ther*, vol. 5, no. 9, pp. 1059–1064, Sep 2006, PMID: 16940750.
- [146] J. C. Arvalo and S. H. Wu, “Neurotrophin signaling: many exciting surprises!” *Cell Mol Life Sci*, vol. 63, no. 13, pp. 1523–1537, Jul 2006, PMID: 16699811.
- [147] Peter J Cullen and Peter J Lockyer, “Integration of calcium and ras signalling.” *Nat Rev Mol Cell Biol*, vol. 3, no. 5, pp. 339–348, May 2002, PMID: 11988768.
- [148] M. J. Berridge, P. Lipp, and M. D. Bootman, “The versatility and universality of calcium signalling.” *Nat Rev Mol Cell Biol*, vol. 1, no. 1, pp. 11–21, Oct 2000, PMID: 11413485.
- [149] L. A. Selbie and S. J. Hill, “G protein-coupled-receptor cross-talk: the fine-tuning of multiple receptor-signalling pathways.” *Trends Pharmacol Sci*, vol. 19, no. 3, pp. 87–93, Mar 1998, PMID: 9584624.
- [150] Nathalie Dhomen and Richard Marais, “New insight into braf mutations in cancer.” *Curr Opin Genet Dev*, vol. 17, no. 1, pp. 31–39, Feb 2007, PMID: 17208430.
- [151] C. Liebmann, “Regulation of map kinase activity by peptide receptor signalling pathway: paradigms of multiplicity.” *Cell Signal*, vol. 13, no. 11, pp. 777–785, Nov 2001, PMID: 11583913.
- [152] Philip J S Stork and John M Schmitt, “Crosstalk between camp and map kinase signaling in the regulation of cell proliferation.” *Trends Cell Biol*, vol. 12, no. 6, pp. 258–266, Jun 2002, PMID: 12074885.
- [153] Patrick Aloy and Robert B Russell, “Structural systems biology: modelling protein interactions.” *Nat Rev Mol Cell Biol*, vol. 7, no. 3, pp. 188–197, Mar 2006, PMID: 16496021.

- [154] Megan Cully, Han You, Arnold J Levine, and Tak W Mak, “Beyond pten mutations: the pi3k pathway as an integrator of multiple inputs during tumorigenesis.” *Nat Rev Cancer*, vol. 6, no. 3, pp. 184–192, Mar 2006, PMID: 16453012.
- [155] L. Huang, F. Hofer, G. S. Martin, and S. H. Kim, “Structural basis for the interaction of ras with ralgs.” *Nat Struct Biol*, vol. 5, no. 6, pp. 422–426, Jun 1998, PMID: 9628477.
- [156] J. A. Girault, A. Costa, P. Derkinderen, J. M. Studler, and M. Toutant, “Fak and pyk2/cakbeta in the nervous system: a link between neuronal activity, plasticity and survival?” *Trends Neurosci*, vol. 22, no. 6, pp. 257–263, Jun 1999, PMID: 10354603.
- [157] Enrique Rozengurt, “Mitogenic signaling pathways induced by g protein-coupled receptors.” *J Cell Physiol*, vol. 213, no. 3, pp. 589–602, Dec 2007, PMID: 17786953.
- [158] Mark R Morgan, Martin J Humphries, and Mark D Bass, “Synergistic control of cell adhesion by integrins and syndecans.” *Nat Rev Mol Cell Biol*, vol. 8, no. 12, pp. 957–969, Dec 2007, PMID: 17971838.
- [159] Yi-Ling Lin, Ya-Ting Lei, Chen-Jei Hong, and Yi-Ping Hsueh, “Syndecan-2 induces filopodia and dendritic spine formation via the neurofibromin-pka-ena/vasp pathway.” *J Cell Biol*, vol. 177, no. 5, pp. 829–841, Jun 2007, PMID: 17548511.
- [160] Eugene Tkachenko, John M Rhodes, and Michael Simons, “Syndecans: new kids on the signaling block.” *Circ Res*, vol. 96, no. 5, pp. 488–500, Mar 2005, PMID: 15774861.
- [161] Nariko Arimura and Kozo Kaibuchi, “Neuronal polarity: from extracellular signals to intracellular mechanisms.” *Nat Rev Neurosci*, vol. 8, no. 3, pp. 194–205, Mar 2007, PMID: 17311006.
- [162] Ruedi Meili, Atsuo T Sasaki, and Richard A Firtel, “Rho rocks pten.” *Nat Cell Biol*, vol. 7, no. 4, pp. 334–335, Apr 2005, PMID: 15803130.
- [163] Igor Vivanco and Charles L Sawyers, “The phosphatidylinositol 3-kinase akt pathway in human cancer.” *Nat Rev Cancer*, vol. 2, no. 7, pp. 489–501, Jul 2002, PMID: 12094235.
- [164] Takeshi Yoshimura, Nariko Arimura, Yoji Kawano, Saeko Kawabata, Shujie Wang, and Kozo Kaibuchi, “Ras regulates neuronal polarity via the pi3-kinase/akt/gsk-3beta/crmp-2 pathway.” *Biochem Biophys Res Commun*, vol. 340, no. 1, pp. 62–68, Feb 2006, PMID: 16343426.
- [165] Mark A Barber and Heidi C E Welch, “Pi3k and rac signalling in leukocyte and cancer cell migration.” *Bull Cancer*, vol. 93, no. 5, pp. E44–E52, May 2006, PMID: 16777617.
- [166] A. J. Ammit and R. A. Panettieri, “Invited review: the circle of life: cell cycle regulation in airway smooth muscle.” *J Appl Physiol*, vol. 91, no. 3, pp. 1431–1437, Sep 2001, PMID: 11509545.
- [167] David J Kwiatkowski and Brendan D Manning, “Tuberous sclerosis: a gap at the crossroads of multiple signaling pathways.” *Hum Mol Genet*, vol. 14 Spec No. 2, pp. R251–R258, Oct 2005, PMID: 16244323.

- [168] Dos D Sarbassov, Siraj M Ali, and David M Sabatini, “Growing roles for the mtor pathway.” *Curr Opin Cell Biol*, vol. 17, no. 6, pp. 596–603, Dec 2005, PMID: 16226444.
- [169] Y. Mamane, E. Petroulakis, O. LeBacquer, and N. Sonenberg, “mtor, translation initiation and cancer.” *Oncogene*, vol. 25, no. 48, pp. 6416–6422, Oct 2006, PMID: 17041626.
- [170] Robert T Abraham and James J Gibbons, “The mammalian target of rapamycin signaling pathway: twists and turns in the road to cancer therapy.” *Clin Cancer Res*, vol. 13, no. 11, pp. 3109–3114, Jun 2007, PMID: 17545512.
- [171] Stephan Wullschlegel, Robbie Loewith, and Michael N Hall, “Tor signaling in growth and metabolism.” *Cell*, vol. 124, no. 3, pp. 471–484, Feb 2006, PMID: 16469695.
- [172] J. F. Youngren, “Regulation of insulin receptor function.” *Cell Mol Life Sci*, vol. 64, no. 7-8, pp. 873–891, Apr 2007, PMID: 17347799.
- [173] Jonathan M Backer, “The regulation and function of class iii pi3ks: novel roles for vps34.” *Biochem J*, vol. 410, no. 1, pp. 1–17, Feb 2008, PMID: 18215151.
- [174] Xiaolin Wan and Lee J Helman, “The biology behind mtor inhibition in sarcoma.” *Oncologist*, vol. 12, no. 8, pp. 1007–1018, Aug 2007, PMID: 17766661.
- [175] Ken Inoki and Kun-Liang Guan, “Complexity of the tor signaling network.” *Trends Cell Biol*, vol. 16, no. 4, pp. 206–212, Apr 2006, PMID: 16516475.
- [176] Janet E Dancey, “Therapeutic targets: Mtor and related pathways.” *Cancer Biol Ther*, vol. 5, no. 9, pp. 1065–1073, Sep 2006, PMID: 16969122.
- [177] Andrew M Arsham and Thomas P Neufeld, “Thinking globally and acting locally with tor.” *Curr Opin Cell Biol*, vol. 18, no. 6, pp. 589–597, Dec 2006, PMID: 17046229.
- [178] Stephen G Dann, Anand Selvaraj, and George Thomas, “mtor complex1-s6k1 signaling: at the crossroads of obesity, diabetes and cancer.” *Trends Mol Med*, vol. 13, no. 6, pp. 252–259, Jun 2007, PMID: 17452018.
- [179] April P Kelly, David K Finlay, Heather J Hinton, Rosie G Clarke, Emma Fiorini, Freddy Radtke, and Doreen A Cantrell, “Notch-induced t cell development requires phosphoinositide-dependent kinase 1.” *EMBO J*, vol. 26, no. 14, pp. 3441–3450, Jul 2007, PMID: 17599070.
- [180] David Shahbazian, Philippe P Roux, Virginie Mieulet, Michael S Cohen, Brian Raught, Jack Taunton, John W B Hershey, John Blenis, Mario Pende, and Nahum Sonenberg, “The mtor/pi3k and mapk pathways converge on eif4b to control its phosphorylation and activity.” *EMBO J*, vol. 25, no. 12, pp. 2781–2791, Jun 2006, PMID: 16763566.
- [181] James A McCubrey, Linda S Steelman, William H Chappell, Stephen L Abrams, Ellis W T Wong, Fumin Chang, Brian Lehmann, David M Terrian, Michele Milella, Agostino Tafuri, Franca Stivala, Massimo Libra, Jorg Basccke, Camilla Evangelisti, Alberto M Martelli, and Richard A Franklin, “Roles of the raf/mek/erk pathway in cell growth, malignant transformation and drug resistance.” *Biochim Biophys Acta*, vol. 1773, no. 8, pp. 1263–1284, Aug 2007, PMID: 17126425.

- [182] Mary B Kennedy, Holly C Beale, Holly J Carlisle, and Lorraine R Washburn, "Integration of biochemical signalling in spines." *Nat Rev Neurosci*, vol. 6, no. 6, pp. 423–434, Jun 2005, PMID: 15928715.
- [183] Nagahiro Minato, Kohei Kometani, and Masakazu Hattori, "Regulation of immune responses and hematopoiesis by the rap1 signal." *Adv Immunol*, vol. 93, pp. 229–264, 2007, PMID: 17383543.
- [184] Ricardo B Medeiros, Deborah M Dickey, Heekyoung Chung, Angie C Quale, Lakshmi R Nagarajan, Daniel D Billadeau, and Yoji Shimizu, "Protein kinase d1 and the beta 1 integrin cytoplasmic domain control beta 1 integrin function via regulation of rap1 activation." *Immunity*, vol. 23, no. 2, pp. 213–226, Aug 2005, PMID: 16111639.
- [185] Gal Mnasch, Stefanie Kliche, Natalie Bezman, and Burkhardt Schraven, "Regulation of t-cell antigen receptor-mediated inside-out signaling by cytosolic adapter proteins and rap1 effector molecules." *Immunol Rev*, vol. 218, pp. 82–91, Aug 2007, PMID: 17624945.
- [186] T. Laux, K. Fukami, M. Thelen, T. Golub, D. Frey, and P. Caroni, "Gap43, marcks, and cap23 modulate pi(4,5)p(2) at plasmalemmal rafts, and regulate cell cortex actin dynamics through a common mechanism." *J Cell Biol*, vol. 149, no. 7, pp. 1455–1472, Jun 2000, PMID: 10871285.
- [187] Christer Larsson, "Protein kinase c and the regulation of the actin cytoskeleton." *Cell Signal*, vol. 18, no. 3, pp. 276–284, Mar 2006, PMID: 16109477.
- [188] M. J. Marinissen and J. S. Gutkind, "G-protein-coupled receptors and signaling networks: emerging paradigms." *Trends Pharmacol Sci*, vol. 22, no. 7, pp. 368–376, Jul 2001, PMID: 11431032.
- [189] Akrit Sodhi, Silvia Montaner, and J. Silvio Gutkind, "Viral hijacking of g-protein-coupled-receptor signalling networks." *Nat Rev Mol Cell Biol*, vol. 5, no. 12, pp. 998–1012, Dec 2004, PMID: 15573137.
- [190] E. Hermans and R. A. Challiss, "Structural, signalling and regulatory properties of the group i metabotropic glutamate receptors: prototypic family c g-protein-coupled receptors." *Biochem J*, vol. 359, no. Pt 3, pp. 465–484, Nov 2001, PMID: 11672421.
- [191] Frances Hannan, Ivan Ho, James Jiayuan Tong, Yinghua Zhu, Peter Nurnberg, and Yi Zhong, "Effect of neurofibromatosis type i mutations on a novel pathway for adenylyl cyclase activation requiring neurofibromin and ras." *Hum Mol Genet*, vol. 15, no. 7, pp. 1087–1098, Apr 2006, PMID: 16513807.
- [192] Kjetil Taskn and Einar Martin Aandahl, "Localized effects of camp mediated by distinct routes of protein kinase a." *Physiol Rev*, vol. 84, no. 1, pp. 137–167, Jan 2004, PMID: 14715913.
- [193] Ivette Hernandez-Negrete, Jorge Carretero-Ortega, Hans Rosenfeldt, Ricardo Hernandez-Garca, J. Victor Caldern-Salinas, Guadalupe Reyes-Cruz, J. Silvio Gutkind, and Jos Vzquez-Prado, "P-rax1 links mammalian target of rapamycin signaling to rac activation and cell migration." *J Biol Chem*, vol. 282, no. 32, pp. 23708–23715, Aug 2007, PMID: 17565979.

- [194] Toshihide Kimura, Hiroyasu Watanabe, Akihiro Iwamatsu, and Kozo Kaibuchi, "Tubulin and crmp-2 complex is transported via kinesin-1." *J Neurochem*, vol. 93, no. 6, pp. 1371–1382, Jun 2005, PMID: 15935053.
- [195] Linda A Amos and Daniel Schlieper, "Microtubules and maps." *Adv Protein Chem*, vol. 71, pp. 257–298, 2005, PMID: 16230114.
- [196] H. Xu and D. H. Gutmann, "Mutations in the gap-related domain impair the ability of neurofibromin to associate with microtubules." *Brain Res*, vol. 759, no. 1, pp. 149–152, Jun 1997, PMID: 9219873.
- [197] Matthias Krause, Erik W Dent, James E Bear, Joseph J Loureiro, and Frank B Gertler, "Ena/vasp proteins: regulators of the actin cytoskeleton and cell migration." *Annu Rev Cell Dev Biol*, vol. 19, pp. 541–564, 2003, PMID: 14570581.
- [198] Nicolas Hulo, Amos Bairoch, Virginie Bulliard, Lorenzo Cerutti, Edouard De Castro, Petra S Langendijk-Genevaux, Marco Pagni, and Christian J A Sigrist, "The prosite database." *Nucleic Acids Res*, vol. 34, no. Database issue, pp. D227–D230, Jan 2006, PMID: 16381852.
- [199] Fabien Bonneau, Igor D'Angelo, Stefan Welti, Gunter Stier, Jari Ylänne, and Klaus Scheffzek, "Expression, purification and preliminary crystallographic characterization of a novel segment from the neurofibromatosis type 1 protein." *Acta Crystallogr D Biol Crystallogr*, vol. 60, no. Pt 12 Pt 2, pp. 2364–2367, Dec 2004, PMID: 15583390.
- [200] B. Sha, S. E. Phillips, V. A. Bankaitis, and M. Luo, "Crystal structure of the *saccharomyces cerevisiae* phosphatidylinositol-transfer protein." *Nature*, vol. 391, no. 6666, pp. 506–510, Jan 1998, PMID: 9461221.
- [201] A. Cleves, T. McGee, and V. Bankaitis, "Phospholipid transfer proteins: a biological debut." *Trends Cell Biol*, vol. 1, no. 1, pp. 30–34, Jul 1991, PMID: 14731807.
- [202] K. W. Wirtz and D. B. Zilversmit, "Participation of soluble liver proteins in the exchange of membrane phospholipids." *Biochim Biophys Acta*, vol. 193, no. 1, pp. 105–116, Oct 1969, PMID: 5349606.
- [203] Günther Daum and Fritz Paltauf, "Isolation and partial characterization of a phospholipid transfer protein from yeast cytosol" *Biochim Biophys Acta*, vol. 794, pp. 385–391, 1984, PMID: n.a.
- [204] J. F. Aitken, G. P. van Heusden, M. Temkin, and W. Dowhan, "The gene encoding the phosphatidylinositol transfer protein is essential for cell growth." *J Biol Chem*, vol. 265, no. 8, pp. 4711–4717, Mar 1990, PMID: 2407740.
- [205] V. A. Bankaitis, J. R. Aitken, A. E. Cleves, and W. Dowhan, "An essential role for a phospholipid transfer protein in yeast golgi function." *Nature*, vol. 347, no. 6293, pp. 561–562, Oct 1990, PMID: 2215682.
- [206] Gilbert Di Paolo and Pietro De Camilli, "Phosphoinositides in cell regulation and membrane dynamics." *Nature*, vol. 443, no. 7112, pp. 651–657, Oct 2006, PMID: 17035995.
- [207] Victoria Allen-Baume, Bruno Ségui, and Shamshad Cockcroft, "Current thoughts on the phosphatidylinositol transfer protein family." *FEBS Lett*, vol. 531, no. 1, pp. 74–80, Oct 2002, PMID: 12401207.

- [208] Scott E Phillips, Patrick Vincent, Kellie E Rizzieri, Gabriel Schaaf, Vytas A Bankaitis, and Eric A Gaucher, “The diverse biological functions of phosphatidylinositol transfer proteins in eukaryotes.” *Crit Rev Biochem Mol Biol*, vol. 41, no. 1, pp. 21–49, 2006, PMID: 16455519.
- [209] Karel W A Wirtz, “Phospholipid transfer proteins in perspective.” *FEBS Lett*, vol. 580, no. 23, pp. 5436–5441, Oct 2006, PMID: 16828756.
- [210] K. W. Wirtz, “Phospholipid transfer proteins revisited.” *Biochem J*, vol. 324 (Pt 2), pp. 353–360, Jun 1997, PMID: 9182690.
- [211] J. W. Crabb, V. P. Gaur, G. G. Garwin, S. V. Marx, C. Chapline, C. M. Johnson, and J. C. Saari, “Topological and epitope mapping of the cellular retinaldehyde-binding protein from retina.” *J Biol Chem*, vol. 266, no. 25, pp. 16674–16683, Sep 1991, PMID: 1715867.
- [212] Achim Stocker and Ulrich Baumann, “Supernatant protein factor in complex with rrr-alpha-tocopherylquinone: a link between oxidized vitamin e and cholesterol biosynthesis.” *J Mol Biol*, vol. 332, no. 4, pp. 759–765, Sep 2003, PMID: 12972248.
- [213] K. Christopher Min, Rhett A Kovall, and Wayne A Hendrickson, “Crystal structure of human alpha-tocopherol transfer protein bound to its ligand: implications for ataxia with vitamin e deficiency.” *Proc Natl Acad Sci U S A*, vol. 100, no. 25, pp. 14713–14718, Dec 2003, PMID: 14657365.
- [214] N. Blomberg, E. Baraldi, M. Nilges, and M. Saraste, “The ph superfold: a structural scaffold for multiple functions.” *Trends Biochem Sci*, vol. 24, no. 11, pp. 441–445, Nov 1999, PMID: 10542412.
- [215] M. A. Lemmon, “Pleckstrin homology domains: not just for phosphoinositides.” *Biochem Soc Trans*, vol. 32, no. Pt 5, pp. 707–711, Nov 2004, PMID: 15493994.
- [216] Toshiki Itoh and Pietro De Camilli, “Membrane trafficking: dual-key strategy.” *Nature*, vol. 429, no. 6988, pp. 141–143, May 2004, PMID: 15141195.
- [217] Jonathan P DiNitto, Thomas C Cronin, and David G Lambright, “Membrane recognition and targeting by lipid-binding domains.” *Sci STKE*, vol. 2003, no. 213, pp. re16, Dec 2003, PMID: 14679290.
- [218] Jong W Yu, Jeannine M Mendrola, Anjon Audhya, Shaneen Singh, David Keleti, Daryll B DeWald, Diana Murray, Scott D Emr, and Mark A Lemmon, “Genome-wide analysis of membrane targeting by *s. cerevisiae* pleckstrin homology domains.” *Mol Cell*, vol. 13, no. 5, pp. 677–688, Mar 2004, PMID: 15023338.
- [219] Mark A Lemmon, Kathryn M Ferguson, and Charles S Abrams, “Pleckstrin homology domains and the cytoskeleton.” *FEBS Lett*, vol. 513, no. 1, pp. 71–76, Feb 2002, PMID: 11911883.
- [220] Mark A Lemmon, “Pleckstrin homology domains: two halves make a hole?” *Cell*, vol. 120, no. 5, pp. 574–576, Mar 2005, PMID: 15766521.
- [221] Mark A Baumeister, Kent L Rossman, John Sondek, and Mark A Lemmon, “The dbp ph domain contributes independently to membrane targeting and regulation of guanine nucleotide-exchange activity.” *Biochem J*, vol. 400, no. 3, pp. 563–572, Dec 2006, PMID: 17007612.

- [222] Anna Godi, Antonella Di Campli, Athanasios Konstantakopoulos, Giuseppe Di Tullio, Dario R Alessi, Gursant S Kular, Tiziana Daniele, Pierfrancesco Marra, John M Lucoq, and M. Antonietta De Matteis, “Fapps control golgi-to-cell-surface membrane traffic by binding to arf and ptdins(4)p.” *Nat Cell Biol*, vol. 6, no. 5, pp. 393–404, May 2004, PMID: 15107860.
- [223] Péter Várnai, Xuena Lin, Sang Bong Lee, Galina Tuymetova, Tzvetanka Bondeva, Andras Spt, Sue Goo Rhee, Gyrgy Hajnczky, and Tamas Balla, “Inositol lipid binding and membrane localization of isolated pleckstrin homology (ph) domains. studies on the ph domains of phospholipase c delta 1 and p130.” *J Biol Chem*, vol. 277, no. 30, pp. 27412–27422, Jul 2002, PMID: 12019260.
- [224] Mark T Uhlik, Brenda Temple, Sompop Bencharit, Adam J Kimple, David P Siderovski, and Gary L Johnson, “Structural and evolutionary division of phosphotyrosine binding (ptb) domains.” *J Mol Biol*, vol. 345, no. 1, pp. 1–20, Jan 2005, PMID: 15567406.
- [225] Kelley S Yan, Miklos Kuti, and Ming Ming Zhou, “Ptb or not ptb – that is the question.” *FEBS Lett*, vol. 513, no. 1, pp. 67–70, Feb 2002, PMID: 11911882.
- [226] K. S. Ravichandran, “Signaling via shc family adapter proteins.” *Oncogene*, vol. 20, no. 44, pp. 6322–6330, Oct 2001, PMID: 11607835.
- [227] Chiara Zuccato, Luciano Conti, Erika Reitano, Marzia Tartari, and Elena Cattaneo, “The function of the neuronal proteins shc and huntingtin in stem cells and neurons: pharmacologic exploitation for human brain diseases.” *Ann N Y Acad Sci*, vol. 1049, pp. 39–50, May 2005, PMID: 15965106.
- [228] Linda J Ball, Thomas Jarchau, Hartmut Oschkinat, and Ulrich Walter, “Evh1 domains: structure, function and interactions.” *FEBS Lett*, vol. 513, no. 1, pp. 45–52, Feb 2002, PMID: 11911879.
- [229] Tadaomi Takenawa and Shiro Suetsugu, “The wasp-wave protein network: connecting the membrane to the cytoskeleton.” *Nat Rev Mol Cell Biol*, vol. 8, no. 1, pp. 37–48, Jan 2007, PMID: 17183359.
- [230] R. Scott Duncan, Sung-Yong Hwang, and Peter Koulen, “Effects of vesl/homer proteins on intracellular signaling.” *Exp Biol Med (Maywood)*, vol. 230, no. 8, pp. 527–535, Sep 2005, PMID: 16118402.
- [231] H. Fried and U. Kutay, “Nucleocytoplasmic transport: taking an inventory.” *Cell Mol Life Sci*, vol. 60, no. 8, pp. 1659–1688, Aug 2003, PMID: 14504656.
- [232] Lucy F Pemberton and Bryce M Paschal, “Mechanisms of receptor-mediated nuclear import and nuclear export.” *Traffic*, vol. 6, no. 3, pp. 187–198, Mar 2005, PMID: 15702987.
- [233] Virginie Gervais, Valérie Lamour, Anass Jawhari, Florent Frindel, Emeric Wasielewski, Sandy Dubaele, Jean-Marc Egly, Jean-Claude Thierry, Bruno Kieffer, and Arnaud Poterszman, “Tfih contains a ph domain involved in dna nucleotide excision repair.” *Nat Struct Mol Biol*, vol. 11, no. 7, pp. 616–622, Jul 2004, PMID: 15195146.
- [234] Reto Meier, Takashi Tomizaki, Clemens Schulze-Briese, Ulrich Baumann, and Achim Stocker, “The molecular basis of vitamin e retention: structure of

- human alpha-tocopherol transfer protein.” *J Mol Biol*, vol. 331, no. 3, pp. 725–734, Aug 2003, PMID: 12899840.
- [235] GE Healthcare, “Amersham ECL PlusTM western blotting detection reagents” *Product Booklet*, vol. RPN2132PL Rev D 2006, pp. 1–32, 2006, <http://www.gehealthcare.com/lifesciences>.
- [236] Eric C Chang and Mark R Philips, “Spatial segregation of ras signaling: new evidence from fission yeast.” *Cell Cycle*, vol. 5, no. 17, pp. 1936–1939, Sep 2006, PMID: 16931912.
- [237] Shuji Ueda, Tohru Kataoka, and Takaya Satoh, “Role of the sec14-like domain of dbl family exchange factors in the regulation of rho family gtpases in different subcellular sites.” *Cell Signal*, vol. 16, no. 8, pp. 899–906, Aug 2004, PMID: 15157669.
- [238] Gábor Sirokmány, László Szidonya, Krisztina Káldi, Zsuzsanna Gáborik, Erzsébet Ligeti, and Miklós Geiszt, “Sec14 homology domain targets p50rhogap to endosomes and provides a link between rab and rho gtpases.” *J Biol Chem*, vol. 281, no. 9, pp. 6096–6105, Mar 2006, PMID: 16380373.
- [239] Runxiang Zhao, Xueqi Fu, Qingshan Li, Sanford B Krantz, and Zhizhuang Joe Zhao, “Specific interaction of protein tyrosine phosphatase-meg2 with phosphatidylserine.” *J Biol Chem*, vol. 278, no. 25, pp. 22609–22614, Jun 2003, PMID: 12702726.
- [240] Ricardo H Alvarez, Hagop M Kantarjian, and Jorge E Cortes, “Biology of platelet-derived growth factor and its involvement in disease.” *Mayo Clin Proc*, vol. 81, no. 9, pp. 1241–1257, Sep 2006, PMID: 16970222.
- [241] Thomas C Cronin, Jonathan P DiNitto, Michael P Czech, and David G Lambright, “Structural determinants of phosphoinositide selectivity in splice variants of grp1 family ph domains.” *EMBO J*, vol. 23, no. 19, pp. 3711–3720, Oct 2004, PMID: 15359279.
- [242] W. Kabsch, “Automatic processing of rotation diffraction data from crystals of initially unknown symmetry and cell constants” *Journal of Applied Crystallography*, vol. 26, no. 6, pp. 795–800, Dec 1993, PMID: n.a.
- [243] T. D. Fenn, D. Ringe, and G. A. Petsko, “POVScript+: a program for model and data visualization using persistence of vision ray-tracing” *J Appl Cryst*, vol. 36, pp. 944–947, 2003, PMID: n.a.
- [244] POV-Team, “Persistence of vision raytracer (POV-Ray)” <http://www.povray.org/>, 2008.
- [245] A. T. Brnger, P. D. Adams, G. M. Clore, W. L. DeLano, P. Gros, R. W. Grosse-Kunstleve, J. S. Jiang, J. Kuszewski, M. Nilges, N. S. Pannu, R. J. Read, L. M. Rice, T. Simonson, and G. L. Warren, “Crystallography & nmr system: A new software suite for macromolecular structure determination.” *Acta Crystallogr D Biol Crystallogr*, vol. 54, no. Pt 5, pp. 905–921, Sep 1998, PMID: 9757107.
- [246] Paul Emsley and Kevin Cowtan, “Coot: model-building tools for molecular graphics.” *Acta Crystallogr D Biol Crystallogr*, vol. 60, no. Pt 12 Pt 1, pp. 2126–2132, Dec 2004, PMID: 15572765.

- [247] R. A. Laskowski, M. W. MacArthur, D. S. Moss, and J. M. Thornton, "Procheck: a program to check the stereochemical quality of protein structures." *J. Appl. Cryst.*, vol. 26, pp. 283–291, 1993, PMID: n.a.
- [248] Steven L Roderick, Wayne W Chan, Diana S Agate, Laurence R Olsen, Matt W Vetting, K. R. Rajashankar, and David E Cohen, "Structure of human phosphatidylcholine transfer protein in complex with its ligand." *Nat Struct Biol*, vol. 9, no. 7, pp. 507–511, Jul 2002, PMID: 12055623.
- [249] Irina N Krylova, Elena P Sablin, Jamie Moore, Robert X Xu, Gregory M Waitt, J. Andrew MacKay, Dalia Juzumiene, Jane M Bynum, Kevin Madauss, Valerie Montana, Lioudmila Lebedeva, Miyuki Suzawa, Jon D Williams, Shawn P Williams, Rodney K Guy, Joseph W Thornton, Robert J Fletterick, Timothy M Willson, and Holly A Ingraham, "Structural analyses reveal phosphatidyl inositols as ligands for the nr5 orphan receptors sf-1 and lrh-1." *Cell*, vol. 120, no. 3, pp. 343–355, Feb 2005, PMID: 15707893.
- [250] Yong Li, Mihwa Choi, Greg Cavey, Jennifer Daugherty, Kelly Suino, Amanda Kovach, Nathan C Bingham, Steven A Kliewer, and H. Eric Xu, "Crystallographic identification and functional characterization of phospholipids as ligands for the orphan nuclear receptor steroidogenic factor-1." *Mol Cell*, vol. 17, no. 4, pp. 491–502, Feb 2005, PMID: 15721253.
- [251] J. Folch, M. Lees, and G. H. Sloane Stanley, "A simple method for the isolation and purification of total lipides from animal tissues." *J Biol Chem*, vol. 226, no. 1, pp. 497–509, May 1957, PMID: 13428781.
- [252] Xuguang Yan, Jeffrey Watson, P. Shing Ho, and Max L Deinzer, "Mass spectrometric approaches using electrospray ionization charge states and hydrogen-deuterium exchange for determining protein structures and their conformational changes." *Mol Cell Proteomics*, vol. 3, no. 1, pp. 10–23, Jan 2004, PMID: 14623985.
- [253] R. O. Caldern and G. H. DeVries, "Lipid composition and phospholipid asymmetry of membranes from a schwann cell line." *J Neurosci Res*, vol. 49, no. 3, pp. 372–380, Aug 1997, PMID: 9260748.
- [254] John E Cronan, "Bacterial membrane lipids: where do we stand?" *Annu Rev Microbiol*, vol. 57, pp. 203–224, 2003, PMID: 14527277.
- [255] G. Daum, "Lipids of mitochondria." *Biochim Biophys Acta*, vol. 822, no. 1, pp. 1–42, Jun 1985, PMID: 2408671.
- [256] R. O. Calderon, B. Attema, and G. H. DeVries, "Lipid composition of neuronal cell bodies and neurites from cultured dorsal root ganglia." *J Neurochem*, vol. 64, no. 1, pp. 424–429, Jan 1995, PMID: 7798942.
- [257] Jean E Vance, "Molecular and cell biology of phosphatidylserine and phosphatidylethanolamine metabolism." *Prog Nucleic Acid Res Mol Biol*, vol. 75, pp. 69–111, 2003, PMID: 14604010.
- [258] H. E. Jones, J. L. Harwood, I. D. Bowen, and G. Griffiths, "Lipid composition of subcellular membranes from larvae and prepupae of drosophila melanogaster." *Lipids*, vol. 27, no. 12, pp. 984–987, Dec 1992, PMID: 1487960.

- [259] W. S. Stark, T. N. Lin, D. Brackhahn, J. S. Christianson, and G. Y. Sun, "Phospholipids in drosophila heads: effects of visual mutants and phototransduction manipulations." *Lipids*, vol. 28, no. 1, pp. 23–28, Jan 1993, PMID: 8446007.
- [260] Trever G Bivona, Steven E Quatela, Brian O Bodemann, Ian M Ahearn, Michael J Soskis, Adam Mor, John Miura, Heidi H Wiener, Latasha Wright, Shahryar G Saba, Duke Yim, Adam Fein, Ignacio Prez de Castro, Chi Li, Craig B Thompson, Adrienne D Cox, and Mark R Philips, "Pkc regulates a farnesyl-electrostatic switch on k-ras that promotes its association with bcl-xl on mitochondria and induces apoptosis." *Mol Cell*, vol. 21, no. 4, pp. 481–493, Feb 2006, PMID: 16483930.
- [261] M. Upadhyaya, J. Maynard, M. Osborn, and P. S. Harper, "Six novel mutations in the neurofibromatosis type 1 (nf1) gene." *Hum Mutat*, vol. 10, no. 3, pp. 248–250, 1997, PMID: 9298829.
- [262] Ineke van der Burgt, "Noonan syndrome." *Orphanet J Rare Dis*, vol. 2, pp. 4, 2007, PMID: 17222357.
- [263] Jacqueline A Noonan, "Noonan syndrome and related disorders: alterations in growth and puberty." *Rev Endocr Metab Disord*, vol. 7, no. 4, pp. 251–255, Dec 2006, PMID: 17177115.
- [264] Robert J Salmond and Denis R Alexander, "Shp2 forecast for the immune system: fog gradually clearing." *Trends Immunol*, vol. 27, no. 3, pp. 154–160, Mar 2006, PMID: 16458607.
- [265] Suzanne Schubert, Gideon Bollag, and Kevin Shannon, "Deregulated ras signaling in developmental disorders: new tricks for an old dog." *Curr Opin Genet Dev*, vol. 17, no. 1, pp. 15–22, Feb 2007, PMID: 17208427.
- [266] Number 4 Collaborative Computational Project, "The ccp4 suite: programs for protein crystallography." *Acta Crystallogr D Biol Crystallogr*, vol. 50, no. Pt 5, pp. 760–763, Sep 1994, PMID: 15299374.
- [267] Elena V Kostenko, Gwendolyn M Mahon, Li Cheng, and Ian P Whitehead, "The sec14 homology domain regulates the cellular distribution and transforming activity of the rho-specific guanine nucleotide exchange factor dbs." *J Biol Chem*, vol. 280, no. 4, pp. 2807–2817, Jan 2005, PMID: 15531584.
- [268] S. Welti, I. D'Angleo, and K. Scheffzek, *Structure and Functions of Neurofibromin*, vol. 16 of *Monographs in Human Genetics*, Karger, Basel, 2008.
- [269] Kan Saito, Lutz Tautz, and Tomas Mustelin, "The lipid-binding sec14 domain." *Biochim Biophys Acta*, vol. 1771, no. 6, pp. 719–726, Jun 2007, PMID: 17428729.
- [270] Erzsébet Ligeti and Jeffrey Settleman, "Regulation of rhogap specificity by phospholipids and prenylation." *Methods Enzymol*, vol. 406, pp. 104–117, 2006, PMID: 16472653.
- [271] Kent L Rossman, David K Worthylake, Jason T Snyder, David P Siderovski, Sharon L Campbell, and John Sondek, "A crystallographic view of interactions between dbs and cdc42: Ph domain-assisted guanine nucleotide exchange." *EMBO J*, vol. 21, no. 6, pp. 1315–1326, Mar 2002, PMID: 11889037.

- [272] I. R. Vetter, C. Nowak, T. Nishimoto, J. Kuhlmann, and A. Wittinghofer, "Structure of a ran-binding domain complexed with ran bound to a gtp analogue: implications for nuclear transport." *Nature*, vol. 398, no. 6722, pp. 39–46, Mar 1999, PMID: 10078529.
- [273] Damara Gebauer, Jiang Li, Gerwald Jogl, Yang Shen, David G Myszka, and Liang Tong, "Crystal structure of the ph-beach domains of human lrba/bgl." *Biochemistry*, vol. 43, no. 47, pp. 14873–14880, Nov 2004, PMID: 15554694.
- [274] Andrew P VanDemark, Mary Blanksma, Elliott Ferris, Annie Heroux, Christopher P Hill, and Tim Formosa, "The structure of the yfact pob3-m domain, its interaction with the dna replication factor rpa, and a potential role in nucleosome deposition." *Mol Cell*, vol. 22, no. 3, pp. 363–374, May 2006, PMID: 16678108.
- [275] J. Peter Geyer, Rolf Dker, Werner Kremer, Xiaodong Zhao, Jrgen Kuhlmann, and Hans Robert Kalbitzer, "Solution structure of the ran-binding domain 2 of ranbp2 and its interaction with the c terminus of ran." *J Mol Biol*, vol. 348, no. 3, pp. 711–725, May 2005, PMID: 15826666.
- [276] Finly Philip, Yuanjian Guo, and Suzanne Scarlata, "Multiple roles of pleckstrin homology domains in phospholipase cbeta function." *FEBS Lett*, vol. 531, no. 1, pp. 28–32, Oct 2002, PMID: 12401198.
- [277] D. Illenberger, F. Schwald, D. Pimmer, W. Binder, G. Maier, A. Dietrich, and P. Gierschik, "Stimulation of phospholipase c-beta2 by the rho gtpases cdc42hs and rac1." *EMBO J*, vol. 17, no. 21, pp. 6241–6249, Nov 1998, PMID: 9799233.
- [278] J. Sambrook and D. W. Russel, *Molecular Cloning: a laboratory manual*, Cold Spring Harbor Laboratory Press, Cold Spring Harbor NY, 2001 edition, 2001.
- [279] S. M. Abmayr et. al., *Current protocols in molecular biology*, Wiley Interscience, 1998.
- [280] E. Gasteiger, C. Hoogland, A. Gattiker, S. Duvaud, M. R. Wilkins, R. D. Appel, and A. Bairoch, *The Proteomics Protocols Handbook: Protein Identification and Analysis Tools on the ExPASy Server*, Humana Press, 2005.
- [281] R. W. Grosse-Kunstleve and P. D. Adams, "Patterson correlation methods: a review of molecular replacement with cns." *Acta Crystallogr D Biol Crystallogr*, vol. 57, no. Pt 10, pp. 1390–1396, Oct 2001, PMID: 11567150.
- [282] S. R. James, A. Paterson, T. K. Harden, and C. P. Downes, "Kinetic analysis of phospholipase c beta isoforms using phospholipid-detergent mixed micelles. evidence for interfacial catalysis involving distinct micelle binding and catalytic steps." *J Biol Chem*, vol. 270, no. 20, pp. 11872–11881, May 1995, PMID: 7744837.
- [283] Jiyao Wang, Alok Gambhir, Gyngyi Hangys-Mihlyn, Diana Murray, Urszula Golebiewska, and Stuart McLaughlin, "Lateral sequestration of phosphatidylinositol 4,5-bisphosphate by the basic effector domain of myristoylated alanine-rich c kinase substrate is due to nonspecific electrostatic interactions." *J Biol Chem*, vol. 277, no. 37, pp. 34401–34412, Sep 2002, PMID: 12097325.
- [284] D. Marsh, *CRC Handbook of Lipid Bilayers*, CRC Press Inc., 1990, ISBN: 0-8493-3255-9.

- [285] I. V. Chernushevich, A. V. Loboda, and B. A. Thomson, “An introduction to quadrupole-time-of-flight mass spectrometry.” *J Mass Spectrom*, vol. 36, no. 8, pp. 849–865, Aug 2001, PMID: 11523084.
- [286] Peter Nemes, Ioan Marginean, and Akos Vertes, “Spraying mode effect on droplet formation and ion chemistry in electrosprays.” *Anal Chem*, vol. 79, no. 8, pp. 3105–3116, Apr 2007, PMID: 17378541.
- [287] M. Wilm and M. Mann, “Analytical properties of the nanoelectrospray ion source.” *Anal Chem*, vol. 68, no. 1, pp. 1–8, Jan 1996, PMID: 8779426.
- [288] Charles E. Mortimer, *Chemie*, Georg Thieme Verlag, Stuttgart, New York, 6. edition, 1995.